Ing. Martin Griesbacher, BSc.

Imidazoline-functionalized silica-based monoliths for the purification of biomolecules and antibodies in particular

MASTERARBEIT

zur Erlangung des akademischen Grades

Diplom-Ingenieur

Masterstudium Chemical and Pharmaceutical Engineering

eingereicht an der

Technischen Universität Graz

Betreuerin

Ass.Prof. Dipl.-Ing. Dr. techn. Heidrun Gruber-Wölfler

Institut für Prozess- und Partikeltechnik

Graz, Mai 2016

EIDESSTATTLICHE ERKLÄRUNG

Ich erkläre an Eides statt, dass ich die vorliegende Arbeit selbstständig verfasst, andere als die angegebenen Quellen/Hilfsmittel nicht benutzt, und die den benutzten Quellen wörtlich und inhaltlich entnommenen Stellen als solche kenntlich gemacht habe. Das in TUGRAZonline hochgeladene Textdokument ist mit der vorliegenden Masterarbeit identisch.

Datum

Unterschrift

Kurzfassung

Proteine im Allgemeinen und Antiköper im Speziellen nehmen eine immer bedeutendere Rolle bei der Herstellung und Produktion von Medikamenten und Therapeutika ein. Die Isolierung und Aufreinigung von (monoklonalen) Antikörpern beruht zurzeit hauptsächlich auf Protein A Chromatographie, eine höchst effiziente aber auch komplizierte und sehr teure Methode.

Das Ziel dieser Arbeit war es, eine effiziente, alternative Methode zur kontinuierlichen Aufreinigung von Antikörpern und Proteinen im Generellen zu entwickeln, die ebenfalls auf chromatographischen Prinzipien beruht. Dieser kontinuierliche, chromatographische Aufreinigungsprozess kann durch den Einsatz von kontinuierlicher annularer Elektrochromatographie (CAEC) erreicht werden. Zu diesem Zweck wurde ein auf Siliziumdioxid-basierende monolithische Säule entwickelt, welche einfach in der Herstellung, und nicht-giftig ist und für CAEC eigesetzt werden kann.
Basierend auf der Funktionsweise von Histidine-Affinitäts-Chromatographie und ihrer speziellen Wechselwirkung mit Antikörpern, wurde diese monolithische Säule mit Imidazolin-Gruppen funktionalisiert.

Die Funktionalisierung mit Imidazolin und deren Dichte innerhalb des Monoliths wurden mittels FTIR und Elementaranalyse festgestellt.
Durch BET-Analyse und Gaspyknometrie wurde ein bimodales Porensystem gefunden, das Mikro- und Mesoporen enthielt. Der Monolith zeigte dazu kein Quellverhalten im Ethanol-Wasser-Gemisch und war resistent in Bezug auf wässrige Puffer im pH-Bereich von 4 bis 10.
Wechselwirkungen wurden in Batch- als auch bei chromatographischen Versuchen mit Albumin, einigen Farbstoffen und in geringer Weise mit bestimmten Aminosäuren festgestellt. Retention und Elution glichen dabei den Sorptionsprozessen eines schwachen Anionentauschers.
In Batchversuchen konnten geringe adsorptive Wechelwirkungen zwischen Monolithmaterial und Antikörper sowie Denaturierungsphänomene festgestellt werden.

Abstract

Proteins in the general and antibodies in particular gain a more and more important role in the preparation and designing of drugs and therapeutics. At present, the isolation and purification especially of (monoclonal) antibodies is dominated by protein A chromatography, which is highly efficient, but also complex and very expensive.

The aim of this study was to develop an efficient alternative method for continuous purification of antibodies and proteins in general based on chromatographic principles. This continuous chromatographic purification process can be achieved by Continuous annular electrochromatography (CAEC). For this purpose, a silica-based monolithic column was prepared by sol-gel processes, which is easy to prepare, nontoxic and might be applicable to CAEC.
Based on histidine affinity principles and their specific interactions with IgG, this silica monolith was functionalized with imidazoline moieties.

The functionalization with imidazolines and their density within the monolith were determined by FTIR and elementary analysis.
Via BET analysis and gas pycnometry a double-sized pore system could be found containing micro- and macropores. Additionally, the monolith showed no swelling behavior in ethanol-water mixtures and was mostly resistant to aqueous buffers in the pH range from 4 to 10.
Interactions could be found with albumins, some dyes and in a minor form with distinct amino acids, tested in batch experiments as well as in chromatographic mode. Retention and elution were performed with sorption processes by weak anion exchange in aqueous mobile phases.
In batch experiments were found slight adsorptive interactions between monolithic material and antibodies as well as denaturing phenomena.

Table of Contents

1 Goals and Motivation....1
2 STATE OF THE ART....3
2.1 Antibody purification....3
2.2 CAEC....6
3 THEORETICAL APPROACH....8
3.1 Proteins and Antibodies....8
3.2 Liquid Chromatography....9
3.2.1 Principles....9
3.2.2 Histidine-Affinity Chromatography....13
3.3 Silica based Monoliths....17
3.3.1 Principles....17
3.3.2 Preparation of silica-based monoliths....20
3.3.3 Substantials for silica-based monoliths....27
3.3.4 Alternative applications....31
4 PRACTICAL WORK....33
4.1 IMEO-monoliths....33
4.1.1 IMEO-monolith preparation....33
4.1.2 Quality control of prepared monolith batches....34
4.1.3 Preparation of IMEO-monolith type A-7....38
4.1.4 Preparation of IMEO-monolith type B-40....39
4.2 Monolith characterization....39
4.2.1 FTIR-Spectra....39
4.2.2 Particle analysis....40
4.2.3 Elementary analysis....44
4.2.4 Microscopy....45
4.2.5 Swelling test....47

4.3 Chromatographic tests 47
4.3.1 Chemical stability 47
4.3.2 Elution of dyes 49
4.3.3 Adsorption and desorption of biomolecules 52
4.3.4 Elution test of biomolecules 61
5 Conclusions 67
6 Outlook 69
7 Experimental 70
7.1 All chemicals 70
7.2 Lab equipment 71
7.3 Other materials 71
7.3.1 For monolith preparation 71
7.3.2 For monolith characterization 71
8 REFERENCES 72
9 List of figures 77
10 List of tables 78
11 APPENDIX 79
11.1 Normal-phase silica preparation 79
11.2 Ninhydrin derivatization 79
11.3 Photometrical analysis 80
11.4 List of monolith batches 81

List of abbreviations and symbols

A	Absorbance
A_0	Initial absorbance
abs	Absolute
ACN	Acetonitrile
ads	Adsorption, adsorbed
AEC, AEX	Anion exchange chromatography
APTES	(3-Aminopropyl)triethoxysilane
ATP	Aqueous two-phase extraction, adenosine triphosphate
AU	Arbitrary unit
Bcg	Bromocresol green
BET	Brunauer-Emmett-Teller (gas adsorption theory)
BSA	Bovine serum albumin
C	Column capacity, constant, Condensation (as index)
c	Molar concentration
C8 / C18	Octyl-, Octadecyl- (see also ODS)
CAEC	Continuous Annular Electro-Chromatography
Calc	Calconcarboxylic acid, calculation
CEC	Capillary electrochromatography
CEX	Cation exchange chromatography
CHN	(Analysis on) Carbon, hydrogen and nitrogen
COOH	Carboxylic acid
CTAB	Cetyltrimethylammonium bromide
Cyt C	Cytochrome C
d	Cuvette thickness, axial diffusion (as index)
DCCA	Drying control chemical additive
D_m	Diffusion coefficient of analyte (mobile phase)
DMF	*N,N*-Dimethylformamide
DNA	Deoxyribonucleic acid
d_p	Particle size
$d_{particles}$	Particle density
e	Eddy diffusion (as index)
E	Separation impedance

elu	Elution, eluted
EOF	Electroosmotic flow
equiv.	Molar equivalents
EtOH	Ethanol
Fc	Fragment crystallizable
FSB	Final sample buffer
FTIR	Fourier transform infrared spectroscopy
Gly	Glycine
H	Theoretical plate height, Hydrolysis (as index)
H_2O	Water
HAc	Acetic acid
HAC	Histidine affinity chromatography
HIC	Hydrophobic interaction chromatography
His	Histidine
HPLC	High performance liquid chromatography
HPT (solution)	(solution of) Histidine, Phenylalanine and Tryptophan
i	individual
IEP	Isoelectrical point
IgG	Immunoglobulin G
IMAC	Immobilized metal ion affinity chromatography
IMEO	4,5-Dihydro-1-[3-(triethoxysilyl)propyl]-1H-imidazol
k_C	Rate of condensation
KCl	Potassium chloride
k_H	Rate of hydrolysis
KSCN	Potassium thiocyanate
L	Length of column
m	weighed mass, mass transfer related to mobile phase (as index)
mAb	Monoclonal antibody
Mb	Methylene blue
MeOH	Methanol
M_N	Atomic mass (of nitrogen)
Mr	Methyl red
Mw	Molecular weight
NaCl	Sodium chloride

N_{BSA}	Molar amount (of albumin)
NH_2	Amino moiety
NH_4OH	Ammonium hydroxide (solution)
ODS	Octadecylsilane (see also C18)
PBS	Phosphate buffer saline
PEEK	Polyetheretherketon
PEG	Polyethylenglycol (see also PEO)
PFTR	Plug flow tube reactor
Phe	Phenylalanine
pI	Isoelectrical point (see also IEP)
pK	Acid dissociation constant
PMMA	Polymethylmethacrylat
PrOH	2-Propanol, Isopropyl alcohol
PS	Polystyrol
PSD	Particle size distribution
Q_{Ads}	Amount (of adsorbed molecules)
R ratio	Molar ratio (of water to precursor)
r	Pore radius
resp.	Respectively
RP	Reversed phase
rpm	Rotation per minute
RRSB	Rosin-Rammler-Sperling-Benett (grain-size distribution)
sc	Side chain
SEC	Size exclusion chromatography
SH	Thiol moiety
sm	mass transfer related to stationary phase (as index)
STD	Standard deviation
Stock	Stock solution
t_0	Dead time of the column
TEOS	Tetraethyl orthosilicate
Term A	Eddy diffusion (mobile phase)
Term B	Axial diffusion (mobile phase)
Term C	Mass transfer (stationary phase)
t_{gel}	Gelation time

TLC	Thin layer chromatography
TMOS	Tetramethyl orthosilicate
tot	Total
Trp	Tryptophan
u	Linear velocity of mobile phase
UPW	Ultrapure water
UV-VIS	Ultraviolet and visible spectroscopy
V	Volume
w	Flow resistance
WL	Wavelength
x_{10}	Particle size limit (10% of the total particles are smaller than x)
Δp	Pressure drop
ε	Molar extinction coefficient
η	Dynamic viscosity
f	Fraction
γ	Surface energy
θ	Contact angle

1 Goals and Motivation

Antibodies are the active ingredients in antisera, vaccines for passive immunization and other therapeutics. More and more therapeutics based on (monoclonal) antibodies push for the pharmaceutical market. In 2007 the pharmaceutical industry generated sales of 9 billion dollars in the United States and in the European Union with 22 approved therapeutics based on antibodies. [1]

But the production of these products has still been enormously costly. The treatment costs are partly invaluable for patients in states with poor health system. Therefore it is a public interest to make the production of antibodies cheaper and more effective. One way to achieve this goal is to optimize the downstream process of antibody production,. The downstream process contains multiple purification and concentration steps focused on protein A chromatography. This main purification step via protein A chromatography is state of the art. Unfortunately, this step represents a high amount of the antibodies' total production costs.

Although protein A chromatography yields the best performance for antibody purification currently, it grapples with drawbacks: A major problem is the isolation of protein A itself, its restricted stability and the leaching of the immobilized protein.

On this account there are a lot of research groups around the world, who try to find alternatives. Some strategies contain the replacement of protein A by small synthetic molecules with higher stability and easier to prepare, but which shows the same effectiveness as protein A: Researchers like Latza et al. [2] try to extract the epitope of protein A and seizes it in small synthetic molecules.

Other strategies plan to purify antibodies via aqueous two-phase extraction or via ultrafiltration, respectively. [3]

Our focus leans on the combination of histidine-affinity chromatography and silica based monoliths.

Hereto, Kanoun et al. [4] found specific interactions between histidine and proteins. With histidine affinity chromatography, it is possible to purify Immunoglobulin G (IgG) directly out of serum. Additionally, optimal process conditions for the antibody isolation were found at a pH of 7.4 and at temperatures of 4°C. But despite of decent results it could not prevail against protein A chromatography.

In the last decades a new trend in chromatography column engineering has been formed: silica based monolithic columns. These monoliths have the benefit of very low backpressures. Low

backpressures warrant high-throughputs. Hence, this work focuses on a monolith with immobilized histidine-like ligands, which can purify biomolecules very effective and fast. The method should be appropriable for continuous annular electrochromatography (CAEC), which would guarantee a possibility for continuous purification of biomolecules and antibodies in particular and a serious cost-cutting alternative to protein A chromatography.

In the next chapters, the reader will find an introduction about antibody purification in general and the theoretical basics for functionalized silica based monoliths.
The sol-gel process is viewed on detail followed by some information about histidine affinity chromatography. We also reason our decision for the use of imdidazoline moieties instead of more histidine-like imidazoles.
The practical work was devoted to the development of imidazole functionalized monoliths, their characterization and their engineering for the biomolecule purification.
After the development, the characterization of the monolith followed: Customized properties should warrant optimal interactions between functionalized monolith and biomolecules like proteins or antibodies in particular. Therefore, it should show definitely delimiting interactions with different functional groups on the basis of adsorption and desorption.
A system of macroporous through-pores provides for high flow rates on the one hand and mesopores for maximal bonding capacity and good chromatographic resolutions on the other hand. Furthermore, the monolithic material should feature chemical and mechanical stability.

In the end, the reader will find a short discussion about the results and a brief outlook for the prospective application of imidazoline functionalized monoliths.

2 STATE OF THE ART

2.1 Antibody purification

Antibodies are glycosylated proteins responsible for immune defense in human bodies. They have a typically Y-form consisting of two heavy and two light protein chains, which are connected via intra-molecular disulfide bonds. Each chain has variable and constant regions. The type of these chains classifies the antibody. The typically form of IgG can be seen in Fig. 1. The size of IgG is about 15 nm. It has 83 lysine groups distributed over the whole molecule (Fig. 1, left side).

By the way, until 2007 all approved antibodies used as therapeutics were IgG. [1, 5]

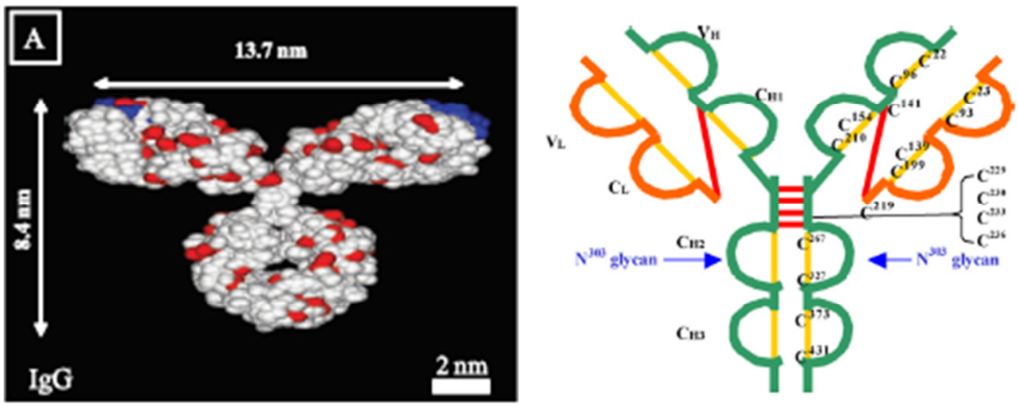

Fig. 1: Structure of IgG. (Left) Rendered model by Chimera [5]: lysine groups (red), antigen binding fragments (blue); (Right) Schematic structure [1]: V =variable chain, C=constant chain, L = light domain, H=heavy domain, red lines=disulfide bridges.

The commercial production of (monoclonal) antibodies start in huge tanks filled with mammalian cell culture. During cultivation (upstream process) the antibodies are secreted into the cell culture media. For their harvest they must be separated from cells and cell debris (start of the downstream process). This is often done by centrifugation, followed by microfiltration (see Fig. 2).

The step is referred as "capture step". The aim is to concentrate the product and separate contaminants (DNA, host cell impurities, virus, endotoxins, etc.).

Viral inactivation and two polishing steps are followed. The viral inactivation is often done by decreasing the pH.

The polishing steps increase the purity by removal of rest DNA, leached protein A and host cell protein impurities. The methods for the polishing and viral inactivation have to be orthogonal to the capture step. A viral- and an ultrafiltration step complete the antibody purification.

A complete pathway for antibody isolation and purification is shown in Fig. 2. [1]

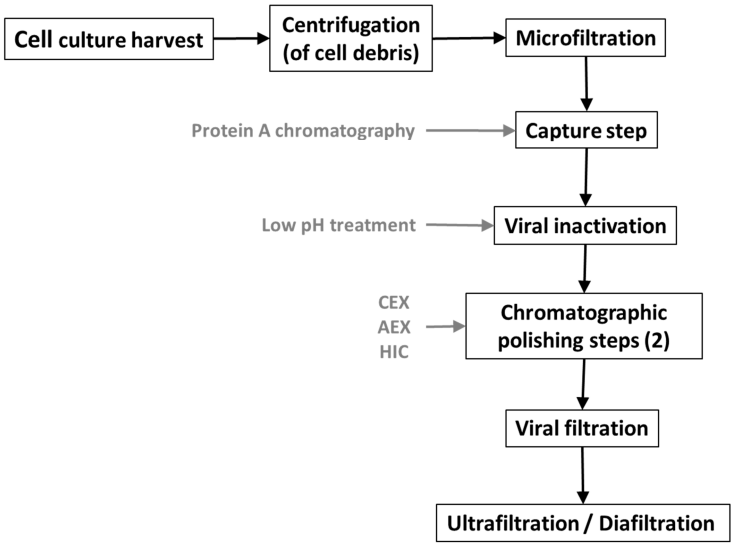

Fig. 2: Typical downstream process for (monoclonal) antibodies. [1]

There are several strategies for the capture step. Among them, the most effective method is protein A chromatography. This chromatography method uses protein A as bioaffinity ligand, which works by the lock-and-key model. [3]

Protein A originates from the cell wall of Staphylococcus aureus and binds specifically immunoglobulins. It interacts with the fragment crystallizable (Fc) region of the antibody via hydrogen bonds and hydrophobic interactions. For that reason, every molecule has five homologous antibody binding sites. The elution, however, can be caused by lowering the pH. [6]

Protein A chromatography can clean up IgG to a purity of 95% with minor protein loss and concurrent DNA and virus clearance. But the process costs outbalance the performance: Protein A is obtained through expensive and complex biochemical pathways.
Moreover, protein A is sensitive to harsh conditions, which, however, are preferable for process cleanings. Additionally, the productivity is limited due to diffusive mass transfer, protein A leaching can occur and in acidic conditions it can form aggregates.
Hence, there are many research groups, which are working to replace protein A by small synthetic molecules. As one strategy, they try to recognize the docking epitopes of protein A and substitute it with similar structured synthetic molecules. [2, 3]
Other approaches try to replace protein A chromatography by non-chromatographic methods.

A promising strategy could be the development of aqueous two-phase (ATP) extraction, which uses concentrated PEG solutions (hydrophobic phase) to separate IgG from the serum phase.
Other experiments were based on precipitation or filtration, respectively. But despite of high recoveries and purities, all these methods could not prevail against protein A chromatography, because of their high effectiveness and the fixed establishment of chromatographic methods in biochemical downstream processes. The non-chromatographic alternatives would require additional support in the process development. That´s why only a chromatographic method could replace protein A chromatography.
Many experiments aimed at replacing protein A ligands by small synthetic mimetics, referred to as "pseudospecific" or "pseudoaffinity" ligands.
Hereby, an attempt is to reduce protein A to its bonding core domain, which can be used to create synthetic molecules that can bind antibodies as good as protein A, but which are resistant to harsh elution conditions and a can be produced easily by a synthetic pathway. [3]

Experiments have shown that even single amino acids like tryptophan and histidine show more or less specific binding effects to antibodies. The binding effect can take place, based on either electrostatic or hydrophobic interactions.
Consequently, various kinds of chromatographic methods served as a basis for alternative antibody purification pathways in the last decades: Size exclusion chromatography (SEC), Anion exchange chromatography (AEC), Cation exchange chromatography (CEC), Immobilized metal affinity chromatography (IMAC) and Hydrophobic interaction chromatography (HIC).
Hereby, a promising candidate is AEC. Along with antibody concentration, it can additionally remove DNA, virus and other contaminants by the displacement principle. The displacement principle works with different bonding affinities of the solutes to the ligand, so that weakly bound antibodies were displaced by contaminates with stronger bonding affinity. This is especially required for flow-through applications.
Remarkable is also IMAC, because of its extraordinary separation principle: Here, the antibodies are retained by immobilized metal ions like nickel, copper, zinc, cobalt or iron, respectively. But the principle is complex and the capacities low.
A similar principle also exploits Hydroxyapatite chromatography (HAC). Hydroxyapatite is a Ca-rich mineral, which adsorbs antibodies via calcium coordination. [3]

HIC, in turn, makes use of the attraction of unpolar domains towards hydrophobic regions and is already a common orthogonal application for aggregate, DNA and host protein removal.
In future, the engineering of stationary supports will also depart from diffusive particles towards monoliths and membranes, respectively, because of the higher possible throughput. [3]

2.2 CAEC

CAEC stands for continuous annular electro-chromatography. It is a chromatographic method for the continuous chromatographic separation of a product flow. The principle works as a combination of thin layer chromatography (TLC) and capillary electro-chromatography (CEC). The column consists of a cylindrical capillary mold.
The product flow is pumped as rotating feed flow onto the top of the column. Mobile phase is permanently fed to the column. An electroosmotic flow (EOF) results through the high voltage between the column´s inlet and outlet and transports the products through the system. The EOF is caused by immobilized (negative) charges on the surface of the solid phase. As a result, there is a voltage drop within the capillary mold´s profile, which induces a continuous flow of the whole mobile phase. A typically scheme of a CAEC can be seen in Fig. 3 and the prototype of such a system is displayed in Fig. 4.
The EOF results in an extremely uniform laminar flow, which are optimal requirements for chromatographic separations. Different fixed product tracks ensued by diverse retention properties of the products. Every product track can be characterized by its own track angle: the more retained, the higher the angle. Multiple product lines can be collected at the column outlet and analyzed by UV-Vis systems. [7]

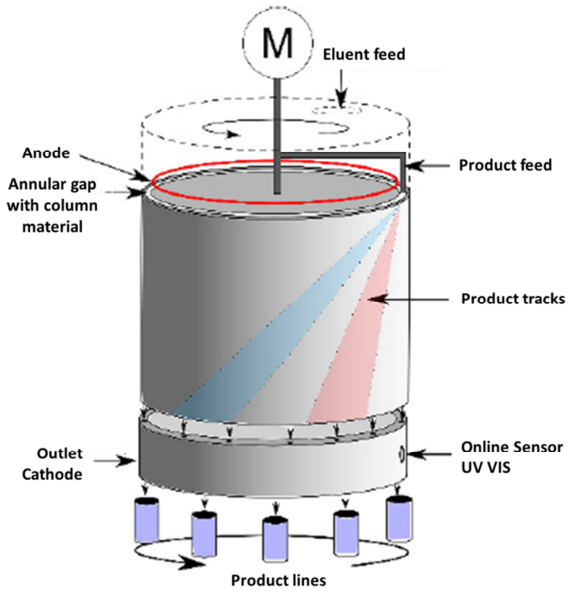

Fig. 3: Scheme of a continuous annular electro-chromatography system. [7]

The suitable application of silica based monoliths for the continuous annular electrochromatography was shown by Braunbruck et al. [8]. They developed a reversed phase (RP) monolith on the basis of alkoxide precursors in a one-pot preparation, which was used to separate small molecules. [8–10]

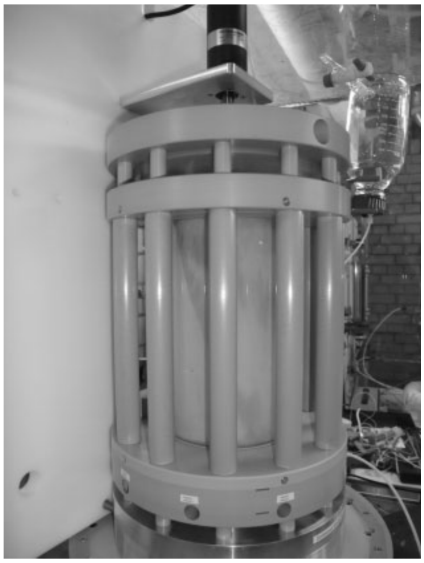

Fig. 4: Prototype of a CAEC with monolithic stationary phase. [8]

3 THEORETICAL APPROACH

3.1 Proteins and Antibodies

Proteins consist of long strands of amino acids and can differ among others in their molecular weight, their surface charges and amount of hydrophobic domains, etc. These properties can be all exploited for chromatographic separation.
For instance, cytochrome C (Cyt C), bovine serum albumin (BSA) and myoglobin are three proteins with totally different isoelectrical point (pI or IEP), ranging from 10.6 to 4.6. This means, that their surface is totally differently charged in the same buffer media.
Furthermore, the amount of hydrophobic domains in the protein influences hydrophobic interactions at the interface and, additionally, the molecular weight effects the diffusion in and out of pores. [11]

For mesoporous silicates a general adsorption effect for proteins has been found depending on pore size, surface modifications, pH and ionic strength, respectively. The adsorption occurs mainly because of electrostatic and hydrophobic interactions between the surface of silicate and protein. It is important for these interactions that the proteins fit into the pore system of the monolith without blockage. This is critically, because too small pores exclude the target proteins, whereas too large pores decrease the surface area. As a consequence, efficiency and capacity would decrease.
Moreover, small pores, labelled as "micropores", initiate an undesired size exclusion effect for small molecules. [11, 12]

Normally, proteins do not adsorb as ideal monolayers on silica surfaces, as Deere et al. [11] could have shown.
In fact, it seems to be a combination of mono- and multilayers. That is, in turn, crucial for the desorption process: It is assumed that proteins in multilayers desorb more easily than proteins bound directly to the surface of mesoporous silicates. For adsorption and desorption of proteins onto mesoporous silicates different pathways have been assumed.
Relevant for protein adsorption, however, is also the surface modification of the silicates. Desorption of Trypsin is relived from surfaces with amino moieties in contrast to unmodified silica, respectively.

Hereby, positively charged proteins adsorb better on unmodified mesoporous silicates. Positively charged proteins (pH below IEP) were physically immobilized on silicates by their terminal silanol groups. The immobilization is partly reversible by changing the pH. [11, 13]

3.2 Liquid Chromatography

3.2.1 Principles

The main part of every (liquid) chromatography system is a column with its stationary phase. The stationary phase is composed of a porous support and terminal functionalized moieties protruded from its surface.

In general, two stationary phase systems are possible: particle-packed columns and monolithic rods, casted in one piece. Both systems have pros and cons: The former one can be easier prepared. The particles bed can be supposed as homogenous bed and their properties are good to characterize. In contrast, monolithic columns need no frits at the outlets. Frits on the outlet lead to a reduced efficiency and to bubble formation. Moreover, monolithic columns have low backpressures. Thus, they can be operated with higher flow rates because of their low backpressures, which, in turn, increase the through-put. Additionally, monolithic columns feature better stability and higher performance than particle-packed columns. [14–16]

The chromatographic efficiency of a chromatographic column is characterized by three main processes, which are described in equation (1) according to [16]: Hereby, Term A corresponds to Eddy diffusion, Term B corresponds to Axial diffusion and Term C is corresponding to the resistance to mass transfer. [14, 16]

$$H = A \cdot \sqrt[3]{u} + \frac{B}{u} + C \cdot u = \frac{1}{\frac{1}{C_e \cdot d_p} + \frac{D_m}{C_m \cdot d_p^2 \cdot u}} + \frac{D_m \cdot C_d}{u} + \frac{C_{sm} \cdot d_p^2 \cdot u}{D_m} \qquad (1)$$

$$\text{with } u = \frac{L}{t_0} \qquad (2)$$

H	…	Theoretical plate height
L	…	Length of column
N	…	Number of theoretical plates
Term A	…	Eddy diffusion (mobile phase)
Term B	…	Axial diffusion (mobile phase)
Term C	…	Mass transfer (stationary phase)
u	…	Linear velocity of mobile phase
C_e	…	Constant for Eddy diffusion
C_m	…	Constant for mass transfer (mobile phase)
C_d	…	Constant for axial diffusion (mobile phase)
C_{sm}	…	Constant for mass transfer (stationary phase)
D_m	…	Diffusion coefficient of analyte (mobile phase)
d_p	…	Particle size
t_0	…	Dead time of the column

The analysis of equation (1) reveals that a reduction of the particle size would increase the column efficiency. But a particle size reduction simultaneously means simultaneously a drastically rise of backpressure leading to a high pressure drop ($\Delta p \sim 1/d_p^2$), as one can see in equation (3).

A further benchmark for the separation efficiency of chromatographic columns is their number of theoretical plates calculated by equation (4).

Consequently, it is obvious from equation (4), that the number of theoretical plates is limited by the pressure drop. Thus, for conventional particle-packed columns, N can just reach 30 000 for HPLC, resp. 100 000 for CEC. [16]

$$\Delta p = \frac{\eta}{t_0 \cdot d_p^2 \cdot L^2} \cdot w \tag{3}$$

$$N = H \cdot L = \sqrt{\frac{t_0 \cdot \Delta p}{\eta} \cdot \frac{1}{E}} \tag{4}$$

H	…	Theoretical plate height
L	…	Length of column
N	…	Number of theoretical plates
u	…	Linear velocity of mobile phase
d_p	…	Particle size
E	…	Separation impedance
η	…	Viscosity of mobile phase
Δp	…	Pressure drop of the column
t_0	…	Dead time of the column
w	…	Flow resistance

By contrast to particle-packed columns, monolithic columns are casted in one piece. They consist of a "skeleton" either made of polymer or silica. This skeleton is interveined by macroscopic throughpores. Tanaka et al. [16] described it, as a "spongy system".
This porous structure results in a rather high permeability. It causes high column efficiencies combined with low backpressures.
The throughpore size distribution can be controlled by the addition of a certain amount of porogen within the preparation phase. The pore size control is mandatory, because the formed micropores (≤ 2 nm) in the structure of polymer monoliths reduce the efficiency. The reasons are size exclusion effects for small molecules and slow diffusive mass transfer.
Another drawback regarding monoliths made of polymers is their low mechanical stability and their volume change in different solvents.
All these disadvantages can be overcome by preparing monoliths on silica basis. These monoliths are based on alkoxysilanes. They can be prepared by the sol-gel process. Once prepared, they have a well-defined mesoporous and macroporous structure with an increased chemical and mechanical stability.
One major problem, however, is the strong shrinkage of silica monoliths during the drying phase. This is also the reason why silica based monoliths has to be cladded with polymer, preferable with polyetheretherketon (PEEK), before they can used as chromatographic columns for HPLC, for example. [15–17]

To avoid the PEEK cladding process, we cancel the drying step after the monolith preparation. Before drying only little shrinkage occurs, but we bear the risk of a reduced mechanical stability.

To get optimal column efficiencies, Rieux et al. [14] recommend keeping the domain size (pore size plus skeleton size) as smallest as possible.

On the other hand, too small pores interfere the mass transfer of analytes in and out of the pores (diffusion-limited mass transfer) and peak broadening occurs.
A high-efficient monolithic column should also exhibit the highest possible surface area with a branched system of homogenous and interconnected pores. Mesopores (between 2 to 50 nm) should also be above 20 nm to prevent peak broadening due to diffusion-limited mass transfer.
This through-pore and mesopore system corresponds to the void and pore system of particle-packed columns.
Commercially monolithic HPLC columns can be obtained from Merck. They are known as 'Chromolith' columns. [14, 15, 17]

A highly effective and modern kind of chromatography is electrochromatography (EC). Capillary electrochromatography (CEC) is based on the same principles as CAEC.
CEC uses small capillaries as column elements vaguely comparable to the mold of the CAEC column.
The flow through the column is caused by an electroosmotic flow (EOF), which is caused by polar groups attached to the wall in an electric field. The formed plug-flow only causes a marginally pressure drop and forms the basis for best performances. [7, 18]

For the preparation of monolithic capillary columns the glass walls have to be activated. It warrants that the monolithic material attaches covalently to the glass walls. Typically, this is made by rinsing the capillary with aqueous 1M sodium hydroxide solution. This process generates free silanol groups, to which silanes can bind and the shrinkage will be reduced. Thankfully, the generated voids are normally in the same scale like the throughpores.
This principle is only valid for small widths and can´t simple implemented for e.g. HPLC columns. Typical HPLC columns have larger gap widths and the shrinkage during the synthesis phase would generate larger voids. Hence, it is necessary to clad HPLC monoliths with a sealant, which is normally done with PEEK, as mentioned elsewhere. [14, 18]

The number of theoretical plates of monolithic CEC columns is 3-4 times higher than for HPLC columns. However, a functionalization with octadecylsilane (ODS) is required for RP properties of a silica based monolith. But the C18 moieties reduce the EOF, which results in slow separation times and low efficiencies. As a consequence functionalization groups have to be found for CEC columns that can either support the EOF and separate efficiently different molecules. [19]

3.2.2 Histidine-Affinity Chromatography

In the 80s, Kanoun et al. [4] found a new purification method for antibodies, referred to as "Histidine-affinity chromatography". His group has succeeded to purify IgG and Carboxypetidase Y using histidine, which was immobilized on a spacer arm. They could show that IgG bind optimally to histidine at low temperatures, when the pH of the buffer medium lies nears the immunoglobulin's pI.

A mixture of charge-transfer, ionic and hydrophobic interactions were made responsible for bonding. Desorption is effected by addition of sodium chloride to the buffer medium. [4]

Generally, affinity chromatography can be divided into two fields: biospecific ligand affinity chromatography and pseudo biospecific affinity ligand chromatography. An overview of the different types of affinity ligands is given in Fig. 5. [20]

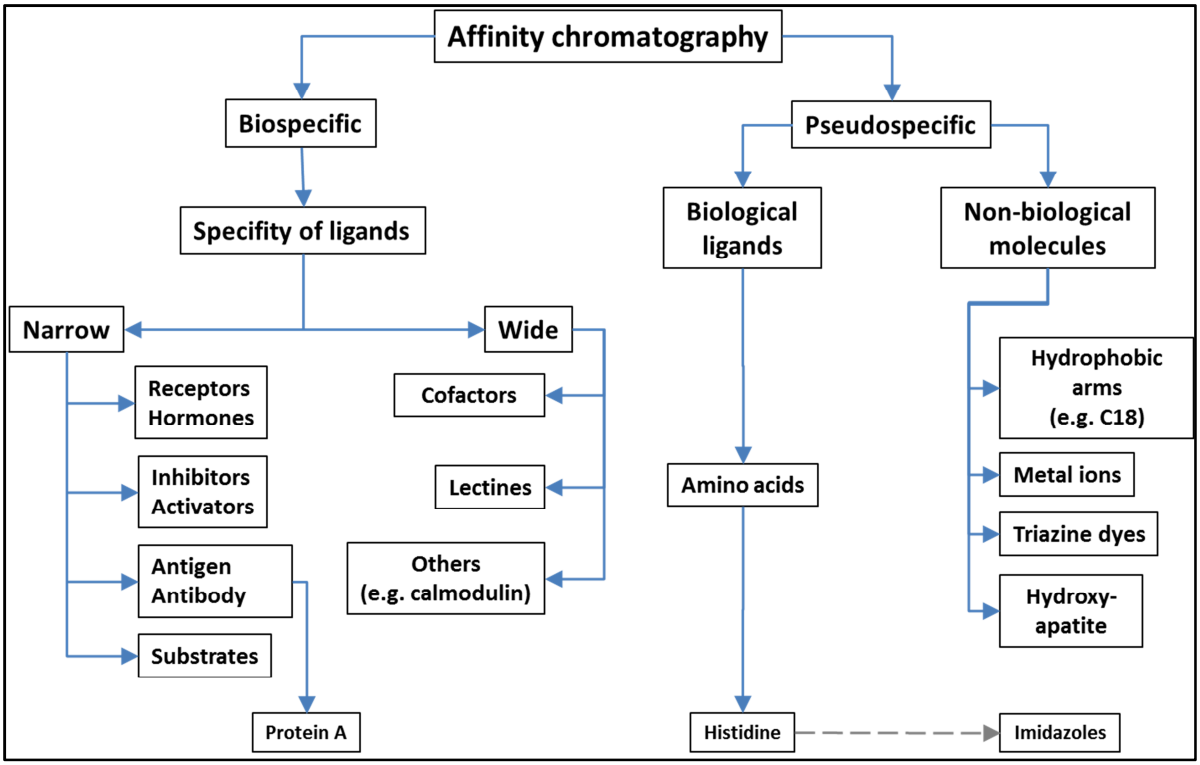

Fig. 5: Overview of chromatographic affinity ligands. Modified according to [20]

All affinity chromatography methods are based on adsorption and desorption effects. However, the mechanism can be completely different: electrostatic and hydrophobic interactions, coordination bonds, antigen-antibody interactions, hydrogen bonds and so on result in specific bonding activities.

In the case of protein A chromatography, interactions are caused by antigen-antibody reactions, whereas selective interactions in histidine affinity chromatography are obtained through a mixed mode of electrostatic and hydrophobic interactions. For the latter method the chromatographic conditions are important: ionic strength, pH, buffer additives and temperature control the selective adsorption and desorption of the analytes. Histidine ligands can interact with proteins by weak charge transfer through the carboxyl and amino groups and proton exchange due to the imidazole ring. Proton exchange, for example, happens, when the pH of the medium is near the pK of histidine and the pI of the protein. This is the case for IgG. Thus, the special bonding mechanism of IgG to histidine can be reduced to imidazole groups. A mixed mode of ion-pairing, hydrogen-bonding and charge-charge interactions between the imidazole nitrogen and IgG could be determined as bonding mechanism. Histidine as protein A binds to the Fc fragment of IgG. Carboxyl groups interfere these bonds. The imidazole nitrogen must be unprotonated for highest bonding effects, and the IgG molecule must have a positive charge.

Nevertheless, the bond strength is weak. But this can also be seen positive for high protein recovery.

The high capacity and reproducibility are good requirements for scale-up processes.

Desorption, in turn, occurs at high ionic strengths. For elution, the NaCl concentration can be increased. [20, 21]

A general comparison between histidine and protein A chromatography can be found in Table 1.

Table 1: Comparison between protein A and histidine affinity chromatography. Slightly modified according to [20]

Parameter	Protein A chromatography	Histidine affinity chromatography
Specificity	High	High (depends on adsorption conditions)
Strength of bonds (K1 values [l/g])	High (10^{-7}-10^{-15})	Low (10^{-2}-10^{-4})
Ease of desorption	Medium	Easy
Capacity	Low (0.1 to 1.0% ligand utilization)	Medium
Reuse and stability	Low (ligand fouling, ligand denaturation; cannot be cleaned with conc. NaOH)	High (cleanable with conc. NaOH)
Flexibility of a particular column matrix	Low	High
Cost	High	Low
Ligand leakage and toxicity of leaking ligand	Medium to High leakage / contamination problem	No leakage / nontoxic

Since there had not been a siloxane coupled to histidine commercially available for our purposes, we had to find an alternative precursor. An alternative ligand must fulfill the following requirements:

- Commercially available
- Nontoxic
- Covalently bound to triethyl orthosilicate
- Similar to histidines or imidazoles as possible

These requirements were found in one siloxane precursor: Triethoxy-3-(2-imidazolin-1-yl)propylsilane (IMEO) has an imidazoline ring (functional group) covalently attached to a silicone atom by a propyl chain, as one can see in Fig. 6.

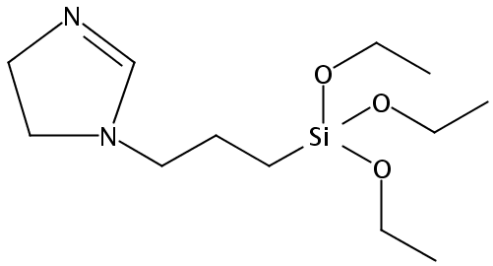

Fig. 6. Precursor for the imidazoline ligand (IMEO).

Anyhow, the imidazoline group features no aromatic system like imidazole and its pKa is far higher predicted at 11.3 [22] than that of imidazole.

Nevertheless, imidazolines and imidazoles bind similarly to IgG classes. A structural comparison of immobilized histidine and IMEO can be found in Fig. 7. [21, 23–25]

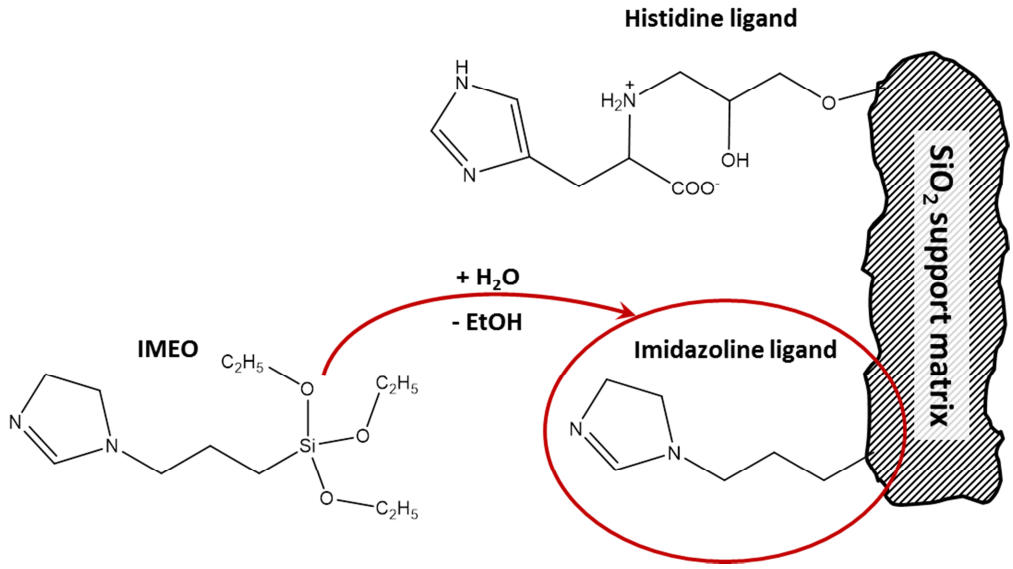

Fig. 7: Structures of the immobilized pseudoaffinity ligands, histidine and imidazoline. IMEO represents the precursor for the imidazoline ligand on silica supports.

Selective interactions of IMEO with IgG could be shown by Öztürk et al. [24, 25]. Her group covered magnetic beads and organic polymer nanoparticles with IMEO, respectively. They could adsorb IgG molecules with both applications directly out of crude human serum samples diluted in simple phosphate buffer.

The elution was done with a chaotropic substance (KSCN) in phosphate buffer. The purity of the isolated IgG antibodies was more than 95% with a high bonding capacity from ca. 0.1 (magnetic beads) to 1 (nanoparticles) gram IgG per gram adsorptive. Both applications also exhibit a low bonding affinity to albumin. Best adsorption could be reached at a pH of 7 and a NaCl concentration of 0.01 to 0.5 M. Hence, optimal IgG adsorption occurs, when the pH of the buffer medium lies around the pI of IgG. However, a rise of ionic strength decreases drastically the amount of bound IgG.

Özturk et al. assume a 'mixed mode' of interactions, such as hydrophobic and electrostatic interactions plus hydrogen bonding, as mechanism for the IMEO-IgG bonding. [24, 25]

3.3 Silica based Monoliths

3.3.1 Principles

Monolithic columns are defined as "one single piece of an adsorbent material (porous silica or polymer) that fills the entire length and width of the column". They have two interconnected types of pores:

- Macro- or throughpores (>50 nm)
- Mesopores (2-50 nm)

Macropores are in the dimension of micrometers and forms the void within the column, where the fluid can flow through. They are responsible for 80% of the total porosity.
Mesopores (and undesirable micropores), however, are very smaller, in the scale of nanometers. They contribute the main part to the surface area.
The literature differentiates between through-pores and skeleton, whereas the latter stands for the silica-backbone, which pervades the whole column and is comparable to the particle size in particle-packed columns. Both, through-pores and skeleton should be as small as possible for optimal separation efficiency. For all chromatographic columns an increase of separation efficiency is always related to an increase of pressure.
Size ratios between through-pores and skeleton are normally in microscopic scale and range from 1.2 to 4. For comparison, particle-packed columns have size ratios of 0.25-0.4 between pores and particles.
The skeleton and the domain size are other critical parameters. The skeleton size, for example, is crucial for the column´s mechanical stability. The domain size, however, is defined by the skeleton size plus adjacent throughpores. [14, 18, 26, 27]

A scheme of an IMEO-functionalized monolith is represented in Fig. 8.

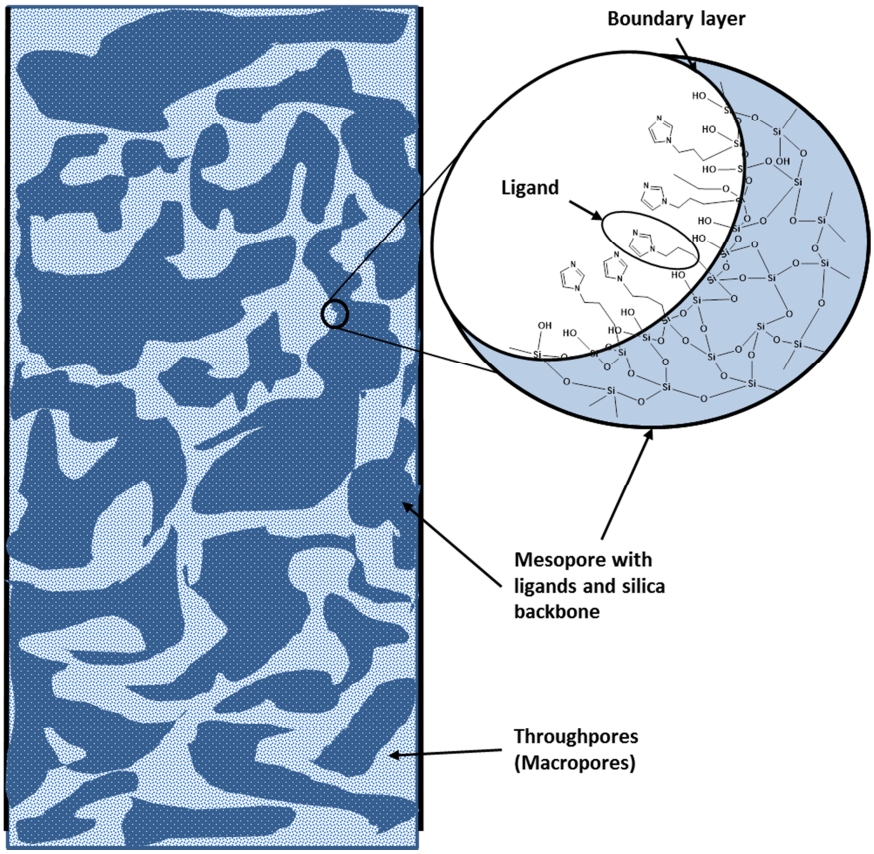

Fig. 8: Structure of an IMEO-functionalized monolithic column.

Benefits of monolithic rods compared to particle-packed columns are the higher permeability and the lower backpressure, which results in a higher efficiency. Furthermore, monoliths don´t need expensive frits at the outlets. And the use of silica instead of organic polymers for monolith preparation gives the advantages of higher mechanical, chemical and thermal stability. [26, 28–30]

Drawbacks concern the preparation and the reproducibility of monoliths. In contrast to large silica particle batches, monolithic columns have to be prepared one by one. In addition, the column properties like permeability, pore size and surface area vary mainly with the silica overall structures and its preparation conditions.

For conventional columns the packing of the column is prevalently critical for reproducibility. Therefore, the preparation of monoliths needs a more intensive control at least for pore size distribution, thickness of the skeleton and external porosity.

In practice, the efficiency of monolithic columns, however, suffers from heterogeneous pore structures.

Furthermore, the pore size distribution is large because of two major phenomena: One of them is the "deformation of coarsening gel domains". The deformation is caused by tensions

between the domains triggered by the volume shrinkage just after the gelation. This is especially relevant for monoliths with high pore volume and skeleton size. The second phenomenon is the "inherent heterogeneity" of the silica skeleton. This feature takes shape in monolithic structures with sub-micro silica domains. In that case, the "roughness" of the silica network influences dominantly the domain volume. A further effect, the so-called "spinodal decomposition" besides forms small-sized pores. [18]

A list of characteristic properties of silica based monoliths is given in Table 2.

Table 2: Properties of typical monolithic columns.

	Dimension	Comment	Literature
Size of mesopores	10-25 nm	Depends on pH, temp. and reaction time; Small mesopores result in high surface area, high capacity and peak broadening	[14, 16]
Size of macropores	1-8 µm		[14, 16]
Skeleton size	1-2 µm		[18]
External porosity	65–80%	In capillary columns higher than in conventional columns	[18]
Total porosity	≥ 80%		[18, 27]
Surface area	ca. 300 m^2/g		[16]
Size ratio of macropores to skeleton	≤ 4		[14]
Density	≤ 80 kg/m^3	Value for aerogels	[31]

Applications for silica-based monolithic material are almost predominantly restricted to chromatography purposes, because of the proposed higher efficiency and lower pressure drops of monolithic columns in contrast to particle-packed columns. Moreover, monoliths made of silica don´t swell or shrink in solvents contrary to organic polymer columns. Functionalization of silica rods make them useful for various kinds of chromatography forms: above all, RP-, electro- and ion-exchange chromatography.

Such a functionalization can be carried out with various moieties: for example with OH, COOH, $^{+}NR_3$; NR_2, and $CONH_2$ groups. One requirement for functionalization is that the functional groups do not react with the groups of the alkoxysilane. [14, 18]

3.3.2 Preparation of silica-based monoliths

A monolithic column can be prepared either by in-situ polymerization of organic polymers or by preparation from alkoxylsilanes via sol-gel process.
In this work, we used tetraalkoxysilanes together with functionalized trialkoxysilanes in a one-pot synthesis to prepare silica based columns. Trialkoxysilanes provide a facility to implement specific functional groups in the silica backbone. As a consequence, the functional groups are covalently bonded to the silicium atom by hydrolytically stable Si-C bond.
The one-pot synthesis has the advantages over postfunctionalization methods that it minimizes the preparation steps and results in higher loadings. It features a more homogenous distribution of functional groups over the whole column and keeps the initial pore structure intact. [14, 18, 26, 32]

A list of various sol-gel preparations and their compositions can be found in a review of Soleimani Dorcheh and Abbasi [27] and the basics for the preparation of silica-based monoliths formed out of alkoxysilanes via sol-gel process is described in a review of Hench and West [31].

3.3.2.1 The Sol-gel process

Sols are defined as "dispersions of colloidal particles in a liquid", whereas the size of the particles can range from 1 to 100 nm.
A gel, however, is an interconnected inelastic network made of polymeric chains longer than a micrometer and submicrometer-sized pores. There are several classification systems for gels. One of them classifies gels in aerogels and xerogels [15, 31]:

- Aerogels are especially low-dense ($\leq$80 kg/m^3), porous (pore volume >98%) and can be produced by hypercritical point drying, which requires complex and expensive equipment
- Xerogels are the more common gels. They can be produced by removing the pore liquid through drying at ambient atmosphere. Xerogels are also called alcogels, when the pores are filled with alcohol.

In this work, we want to use alcogels to prepare functionalized monoliths.

In general, there are three methods to generate silica based monoliths [27, 31]:

1. Gelation of solute colloidal powders
2. Hydrolysis and polycondensation of precursors with subsequent hypercritical drying
3. Hydrolysis and polycondensation of alkoxide precursors, mainly alkoxysilanes like TEOS or TMOS with subsequent aging and drying in mild conditions (ambient atmosphere)

Since we exclusively prepared monoliths by method 3 (Hydrolysis and polycondensation of alkoxysilanes), the following remarks are only referred to this method, unless stated otherwise.

Method 3 was theoretically divided into seven process steps on closer inspection by Hench [31]. In this study, a previous step (Step 0) was introduced:

Step 0: Activation of the glass walls (for capillaries and small molds)
Step 1: Mixing
Step 2: Casting
Step 3: Gelation
Step 4: Aging
Step 5: Drying
Step 6: Dehydration or Stabilization
Step 7: Densification

Critical hereby is the drying process (Step 5) because of the intense capillary pressure inside the pores. The pressure results in a massive shrinkage followed by cracks in the still weak monolith structure. [31]
To avoid this shrinkage we have canceled the drying process. Instead, we have kept the prepared monoliths immersed in a storage buffer after aging.
The prepared monoliths are intended for chromatography purposes only and keep immersed at all times. Therefore, the steps Drying (Step 5), Dehydration (Step 6) and Densification (Step 7) were considered as not unconditionally required. But for the sake of completeness, all steps are described in detail:

Step 0: Pretreatment of the glass walls

For capillaries and small molds the glass walls were typically cleaned and activated by incubating them in aqueous sodium hydroxide solutions. This step improves the adhesion of the gel to the glass wall by generating more covalent siloxane bonds (Si-O-Si) between gel and wall. [18, 29]

Step 1: Mixing (Hydrolysis and Condensation reactions)

A sol is formed through hydrolysis and polycondensation reactions, when alkoxysilanes are mixed with water. A simplified reaction model for this gel forming process is shown in Fig. 9. [31]

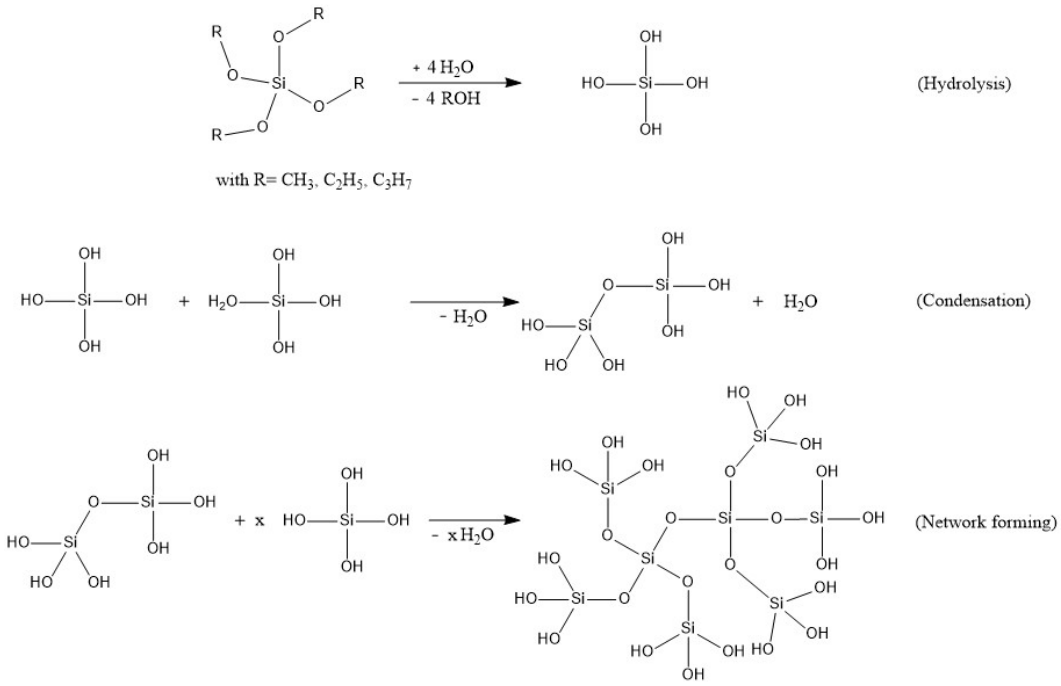

Fig. 9: Hydrolysis and Condensation reactions of alkoxysilanes. Modified after [31]

Hydrolysis and condensation are responsible for the formation of the prospective gel network. Through adding a catalytic amount of acid or base to the mixture of water and alkoxysilanes, the latter will be hydrolyzed and forms alcoholic molecules as byproduct. Ideally, the formed alcohol acts as additional solvent. In consequence, silanol groups of the hydrolysated precursors condensate either with other silanol groups or with other alkoxysilane molecules to form a colloidal solution (sol), firstly. This sol transmutes to a complex gel network through continued (poly)condensation reactions. [29]

The ongoing processes form a gel network with nanometer-sized pores filled with water and alcohol. The formed pore size can be enlarged by thermal treatment or chemical washings. The growth of the silica backbone is mainly influenced by the rates of hydrolysis (k_H) and condensation (k_C). These rates depend above all on following parameters [31]:

- Reaction temperature
- Type and concentration of acid or base

- Solvent
- Type and amount of alkoxide precursor
- Molar ratio of water to precursor (labelled as R ratio according to [31])
- Pressure

In the process, slow hydrolysis together with fast condensation favors large, bulky and highly-branched structures.

Generally, the hydrolysis rate increases with decreasing pH in acidic media and with decreasing pOH in basic media, respectively. Typically rates of hydrolysis are $9 \cdot 10^{2}$ mol L^{-1} s^{-1} $[H^{+}]^{-1}$ in acidic media and $4 \cdot 10^{-2}$ mol L^{-1} s^{-1} $[OH^{-}]^{-1}$ in basic media, respectively. [31]

The correlation of hydrolysis and condensation of alkoxysilanes with the pH of the reaction mixture can be found in Fig. 10.

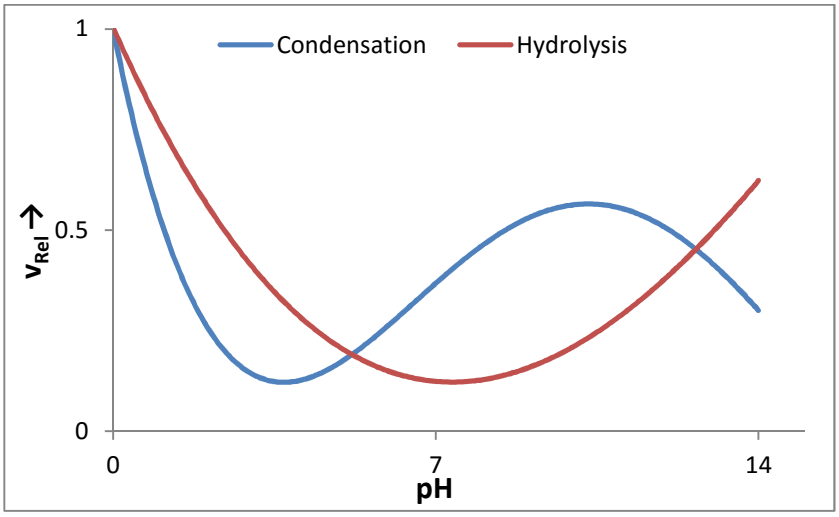

Fig. 10: Relative hydrolysis and condensation rates vs pH of the reaction mixture. [27]

The slowest condensation rates can be found at the isoelectrical point of the precursors, The IEP of silica can be found at a pH of 2 to 3.

Besides, the hydrolysis can be promoted through sonication in acidic media. [15, 16]

Step 2: Casting

As a next step, the mixture had to be filled in a mold. This must happen before the gel can solidify. Typically molds are either in the size of HPCL columns or fused-silica capillaries. The length of classical monolithic HPLC columns is limited to 25 cm because of the deformation of the rods, otherwise. [18, 31]

For CAEC two different gap widths are used: 4 and 10 mm. But because of a better heat exchange a gap width of 10 mm has become prevalent. [7]

Step 3: Gelation

With continued condensation reactions, network-like structures are slowly formed. Simultaneously, the viscosity also increases. The sol is transformed to a gel, when it reacts elastically to stress. The required time for this stiffening effect is called "gelation time" (t_{gel}). This gelation time is among others dependent on the size of the mold and can last from seconds to days, even months are possible. During gelation the material changes its viscosity characteristics from Newtonian to viscoelastic. [15, 27, 29, 31]

In this study, the gelation time is defined as the time, when the reaction mixture in the mold visually stops to flow.

A well-known process related to gel-formation is the already mentioned effect of "spinodal decomposition". Hereby, local phase separations occur because of minute concentration fluctuations during the reaction. Because of the competition of phase separation and gel formation an open pore network can be generated [16, 18]

Critical parameters for the gelation time and the corresponding phase separation are mainly type and concentration of the starting components and the pH of the reaction mixture. At low pH the hydrolysis may superimpose over condensation, which prolongs the gelation time. In addition, small throughpores will be developed. [14]

Step 4: Aging

Aging labels the phase, in which molecule strands have already been formed, but reactions continue long after the gelation. Three reactions, polycondensation, syneresis and coarsening, dominate this phase and can be used to increase either the structure´s stability or the pore size. Unfortunately, an increase in stability is also accompanied by a decrease of surface area.

When aging starts, a fragile network immersed in liquid exists. Molecules consequently aggregate, dissociate and reprecipitate. To a certain extent, this effect can be interpreted as a maturation process, which is called Oswald ripening. In this step, the amount of bridging bonds rises and results in higher structure stability. But simultaneously, this process also decreases the porosity. Such a coarsening changes the average pore size of

small particles. A critical factor for Oswald ripening is the pH of the mixture. But in contrast to gelation, it is independent of the type of the acid or base [31].
Continued polycondensation reactions, however, strengthen the integrity of the gel network. They can be influenced by temperature. [15, 31, 33]

Syneresis describes the shrinkage effect of the gel accompanied by an expulsion of the pore´s liquid. It is assumed that syneresis is caused by newly formed bridging bonds, which contract the network. The effect of syneresis has its minimum at the gel´s IEP (for silica gels the IEP is 2). Besides of the pH, syneresis can be influenced by time, temperature, solvent and concentration of the available silanol groups. A linear shrinkage by syneresis during the gelation and aging steps can be supposed with 10%. [14, 27, 31]

According to [27] it is recommended to age the gel in solutions with a pH of 3.5 at 60°C for 24 h.
Ethanol-water washes increase the permeability by "dissolution reprecipitation processes" and immersing in mother liquor strengths the silica network, but decreases the permeability.
On the other hand washes in solvents with pH >8 turn can turn micropore structures into mesoporous ones.
In other cases, aqueous ammonium hydroxide solutions and elevated temperatures are used for postreatment to fit the size of the mesopores. [14–16, 27, 33]

Step 5: Drying

As mentioned, drying (Step 5), dehydration (Phase 6) and densification (Step 7) are not required for this study, but they are shortly outlined here for the sake of completeness.

During drying the total pore liquid will be removed. This is a very critical step because of high capillary pressures formed inside the pores. These pressures can result in massive shrinkage and cracking of the monoliths. The prevalent capillary stress inside the pores can be calculated by (5) and depends on specific surface energy, contact angle of the interface and the pore radius [31]:

$$\Delta p = 2 \cdot \gamma \cdot \cos(\theta) \cdot \frac{1}{r} \qquad (5)$$

Δp	…	Capillary stress [N/m²]
γ	…	Specific surface energy [J/m²]
θ	…	Contact angle [°]
r	…	Pore radius [m]

As can be seen from (5), shrinkage and cracking can be reduced by a reduction of specific surface energy or surface tension, respectively. This can be achieved either by adding surfactants to the reaction mixture, by hypercritical evaporation or by controlling k_H and k_C for a pore size distribution as monodisperse as possible. [31]

Generally, drying is divided in three stages, whereas stage 1 is separated from stage 2 by the so-called "leatherhard point".
Critical parameters in this step are gel strength, the pore size distribution and the drying solvent. Thus, a careful choice of the drying solvent can reduce the probability of cracks, for example: In [14] isobutanol, 2-pentanol or isooctane is suggested for this purpose.
The pore size, however, shouldn´t come below 20 nm. Since smaller pores have to withstand extremely high pressures during the drying process. [15, 15, 31]

Common drying methods to obtain aerogels are Supercritical drying (SCD), Ambient pressure drying and Freeze drying. [27]

Step 6: Stabilization

Stabilization is required as pretreatment for the preparation of so called "type VI gelsils", which are porous transparent glasses used as optical material.
The task of this step is to remove the remaining silanol bonds from the surface of the monolithic network via chemical and thermal stabilization. [31]

Step 7: Densification

Densification (final phase) of the gel network takes place at temperatures above 1000°C. Through this process the pores remove and an amorphous dense fused-silica material is emerged. It is critical to get rid of all pores. Otherwise, the glasses become opaque and shady. [31, 34]

3.3.3 Substantials for silica-based monoliths

Hereafter, the principal constituents for the preparation of silica-based monoliths will be presented and explained.

3.3.3.1 Precursors (Tetraalkoxysilanes)

The common used alkoxysilanes are tetramethylsilane (TMOS) and tetraethylsilane (TEOS). In combination with water a gelation starts in acidic or basic conditions, typically within a few days. This process is driven by hydrolysis and condensation reactions as in Fig. 9 described.

Whereby the hydrolysis rate is affected (decreasing) by the (increasing) length of the precursor´s alkoxy chain.
In this context, a use of TMOS can improve the pore size distribution and increases the surface area. Nevertheless, TMOS is forming methanol as byproduct during the reaction, which is highly toxic. Because of this high toxicity, we have avoided the use of TMOS. As compensation, we preferred TEOS, which only generates ethanol as byproduct and additionally lowers the hydrolysis rate. [15, 15, 27, 31]

The gelation time of TEOS systems shows a minimum at a pH of 3. Gel networks can only be found under acidic conditions, whereas droplets and beads are mainly formed under basic conditions.
Furthermore, an intensified formation of beads was observed with high water and catalyst concentrations in basic media.
Generally, all alkoxysilane precursors are low soluble in water and need solvents like alcohols for preparing a solution as seen in Fig. 11. [27, 29]

3.3.3.2 Solvents

As mentioned above, silicone alkoxides are barely soluble in water (Fig. 11). Hence, for preparation of solutions a solvent is required. Alcohols are common, but also *N,N*-dimethylformamid (DMF), acetonitrile (ACN) or even ionic liquids are in use.
Solvents can affect hydrolysis reactions as an example in the following order:

ACN>MeOH>DMF

Generally, alcohols reduce the hydrolysis rate, but also alcoholysis can occur. Alcoholysis causes that formed siloxane bonds were resolved. This process affects the formation of the gel

network negatively. To avoid this effect, an ethanol concentration of 3.5 M was recommended in aqueous systems by Constantin et al. [29]. [14, 27, 31]

Regarding this, a ternary phase diagram of TEOS-Alcohol-Water is shown in Fig. 11.
For optimal porous monoliths the alkoxysilane concentration in alcohol should be located within 5 to 10%. [15]

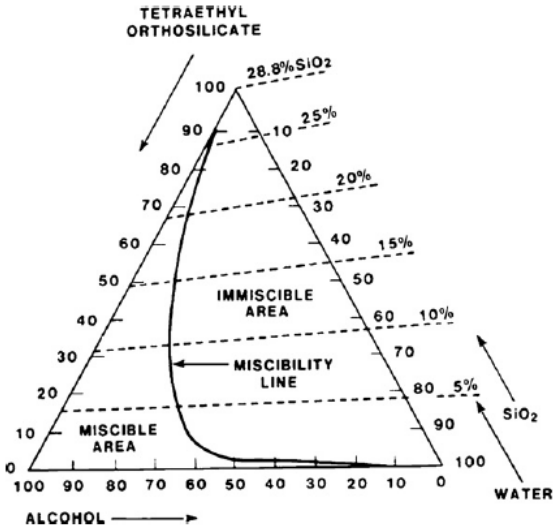

Fig. 11: Ternary phase diagram of TEOS-alcohol-water. [27]

3.3.3.3 Water

One of the most critical variables for the gel preparation is the ratio of water to alkoxysilane, expressed as R ratio.
High R ratios are required in acidic media to enhance k_C, because here hydrolysis dominates over condensation. According to [29] the minimum amount of water can be calculated by (6).

$$R_{min} = \frac{1}{2} \cdot \frac{(4m + 3n)}{(m + n)} \tag{6}$$

R_{min}	…	Minimum molar ratio of water to precursor [-]
m	…	Molar amount of tetraalkoxysilanes [mol]
n	…	Molar amount of trialkoxysilanes [mol]

The minimum ratio R_{min} is required for maximal reaction rates, with m related to the moles of tetraalkoxysilanes and n related to moles of ligand-bonded alkoxysilanes [29]. Salamani Dorcheh and Abbasi [27] have stated this R ratio to a minimum of 2 for total hydrolysis. Although, R ratios over 2 apparently decrease the hydrolysis rate as in [31] mentioned. In

general, however, a high R ratio seems to decrease the gelation time [27] and R ratios above 2 are apparently necessary for complete hydrolysis.
Elsewhere [15], aerogels with high porosities were achieved with R ratios between 2 to 5.

3.3.3.4 Acids and bases

The formed structures during the gelation depend critically on the type of (hydrolysis) catalysts: Acid forms mainly a linear network, whereas alkaline based catalysts generate a branched network of beads and particles. It is not only the pH, which affects the gelation, but also the type of the acid or base. Small addition of hydrogen chloride, for example, accelerates the hydrolysis immensely, whereas the same amount of acetic acid barely has an effect on the hydrolysis. [31]
In conflict with this statement, Soleimani Dorcheh and Abbasi [27] predicted longer gelation times in low pH solutions for acidic conditions. They stated a prolonged gelation time by the use of hydrogen chloride (HCl) instead of acetic acid (HAc).

Typical acidic catalysts are hydrogen fluoride (HF), acetic and formic acid (FA). A typical basic catalyst is ammonium hydroxide (NH_4OH). [27, 31]

3.3.3.5 Porogens and Drying additives

Porogens are structure-directing agents that directly affect the pore size distribution of the monolith. They act as "throuph-pore templates" [27] and solubilizer [15]. Their task is to initiate microscale phase separations [18].
With their help silica-based monoliths can be produced with both well-defined macroporous and mesoporous structures.
Typical porogens are Polyethylene glycols (PEG, also called PEO for Mw >35 000 g/mol) or Cetyltrimethylammoniumbromid (CTAB).
CTAB is a cationic detergent. It can improve permeability and structure homogeneity of a silica-based monolith. Thereby, it increases the amount of negatively charged silanol groups on the silica interfaces, which is an undesirable effect for the IMEO-functionalized monoliths in this study.
For that reason we have given preference to PEG as used porogen for monoliths in this study. PEG is used in most cases for preparing chromatographic monoliths and can, in turn, either strengthen the silica network in low concentrations or weaken it in high concentrations. The

molecular weight is also important: A high molecular weight of the PEG corresponds to large pore structures. [10–12, 14, 15, 28, 35]

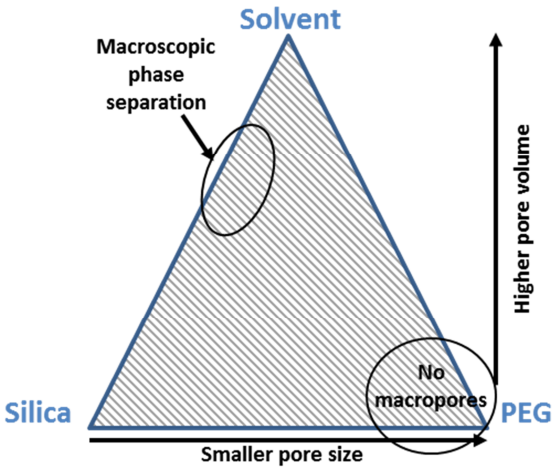

Fig. 12: Relationship of Silica-PEG-solvent mixtures for monolith preparations. [16]

Fig. 12 displays the relations of silica to PEG and solvent: As can be seen, gels with high amount of silica generate smaller pores sizes and more stable skeletons right up to dense materials without macropores.

Besides, higher PEG amounts are reflected in higher pore volumes. These silica-PEG interactions are explained by formed hydrogen bonds between silanols and glycols, which lower the solubility and support the precipitation. This effect finds expression in a deferred phase separation and smaller domain sizes.

Attention is to pay on the ratio between silica and solvent. Low concentrations of silica in high concentrations of solvent can cause macroscopic phase separation during the gelation. [14, 16, 18]

Additives, which minimize drying stresses, are labelled as "Drying Control Chemical Additive" (DCCA). For that purpose, an often used and appropriate substance is glycerol: It can reduce shrinkage and increase transparency at the same time. [36]

3.3.3.6 Functionalized silanes (Trialkoxysilanes)

It is common to prepare silica gels from mixtures of different alkoxysilanes in copolymerization processes. In many cases, the gel contains tetraalkoxysilanes and trialkoxysilanes mixed together. Trialkoxysilanes have an additional functional moiety (ligand), which is crucial for the preparation of functionalized chromatographic monoliths. In this

study a 1-propyl-2-imidazoline group is used for functionalization. This group had already shown specific interactions with antibodies via electrostatic effects in the past [24, 25].
Ligands should be especially found on the surface of monoliths, where they interact with specific target molecules in the mobile phase. Typical groups are octyl chains (C8), amino (NH2) or mercapto (SH) moieties linked over a spacer (mostly alkyl chains) to the silanes. The covalent bonds of the functional groups to the silicium atom defend them from hydrolysis. [9, 12, 27, 35]
Constantin et al. [29] found a maximal mixing ratio of 7:3 for TEOS and functionalized triethoxysilane (C_8-TEOS). Above this ratio a phase separation was observed. Indeed, they were unable to prepare a monolith made of pure triethoxysilanes. They assumed that this would be the result of steric hindrance of the ligand.

Amines intensely accelerate the gelation time of monoliths. Hence, a short gelation time can be supposed for IMEO-functionalized monoliths. [9, 35]

Functionalized mesoporous material is also very helpful as support for catalysts. The high surface area of monoliths can be loaded with catalytic material and applied as plug flow tube reactor (PFTR). [35, 37]
An example for IMEO-functionalized mesoporous silica for catalytic purposes can be found in the work of Hruby and Shanks [38]. They prepared this kind of silica as solid-phase catalyst for the Knoevenagel condensation.
Some others, again, prepared mesoporous silica particles and monoliths functionalized with aminopropyl groups by mixing 3-aminopropyltriethoxysilane (APTES) to TEOS. [9, 35, 39]

3.3.4 Alternative applications

A commercial monolithic HPLC column is available from Merck, known as Chromolith [18], as already mentioned.
Moreover, it is also possible to prepare monolithic glasses and low-density aerogels by sol-gel processes. Monolithic silica glasses are characterized by outstanding transparency to deep-ultraviolet and used for all kind of optical components. [34]
Silica aerogels on the contrary have unique properties, extreme low density, enormous surface area and porosities of over 80%. For this class of material numerous applications are proposed for prospective applications like storage media for liquid rocket propellants, thermal

superinsulators or as catalytic supports. But at the moment the range of commercial available products are rather negligible. [40]

4 PRACTICAL WORK

4.1 IMEO-monoliths

First of all, it was necessary to produce a silica based monolith with imidazoline moieties on the surface. The functionalized monolith had to feature the following characteristics for (electro)chromatographic purposes:

- Covalent bonds to the glass wall
- Permeable for aqueous solutions
- Chemically and mechanically stable
- Gelation within an acceptable time range (at a max of one day)
- Easy to prepare
- Nontoxic

Because of the characteristics of a monolith, the gelation had to be directly in the terminal mold, where it could bind covalently to the glass wall (see also chapter 3.3.2., p. 20).
To get an appropriate monolith various batches with different compositions and conditions were checked for their (1) appearance, (2) gelation time and (3) permeability (further details see below). All these tests were performed with small monolith batches filled in conventional activated Pasteur glass pipettes. A table of all batches, their components and conditions is listed in the appendix, pp. 78.
A general preparation of imidazoline functionalized monoliths can be found below, on pp. 33.

4.1.1 IMEO-monolith preparation

In general, the monolith synthesis consisted of three steps and ended after the washing phase (aging). The batches can be grouped in different classes. There were two main classes: Type A (with PEG and PrOH) and type B (CTAB and EtOH). The two digits after the code letter classify the used amount of porogen.

Step 0: Activation of the glass walls

An activation of the glass wall cleans the surface from dust, removes electrostatically bound interfering molecules and activates terminal hydroxyl groups of the glass.
To begin with, the glass templates were washed with EtOH and filled with 1M hydrochloride solution subsequently. The solution was incubated in the template at 40°C for 30 min. Then it

was washed with ultrapure water (UPW) until the wash solution was pH neutral. Afterwards, the template was filled with 1M sodium hydroxide and incubated again at 40°C for one hour. The solution was removed and the template was washed again with UPW until pH neutral. The purified glass was dried in an oven at 100°C for at least two hours and sealed with paraffin film until use.

Step 1: Activation of the TEOS mixture (Hydrolysis)

TEOS was prehydrolysed in acidic media before reacting with IMEO, unless stated otherwise. For all experiments one equivalent (equiv.) of TEOS was solved in an alcohol (PrOH, EtOH or MeOH). The solution was mixed with various equiv. of UPW, porogen (PEG or CTAB) and acid. The mixture was stirred at 60°C in a closed vessel (round-bottom flask) for at least 30min until complete activation. Then the reaction mixture was cooled in an ice bath for 5 min and finally brought to ambient temperature.

(Note: One equivalent is exclusively related to the molecular amount of used tetraalkoxysilane precursor.)

Step 2: Filling, Gelation and Aging

Just before the filling process, IMEO was added under stirring to the reaction mixture and immediately filled in the final (glass) template or mold. The time was measured from addition of IMEO to gelation (gelation time). After gelation, the test specimen was sealed and left in mother liquor overnight at ambient temperature (aging phase).

Step 3: Remove of remaining reagents

To remove educts, byproducts and porogen, the monolith had to be washed with an appropriate washing solution (EtOH or water) until the washing solution was clear. The drop rate for the permeability test was determined in this phase, when the wash solution was clear.

4.1.2 Quality control of prepared monolith batches

Different batches of various components and compositions were at first prepared in Pasteur pipettes and tested for monolithic characteristics. These characteristics were tested in three test procedures: (1) Appearance, (2) Gelation time and (3) Permeability.

(1) Appearance

The appearance was either transparent, milky or a multi-phase system. A milky appearance was assumed as porous material. The test was done via visual inspection of the prepared batches after aging and washing. Additionally, it was also paid attention to the homogenous structure of the monolith.

A figure of several monolith batches with different appearances and possible defects is presented in Fig. 13.

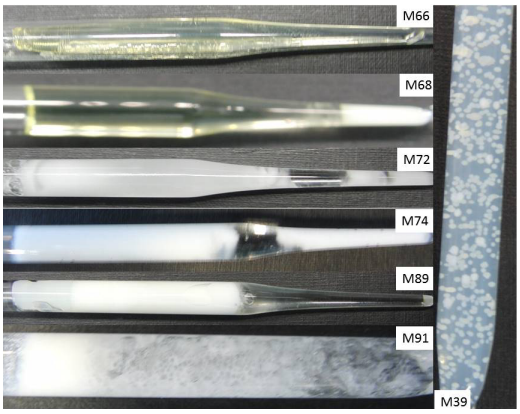

Fig. 13: Defects of IMEO-monoliths. Transparent gel (M66), Phase separation (M68), Bad spots and non-uniform (M72, M74, M89, M91), enclosed PEG particles in a silica gel block (M39)

(2) Gelation time

The gelation time determined the required time for the reaction mixture to solidify (gelation). Afterwards, a reforming or refilling is not possible anymore. For the test, the test specimen was swiveled. It was measured the time, when the batch stopped flowing. For processing, the gelation time had to be higher than at least two minutes but within a day.

(3) Permeability

The permeability was required for further processing, that the monolith could be washed with aqueous solvent mixtures for purification from reagents and byproducts. Moreover permeability was required to ensure an acceptable flow rate for subsequent chromatographic tests.

Permeability was simply tested during the wash phase by adding eluent on the top of the monolith and measuring the number of drops within one minute (drop rate). A drop rate higher than 0.3 drops per minute was decided as acceptable. If the eluent rinsed through without forming drops, the result was evaluated as 'Rinse through'. In this case, no contact between glass wall and monolith was supposed.

For visualization, a whole monolith was dyed with methyl red in Fig. 14. The monolith was dyed homogenously. Consequently the monolith had to exhibit an interconnected porous system.

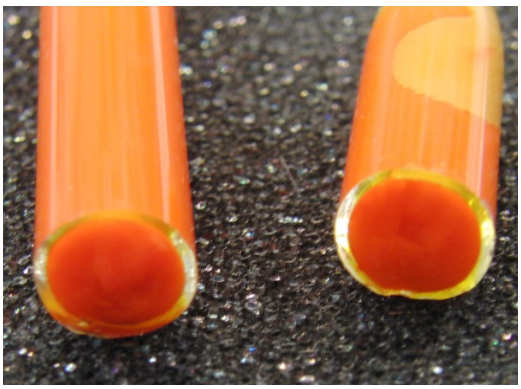

Fig. 14: Methyl red stained IMEO-monolith.

Acceptable criteria have been set as follows in detail:

(1) Gelation: 2 min to 5 hours
(2) Appearance: uniform, milky and homogenous with no phase separation or bad spots
(3) Permeability for water and EtOH: 0.3 drops/min to 120 drops/min (no 'Rinse through')

Table 3 lists a selection of used monolith batch components with their measured concentration range and the valid range within acceptable monoliths could be prepared.
However, a majority of all batches have failed in one of the three quality controls: From 91 tested monolith batches have fulfilled 27 batches the criteria listed above.

Table 3: Overview of selected components for the IMEO-monolith synthesis and their valid range for appropriate IMEO functionalized monoliths.

Components	Measured Conc. Range [equiv.]	Valid Conc. Range [equiv.]	Notes
Silica precursor			27 of 91 prepared batches fulfilled the criteria *
TEOS	1 equiv. was from 2 to 36 mmol		
Solvent			One equivalent is related to the molar quantity of used TEOS for each batch. *
EtOH	6-10	6-10	
MeOH	10-11	n/a	
PrOH	4-31	5-10	
DMF	10	n/a	With HCl the monolithic appearance tends more to transparent form *
Porogen			
CTAB	0.04-0.1	n/a	A pH different from 4 apparently weakens the monolithic structure and causes bad spots. *
PEG300	$2\cdot10^{-3}$-$3\cdot10^{-3}$	n/a	
PEG6000	$1\cdot10^{-3}$-0.05	0.003-0.5	
Acid / Base (for hydrolysis)			In continuative experiments catalyst and water were replaced by pH buffer. *
HCl	$5\cdot10^{-3}$-0.01	n/a	
HAc	$3\cdot10^{-4}$-0.2	$3\cdot10^{-4}$-0.1	
H3PO4	0.01	n/a	
HNO3	0.01	n/a	IMEO influences the gelation time and weakens the monolithic structure up to liquefaction of the batch.
NaOH	0.01	n/a	
Formic Acid	0.1	n/a	
Aqueous component			
Water	1.5-43	1.5-14	
Buffer (pH 3-12)	3-43	3-14 (pH 4)	
Ligand			
IMEO	0.1-25	0.5	

Note: The measured conc. Range can vary strongly within a component group. When the criteria were not fulfilled with this component in a few first trials, no further tests were conducted with the respective component.

The low number of acceptable monoliths is attributed to complicate interactions of each reagent, which prevents a prediction of the batch properties. On the other hand IMEO had to be applied in high concentrations for good functionalization. But at the same time, IMEO extremely shortens the gelation time as well as weakens the monolithic structure.

Table 3 shows that appropriate IMEO-monoliths based on TEOS could only be obtained by the use of PEG_{6000} (porogen) and EtOH resp. PrOH (solvent) with acetic acid or acetate buffer (25mM, pH 4) for hydrolysis.

From all tested IMEO concentrations 0.5 equiv. of IMEO seemed as a good compromise for both high ligand density and high functionalization.

Consequently, further chromatographic and adsorptive tests were performed with IMEO-monoliths based on these components mentioned above. The composition of the two main IMEO-monolith systems for further experiments is listed in Table 4. The two IMEO-monolith compositions are grouped in monolith type A and monolith type B. Type A was the most promising monolith candidate and type B was considered as an alternative. The number after the code letter divided by 1000 defines the equiv. of porogen.

Type A monoliths were prepared from TEOS, PEG_{6000}, PrOH, HAc, water and IMEO if not stated otherwise. Within the development water and acetic acid was replaced by an acetate buffer (25mM, pH 4).

For the preparation of type B monoliths, in turn, were used CTAB and EtOH instead of PEG and 2-propanol.

Table 4: Composition (molar equivalents) of the two IMEO-monolith systems used for further tests.

	Precursor	Porogen		Solvent		Acid	Reagent	Ligand
	TEOS [1)]	**PEG_{6000}**	**CTAB**	**PrOH** [2)]	**EtOH**	**HAc** [3)]	**H2O** [3)]	**IMEO**
Type A-7	1	$7 \cdot 10^{-3}$	-	5	-	$8 \cdot 10^{-2}$	7	0.5
Type B-40	1	-	0.04	-	6	-	3	0.5

[1]) *TEOS scale: 9 to 13 mmol*
[2)] *PrOH was selected because of practical reasons (higher purity and costs).*
[3)] *In ongoing experiments acetic acid and water were replaced by 7 equiv. of 25mM acetate buffer (pH 4)*

The special preparations of these two IMEO-monolith systems are explained in detail below.

4.1.3 Preparation of IMEO-monolith type A-7

In a round-bottom flask 0.007 to 0.015 equiv. of PEG_{6000} were solved in 5 equiv. PrOH and 7 equiv. water, at a later time replaced by acetate buffer (25mM, pH4). One equiv. of TEOS was added and the mixture was heated up to 60°C - 70°C in the closed vessel while stirring for 0.5 - 1 hour. The mixture was cooled down to ambient temperature and 0.5 equiv. of IMEO were added while stirring. The emulsion was immediately filled in the activated mold via a syringe. The batch was sealed and allowed to age at ambient temperature in mother liquor overnight. The aged monolith was washed with 60% EtOH until the wash solution was visually clear. The monolith was stored in 60% EtOH (storage buffer) until used. Such a prepared IMEO monolith of A-7 type is shown in Fig. 15.

Fig. 15: IMEO-monolith type A-7.

4.1.4 Preparation of IMEO-monolith type B-40

In a round-bottom flask 0.004 equiv. of CTAB were solved in 6 to 10 equiv. EtOH and 3 equiv. of water. One equiv. of TEOS was added and the mixture was heated up to 70°C in the closed vessel while stirring for 15 minutes. The mixture was cooled down to ambient temperature and 0.5 equiv. of IMEO were added while stirring. The emulsion was immediately filled in the activated mold via a syringe. The batch was sealed and was allowed to age at ambient temperature in mother liquor overnight. The aged monolith was washed with 60% EtOH until the washing solution was clear. The monolith was stored in 60% EtOH (storage buffer) until used. Typically IMEO monoliths B-40 look like as shown in Fig. 16.

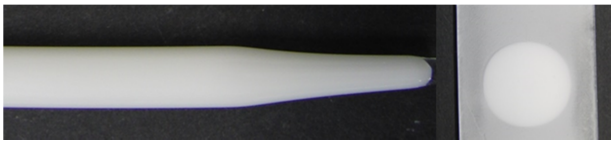

Fig. 16: IMEO-monolith type B-40. (Left) monolith in glass mold; (Right) monolith between two glass slides

4.2 Monolith characterization

4.2.1 FTIR-Spectra

For the control, that IMEO was covalently bound to the monolith, an FTIR analysis of the monolith was done. Therefor the monolith material was dried on air, grinded to a fine powder, washed with 60% EtOH and dried again. The samples were analyzed in powder form on a Bruker VERTEX 70 with ATR unit in absorbance mode. The wavelength was from 600 cm^{-1} to 4500 cm^{-1} with a resolution of 4 cm^{-1} and air as background.

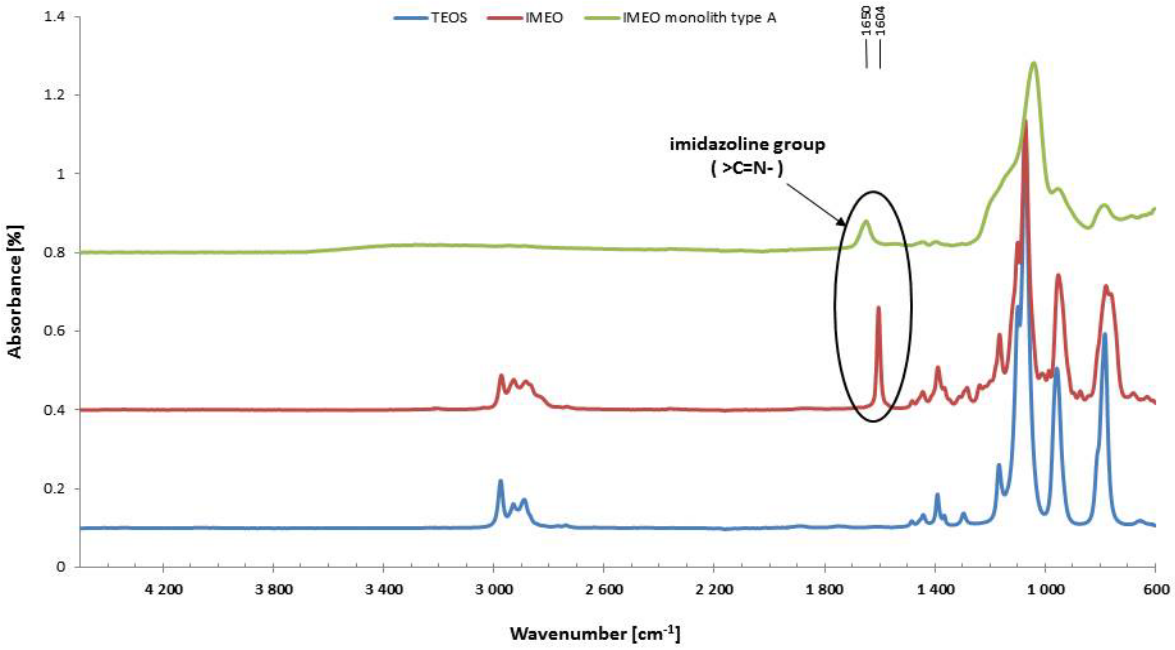

Fig. 17: FTIR spectrum of an IMEO monolith type A with IMEO and TEOS as reference substance.

The FTIR spectrum of the IMEO monolith type A (Fig. 17) shows a typical band at 1650 cm^{-1} (>C=N- group) for imidazoline groups (compare with [24, 25]).

Therefore, it can be assumed, that it is functionalized with imidazoline moieties.

4.2.2 Particle analysis

4.2.2.1 Particle size

For the protein adsorption and for calculating the specific binding capacity it was necessary to know the particle size distribution (PSD) of the used IMEO silica material.

A powdered IMEO-monolith sample equally prepared as for protein adsorption tests, was analyzed by laser diffraction with a HELOS/BR system with dry dispenser unit RODOS (Sympatec GmbH).

The particle size distribution of IMEO-silica powder is shown in Fig. 18.

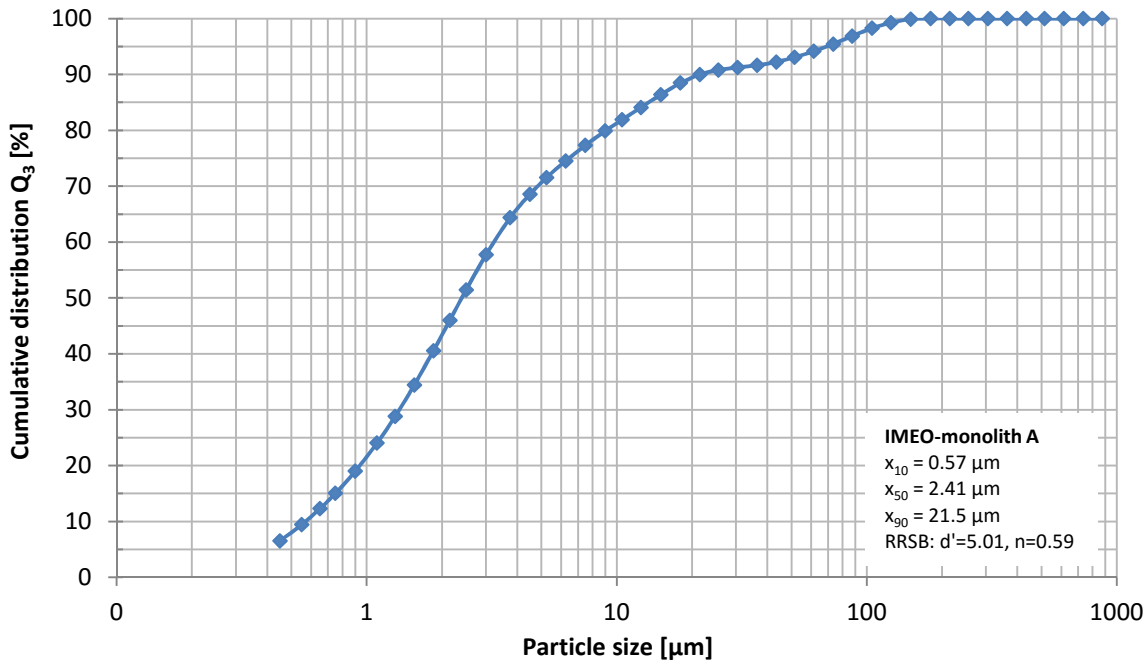

Fig. 18: Particle size distribution of powdered IMEO monolith A-7.

The diagram shows that the PSD of the IMEO-sample ranges from 0.6 µm (x_{10}) to 120 µm (x_{99}), whereby 50% of all particles are smaller than 2.4 µm.

4.2.2.2 BET gas adsorption analysis

BET gas adsorption analysis is a classical method to determine the porosity of a dried and degassed test specimen. The adsorbed amount of gas on a test specimen at the atmospheric boiling point of the gas is measured. In most cases, nitrogen is used as standard gas for BET measurements. [26]

In our case, several dried IMEO-monoliths were measured for their specific surface area, pore volume and pore size. All measurements were performed with TriStar II 3020 (Micromeritics Instr. Corp.) and nitrogen as adsorptive gas.
All results of these analyses are given in Table 5. The isotherm plot of an IMEO-monolith A-7 test specimen is shown in Fig: 19.
All measured (type A) monoliths were prepared by the use of TEOS and IMEO solved in PrOH. Acetic acid was used as catalyst for hydrolysis and PEG_{6000} as porogen. The amount of porogen was 0.007 equiv. for type A-7, 0.011 equiv. for A-11 and 0.015 equiv. for A-15, respectively. Additionally, two of the monoliths were washed in ammonium hydroxid solution

within the aging phase. Additionally, a pulverized IMEO-monolith with the same composition like type A-7 was measured for comparison.

Table 5: BET nitrogen adsorption analyses of several monolithic test specimen and powdered IMEO-silica.

Sample	Surface area [m^2/g]	Pore Volume [cm^3/g]	Pore size [nm]	Isotherm plot type
IMEO-silica A-7 (powder)	9.83	0.028	11.66	II
Type A-7	51.5	0.046	7.06	IV (H4)
Type A-15, Washed with H_2O	35.2	0.027	6.34	IV (H4)
Type A-15, Washed with 0.01M NH_4OH	37.8	0.032	6.33	IV (H4)
Type A-15, Washed with 0.1M NH_4OH	38.6	0.028	5.60	IV (H4)
Type A-11	45.5	0.036	6.18	IV (H4)

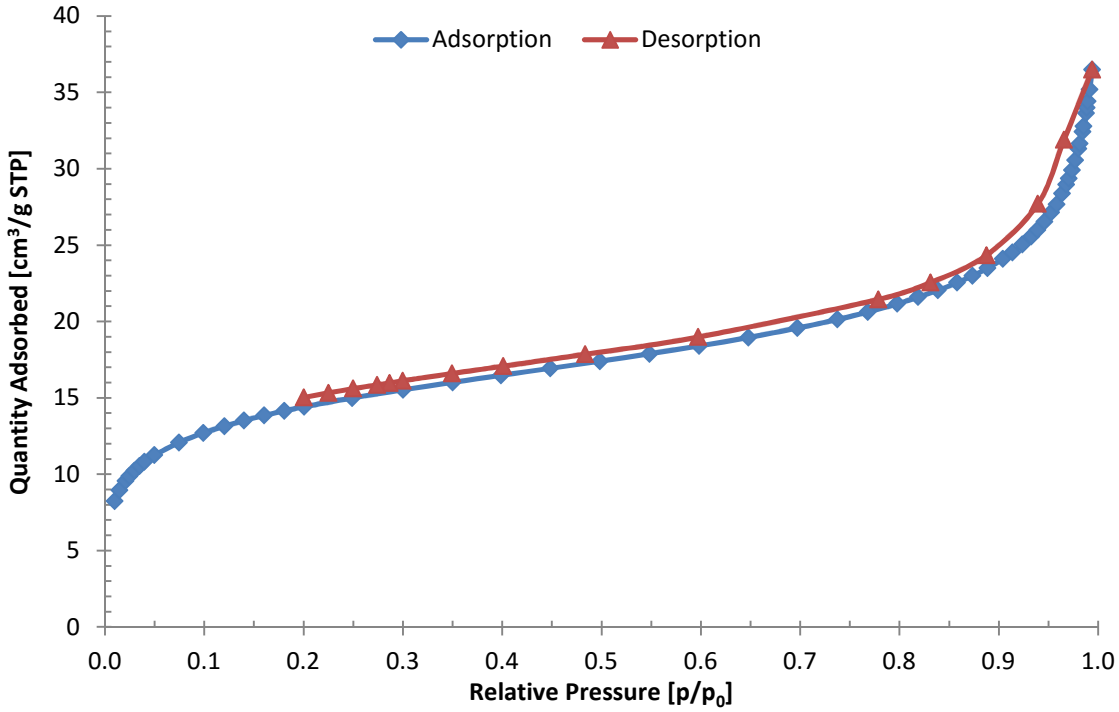

Fig: 19: Isotherm Linear Plot of an IMEO-monolith type A-7.

The curve of the BET analysis of monolith type A-7 with its hysteresis loop, shown in Fig: 19, can be classified as a type IV isotherm with a H4 hysteresis according to Sing et al. [41]. It is typical for structures with micro- (pore width <2nm) and mesopores (pore width from 2 to 50 nm). Furthermore, the form of the hysteresis loop indicates narrow slit pores in the micropore range.

This is in contrast to the powder form, where desorption and adsorption curve overlaps (BET plot form II, figure not shown) as consequence of a non-double pore structure.

From Table 5 it is obvious that the pore volume and the surface area decrease with rising PEG concentrations from $7 \cdot 10^{-3}$ to $1.5 \cdot 10^{-2}$ equivalents.

The pore size appears to follow no trend and displays a minimum for type A-11. Furthermore, based on the comparison between powder and monolith form, one can see a five times higher surface area of the monolith than of the powder form. This indicates a much higher porous structure of the monolithic form.

Moreover, a curing (wash) of the monolith with aqueous ammonia hydroxide (NH_4OH) solutions seems to increase the surface area slightly. However, it has only slight influence on pore volume and size.

4.2.2.3 Gas pycnometry

Gas pycnometry measures the true density of the monoliths. This was done with an AccuPyc II 1340 (Micromeritics Instr. Corp.) device. Measurements were made with nitrogen. All samples were dried before the measurements.

All monolithic samples were produced in a plastic syringe (2 ml) with a sealed nozzle. After aging, the samples were washed with storage buffer as long as the washing solution became clear. The monoliths were pressed out of the mold keeping by compressed air. The samples were dried in air at ambient temperature gently. During the press out and drying process it was observed that the monoliths kept their form.

Powdered samples were prepared in the same way as for the chromatographic tests.

The measured true densities for several IMEO-monolith specimens and for IMEO-silica powder are listed in Table 6.

Table 6: True density of IMEO-monolith specimen. Measured by nitrogen pycnometry

Sample	True Density [g/cm^3]
IMEO-silica A-7 (powder)	1.88 ± 0.02
Type A-7	2.22 ± 0.02
Type A-15	2.11 ± 0.02
Type A-15; Wash with 0.01M NH4OH	2.12 ± 0.02
Type A-15; Wash with 0.1M NH4OH	2.10 ± 0.02
Type A-11	1.67 ± 0.01
Type A-15, after chromatographic test[1)]	1.89 ± 0.01
Type B-40	1.21 ± 0.00

1) *This monolith was used for the chromatographic tests. The density measurements were made after the tests.*

The true density measured with gas pycnometry can also include closed pores. Hence, materials with high amounts of closed pores appear to have lower particle densities as in reality. This could be the reason for the lower densities of type A-11 and type B-40. A curing with aqueous ammonia hydroxide solution only has minor influence on the true density as well as on the pore size and volume (compare with chapter 4.2.2.2). The curing did not change the density by altering the PSD as presumed elsewhere [33, 42]. However, it is to mention that the curing with ammonia hydroxide solutions in this study was done at ambient temperature and within a short time (1 to 2 hours).

4.2.3 Elemental analysis

For an elemental analysis, an IMEO monolith type A-7 was dried and grinded in a mortar to a fine powder. 10 mg of the samples were analyzed by a varioEL III Element Analyzer (elementar Analysensysteme GmbH, analyzed by the Institute of Anorganic Chemistry, TU Graz) for the elements carbon, hydrogen and nitrogen (CHN). From nitrogen content and surface area (see also chapter 4.2.2.2 on p. 41) the concentration of imidazoline moieties within the monolith could be calculated by equation (7).

Table 7: CHN Elemental analysis of IMEO monolith A. n=3

	%N	%C	%H
Measurement 1	5.13	13.60	3.56
Measurement 2	5.04	13.64	3.60
Measurement 3	5.09	13.62	3.56
Mean:	**5.08**	**13.62**	**3.57**
STD:	**0.05**	**0.02**	**0.02**

The imidazoline moiety possesses two nitrogen atoms as can be seen in Fig. 20, and has a molecular weight of 112.17 g/mol.

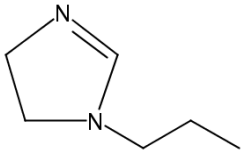

Fig. 20: Imidazoline moiety with propyl chain (ligand) from IMEO.

According to gas pycnometry measurements the particle density is 1.88 g/cm^3 (see also chapter 4.2.2.3, p. 43). The surface area was set to 9.83 m^2/g monolith according to the BET analysis (see also chapter 4.2.2.2, p. 41).

With this information, the ligand concentration was calculated as already mentioned by eq. (7):

$$c_{IMEO} = \frac{\%N}{2} * \frac{1}{M_N} \cdot 10^4 \cdot d_{particle} \qquad (7)$$

c_{IMEO}	…	Concentration of IMEO [µmol /cm³]
%N	…	Content of nitrogen in sample [%]
M_N	…	Atomic mass of nitrogen [14.01 u]
$d_{particles}$	…	Particle density [1.88 g/cm³]

As a result, a concentration of 3.40 mmol IMEO per cm³ monolith was calculated. The dried mass of 9 ml IMEO column was related to a mass of 5.9 gram. In consequence, an IMEO concentration of 5.2 mmol per gram IMEO monolith could be found.
This concentration outperforms by far the concentrations found by Oztürk et al. [24, 25]. There, IMEO concentrations about 0.13 mmol IMEO per gram beads and 0.24 mmol IMEO per gram nanoparticles have been found on the surface. However, the concentration of imidazolines in this study could only be calculated for the monolith´s total volume.

4.2.4 Microscopy

To get a more detailed view of the monolithic structure, single monoliths (type A) with PEG amounts of 0.004 (A-4, low-PEG), 0.01 (A-11, medium-PEG) and 0.02 (A-19, high-PEG) equivalents were produced in a plastic mold (PP) and carefully dried on air at ambient temperature. As shown in Fig. 21, microscopic images were taken in bright field mode.
Samples prepared in the same way as before were also filled between two activated microscopic slides, dried gently and viewed in dark field mode, as shown in Fig. 22.
Additionally, a sample of IMEO monolith type B-41 with CTAB as porogen was also prepared and viewed on a microscope in bright and dark field mode. This is shown in Fig. 23.
All samples were examined with a DM 4000 microscope (Leica) with a magnitude of fifty.

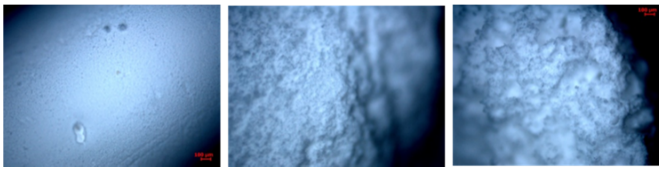

Fig. 21: Outer structure of dried IMEO monoliths (type A). From left to right: low - middle - medium porogen content, (bright field mode)

In Fig. 21 it is obvious that the porous character of the sample increases with rising PEG content. However, the solid monolithic form (low-PEG) turns into a loosely network of agglomerates (high-PEG).

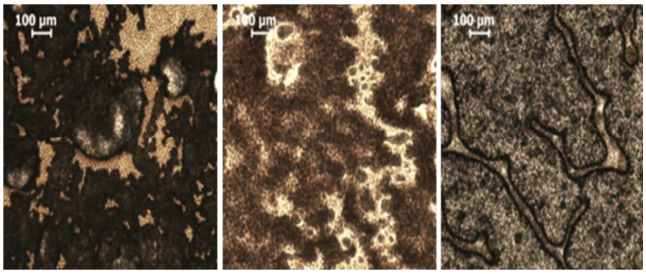

Fig. 22: Structure of dried IMEO monoliths (type A). From left to right: low - middle - medium porogen content, (dark field mode)

As shown in Fig. 22, the bright field mode presents a similar picture as before: The monolith type A-4 (low-PEG content, left side) shows high densified and interconnected particles with spacious voids between them. However, the permeability is low and the true density is high, respectively. As a result, the macroporous system appears to be non-interconnected and includes closed pores.

With higher amounts of PEG the samples are more extensively allocated, which decreases the particle density and leads to shrinked voids. As a consequence the permeability increases.

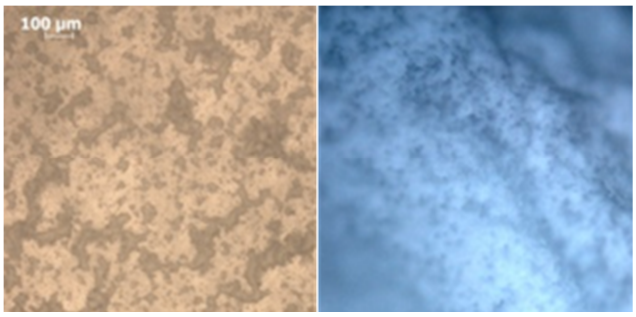

Fig. 23: Structure of dried IMEO monolith (type B). (Left) bright field mode, (Right) dark field mode

The IMEO monolith type B-41 (high-porogen content) in Fig. 23 shows similar characteristics as the high-PEG containing samples of type A: a fluffy network of agglomerates with low mechanical stability, but high permeability. In the opposite to the high-PEG containing samples the CTAB sample displays fainter interfaces between silica and voids and the distribution is more homogenous as visible in the dark field mode.

4.2.5 Swelling test

For a single test, a measuring cylinder was filled with dried powder of an IMEO-monolith type A-7 up to 2.0 ml. The powder was tapped after pouring until the volume kept constant. The total start volume was noted.

Then, the sample was mixed with 5 ml of 60% EtOH to a slurry, which rested for three days until the sample settled again. The volume change of the powder sample was measured.

(Note: A 60% EtOH solution was used as storage and washing solution in this study as not stated otherwise.)

A comparison between dry and wetted powder of IMEO-silica immersed in 60% EtOH is shown in Fig. 24.

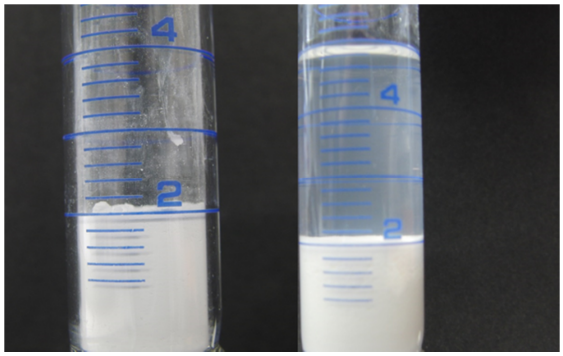

Fig. 24: Swelling test of an IMEO-silica powder (type A-7). (Left) dry, (Right) immersed in 60% EtOH

Based on Fig. 24 it is evident that a solution of 60% EtOH had no swelling effect on the IMEO sample type A-7. The volume of the powder kept constant. It was also noticeable, that the wettability of the IMEO sample was low with both ethanol and water.

4.3 Chromatographic Tests

4.3.1 Chemical stability

This test should examine the (chemical) resistance of IMEO-monolith to various pH buffers intended to be used as mobile phases. No loose or dissolved IMEO-silica material should be found in the eluates.

For this analysis, a 9 ml seized IMEO-monolith (type A-15) was prepared. The column was equilibrated with 12 ml of pure water before the test started. During the equilibration the drop rate was determined as 9 drops per minute (0.05 ml/drop, 0.5 ml/min). Afterwards, various

aqueous pH buffers, as shown in Table 8, were rinsed through the column. The eluate was collected in 1 ml-fractions for photometrical analysis.

Table 8: Test for chemical resistance to mobile phases of IMEO-monolith A.

Elution volume [ml]	Mobile Phase	Drop rate [1] (Flow rate)
0	Equilibration (12 ml pure water)	9 (0.5)
1-8	Carbonate buffer (25mM, pH 10)	n/a
9-17	Acetate buffer (25mM, pH 6)	n/a
18-28	Acetate buffer (25mM pH 6) with 2M NaCl	n/a
29-43	KCl buffer (50mM, pH 12)	8 (0.4)
44-56	Acetate buffer (25mM, pH 4)	8 (0.4)
57-69	60% EtOH	7 (0.1)
-	Stored in 60% EtOH overnight	n/a
70-80	Wash water after storage	10 (0.5)
81-93	25mM KCl buffer (pH 2)	n/a

1) *Drop rate in drops/min; Flow rate in ml/min: One drop of 60% EtOH has a volume of 0.02 ml. One drop of water has a volume of 0.05 ml.*

For the photometrical analysis the eluates were mixed with ninhydrin and analyzed at 568 nm. IMEO is also able to react with ninhydrin like amino acids and forms a reddish solution (absorption maximum at 568 nm), as stated in [46]. For the mass extinction coefficient of IMEO mixed with ninhydrin at 568 nm a value of 27.3 ml g^{-1} cm^{-1} was determined.

The recovered IMEO concentrations in the eluates are displayed in Fig. 25.

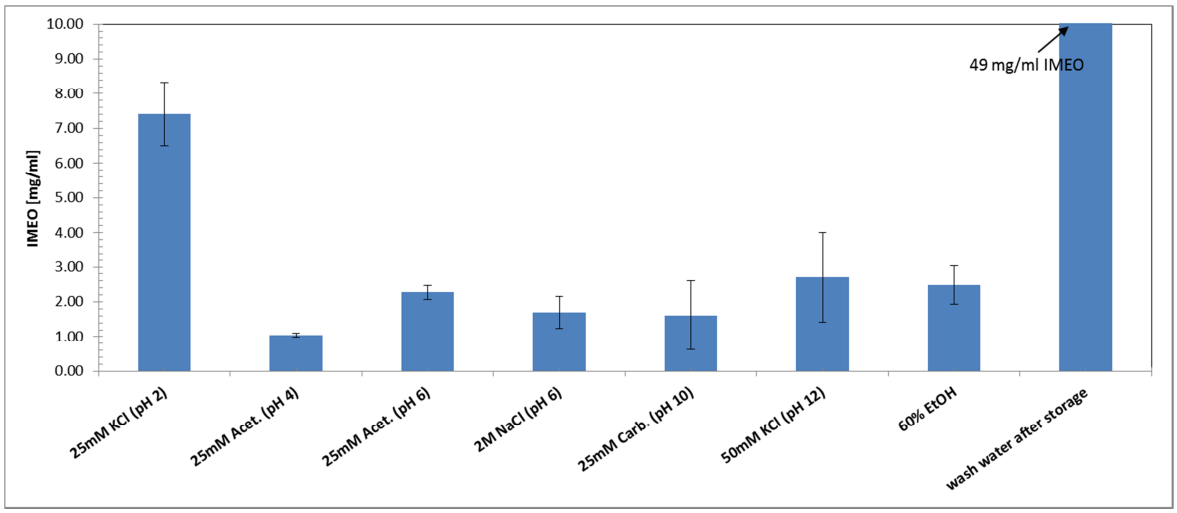

Fig. 25: Concentrations of IMEO recovered in various elution buffers.

The monolith degraded intensively at pH 2 or when stored in 60% EtOH for longer time (overnight), as shown in Fig. 25.

A minimal loss of material of around 2 mg IMEO per ml buffer was detectable for all pH buffers, but amplified when acetate buffer (pH 6) and KCl buffer (pH 12) were used. Moreover, high concentrations of IMEO could be retrieved in the storage buffer, which could be a consequence of continuative aging and resolvation processes.

4.3.2 Elution of dyes

As an optical evaluation for the adsorption performance, different kinds of dyes were eluted from an IMEO-monolith.

In this case, four dyes Calconcarboxylic acid (Calc), Bromocresol green (Bcg), Methylene blue (Mb) and Methyl red (Mr) were used.

For the selection, it was crucial, besides their availability in the laboratory, that possible interactions between tested monoliths and biomolecule´s representative moieties (amines, carbon acids, heterocyclic aromatic rings) could be visualized. Respectively, the dyes had to be preferably diverse functional groups. The molecular structures of the used dyes are presented in Fig. 26.

A little volume of dye solution (1 - 0.2 mg dye/ml, ca. 0.5 to 1 ml) was put on the top of the IMEO monolithic column and eluted with mobile phase. The eluate was collected in volumes of 1 ml and analyzed photometrically.

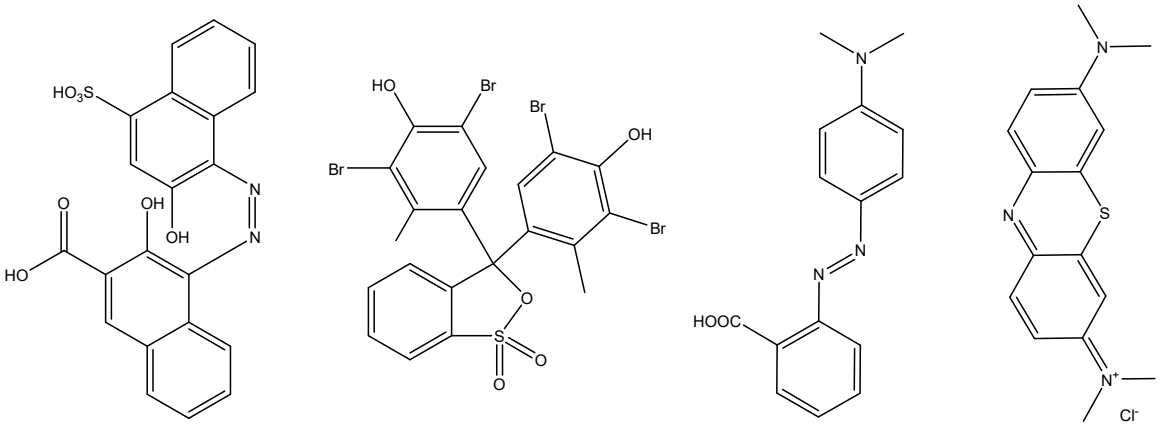

Calconcarboxylic acid (Calc) | **Bromocresol green** (Bg) | **Methyl red** (Mr) | **Methylene blue** (Mb)

Fig. 26: Molecular structures of the used dyes.

In the following experiments with single dye solutions and with a mixture of all dyes were performed.

4.3.2.1 Elution of single dye solutions

Single dye solutions were eluted separately through an IMEO-monolithic column (type A-7) with a volume of 2 ml. The drop rate fluctuated during the test between 5 to 10 drops per minute (0.05 ml/drop, 0.3 – 0.5 ml/min). The total elution progress (elution profile) of all single dye solutions are shown in Fig. 27. The Greek letters in Fig. 27 sign the used mobile phases for that volume range. Each elution of a dye solution is indicated as one series.

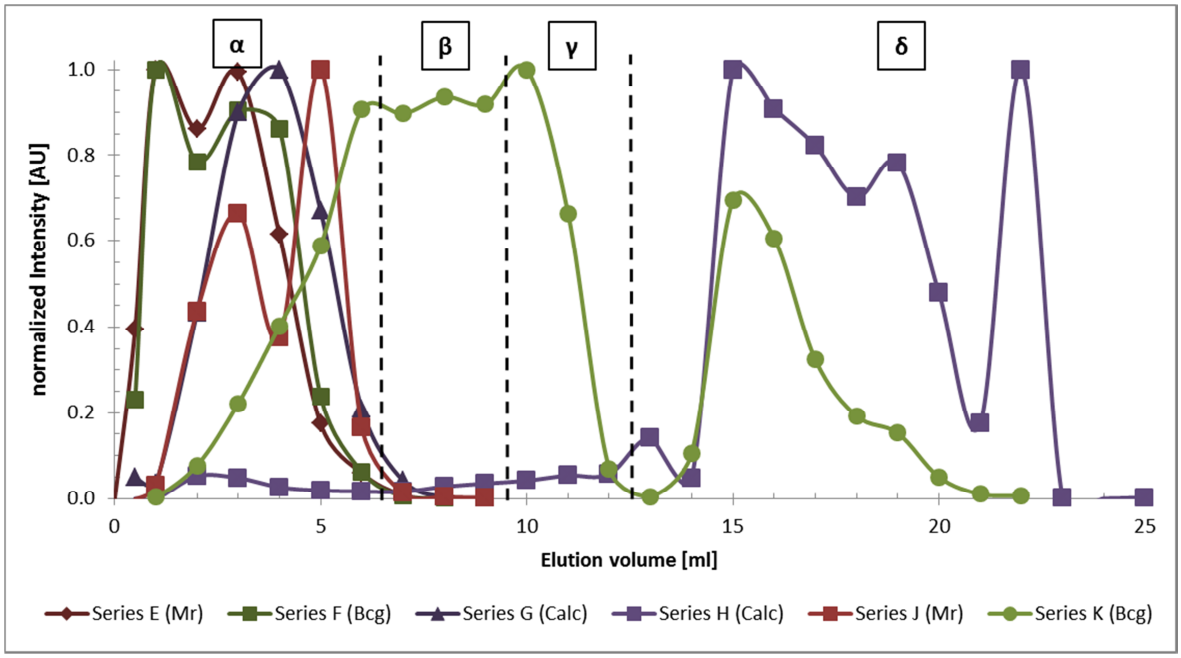

Fig. 27: Separate elution of various dye solutions. Sectors α, β, γ and δ characterize mobile phase changes (see also Table 9)

The used mobile phases for each dye solution are listed in Table 9.

Table 9: Used mobile phases for the elution of the single dye solutions.

			E Mr	F Bcg	G Calc	H Calc	J Mr	K Bcg
Sectors in Fig. 27	**Fraction #**	**Volume [ml]**	**Mobile Phase**					
α	1-2	0.5	I	I	I	II	III	III
	3-7	1.0	I	I	I	II	III	III
β	8-9	1.0	I	I	I	IV	III	III
γ	10	1.0	-	-	I	IV	III	VI
	11-13	1.0	-	-	-	IV	-	VI
δ	14	1.0	-	-	-	V	-	VI
	15-23	1.0	-	-	-	V	-	IV
	24-28	1.0	-	-	-	V	-	-

Mobile Phases: (I) Phosphate buffer (25mM, pH 7):EtOH, 4:6; (II) Phosphate buffer (25mM, pH 7); (III) PBS (pH 7); (IV) 2M aqueous NaCl solution; (V) Phosphate (25mM, pH 12); (VI) 60% EtOH.

As shown in Fig. 27, Mr (Series E) and Bcg (Series F) did not retard, when a mix of phosphate buffer (pH 7) and EtOH (I) was used as mobile phase. However, the elution time of Calc (Series G) was increased with that mobile phase.

Remarkably, Mr (Series E and J) and Bcg (Series F) formed shoulder peaks, which might result from bypass effects near the wall.

Calc (Series G) were eluted by a mixture of phosphate buffer and EtOH. It was the only dye, which showed a limited retention effect.

A strong adsorption effect for Calc (series H) was detectable, when eluted with aqueous neutral solutions. Bcg, in turn, kept adsorbed, when eluted with ethanol-water (series K). Both, Bcg and Calc, retarded massively by using PBS as mobile phase. Calc even kept completely adsorbed on the column by using neutral phosphate buffers or solutions with high salt concentrations. However, a buffer with a pH of 12 could elute the immobilized Calc slowly forming two broad peaks.

4.3.2.2 Elution of a mixture of all dyes

An IMEO-monolithic column (type A-7) of 2 ml volume was equilibrated with 10 ml of citrate buffer (25mM, pH 3.2).

Then, 1 ml of a mixture of Calc (0.05 mg/ml), Bcg (0.05 mg/ml), Mb (0.25 mg/ml) and Mr (0.05 mg/ml), dissolved in 40% EtOH, was put on the top of the column. The drop rate was determined to 7 drops per minute (0.02 ml/drop, 0.1 ml/min). The collected volume of each fraction was 0.5 ml and the ionic strength of all mobile phases was accounted to 25 mM. The used mobile phases and the coloration of the eluates are listed in Table 10.

Table 10: Elution of a dye mixture from an IMEO monolith (A-7).

Fraction	Mobile Phase /pH	Coloration
0	Citrate buffer, pH 3	-
1-7	Citrate buffer, pH 3	Turquoise
8-10	Phosphate buffer, pH 7	Turquoise
11-14	Phosphate buffer, pH 7	Greenish
15-16	Phosphate buffer, pH 12	Pale
17-30	Phosphate buffer, pH 12	Purple
31-39	Phosphate buffer, pH 12	Blue
40-42	Phosphate buffer, pH 12	Pale

The elution progress of each dye component was tracked photometrically. Thus, the complete elution profiles of each component of the dye mixture were shown in Fig. 28. The absorbance of each dye was normalized by division through the maximum absorbance and set as 'normalized absorbance' with arbitrary units [AU].

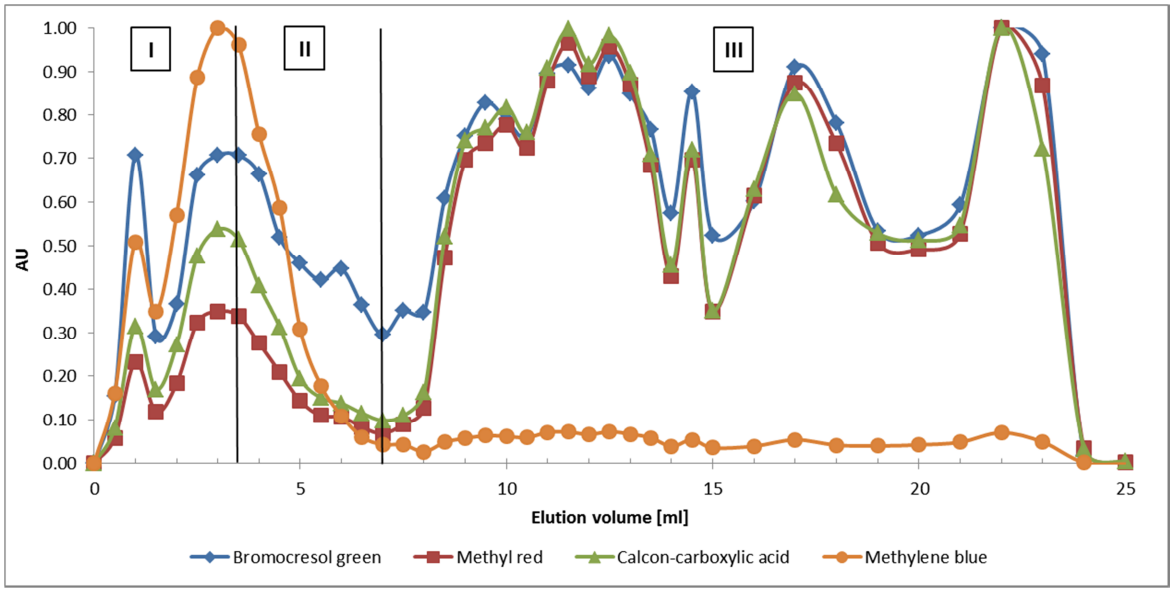

Fig. 28: Elution profile of the dye mixture eluted from an IMEO monolith (type A-7).
(Section I) Citrate buffer (25mM, pH 3), (Section II) Phosphate buffer (25mM, pH 7),
(Section III) Phosphate buffer (25mM, pH 12)

Methylene blue was the first that was eluted and barely immobilized on the column.

Calc and Mr were mainly adsorbed on the top of the column at a pH range of the mobile phase from 3 to 7. Their elution only started, when the pH of the mobile phase was increased to 12.

Bcg eluted over the whole range of elution buffers. Each dye formed broad bands.

The drop rate kept constant during the whole elution process.

After the complete run the column looked regenerated and was completely colorless again.

4.3.3 Adsorption and desorption of biomolecules

The adsorption and desorption behavior of IMEO-monoliths for biomolecules such as amino acids and proteins were examined. As model biomolecules served several kinds of amino acids as well as bovine serum albumin (BSA) and antibodies.

4.3.3.1 Adsorption of amino acids

The adsorption behavior of amino acids on IMEO-monoliths was examined. It was assumed, that the binding capacity depends on pH and ionic strength of the adsorption buffer as well as on the isoelectrical point (pI) of the amino acids. However, they are much smaller than proteins and have free carbon acid and amine moieties, which could affect the adsorption additionally.

For the experiments in this study, the amino acids Glycine (Gly), Histidine (His), Phenylalanine (Phe) and Tryptophan (Trp) were chosen as representatives because of their availability at the institute.

Table 11: Relevant data about the used amino acids. The indices stands for the amino acids functional moiety: (COOH) terminal carbon acid, (NH2) terminal amine, (SC) side chain; taken from [43]

	Mw [g/mol]	Solubility in H_2O at 25°C [g/l]	pI	pK_{COOH}	pK_{NH2}	pK_{Sc}
Glycine	75.07	239	5.97	2.34	9.58	-
L-Histidine	155.15	43.5	7.59	1.7	9.09	6.04
L-Phenylalanine	165.19	27.9	5.48	2.18	9.09	-
L-Tryptophan	204.23	13.2	5.89	2.38	9.34	-

The adsorption behavior was tested in various buffer systems. For the detection of all amino acids a derivatization of the amino acids with ninhydrin (see also chapter 11.2) was done. Because of the aromatic system, tryptophan can also be detected photometrically at 280 nm.

For the experiment 10 mg to 20 mg of dried and grinded monolithic material (sample) was exactly weighed in a microcentrifuge tube. 50 mg of each amino acid were dissolved separately in 10 mL distilled water (amino acid stock solutions). The stock solutions were together diluted in various pH-buffers and brought to an end concentration of 0.1 mg/ml (amino acid test solution). The sample material was suspended in one ml of the amino acid test solution and incubated at 25°C with a mixing rate of 1400 rpm for 2 hours.

After the incubation each sample suspension was centrifuged at 25°C with 10 000 rpm for 10 min. 0.8 ml of the clear supernatant were dropped in semi-micro disposable cuvettes and analyzed photometrically at 279 nm for Trp at first. Then, all supernatants were derivatized with ninhydrin and analyzed at 560 nm for the total amino acid concentrations.

The molar concentration coefficient of Trp in phosphate buffer (pH 7) was determined 5.48 mM^{-1} cm^{-1} (comp. to 5.69 mM^{-1} cm^{-1} in water, [48]).

The total amount of adsorbed amino acids was calculated by equation (8).

$$Q_{ads} = (1 - A/A_0) \cdot \frac{V_{amino\ acid} \cdot c_{amino\ acid}}{m_{silica}} \cdot 10^6 \qquad (8)$$

Q_{ads} … Amount of adsorbed amino acid [µmol /g sample]

A_0 … Absorbance of amino acid test solution [-]

A … Absorbance of supernatant [-]

$V_{amino\ acid}$ … Volume of amino acid test solution [ml]

$C_{amino\ acid}$ … Conc. of each amino acid in the test solution [mmol/ml]

m_{silica} … Mass of silica [mg]

The calculated amounts of adsorbed tryptophan on variable amounts of IMEO-silica (powder form) are shown in Fig. 29.

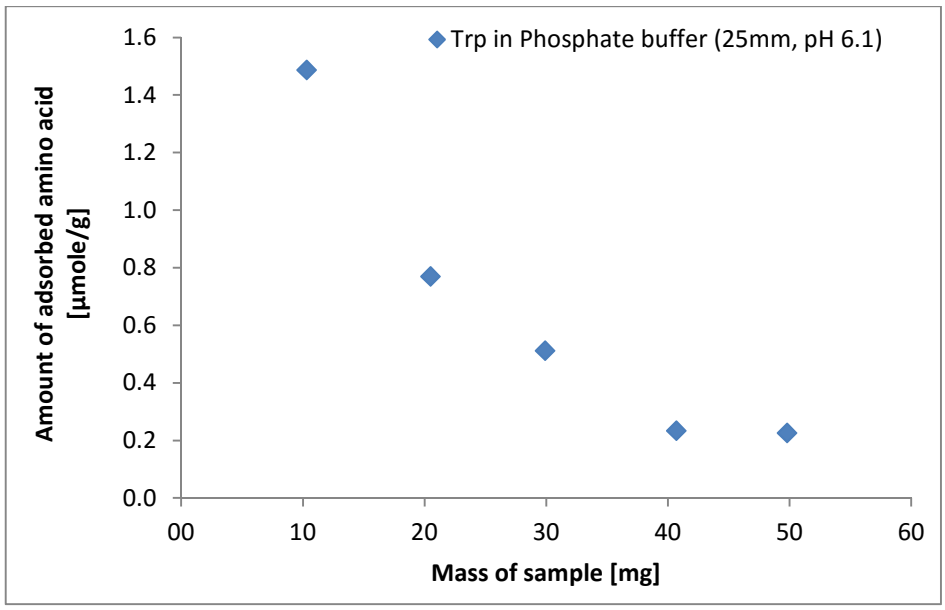

Fig. 29: Adsorption of Trp on IMEO-silica (A-7, powder). Adsorption buffer was a phosphate buffer (25mM, pH7)

Different masses of IMEO-silica in powder form were suspended in one ml of a Trp test solution (50 µg Trp/ml phosphate buffer (25mM, pH 7)) and incubated as described above. The results are shown in Fig. 29. With this experiment the maximal adsorption capacity for Trp on IMEO-silica should be determined. But the adsorbed amount depended on weighed mass of silica as one can see in Fig. 29: The amount of adsorbed Trp decreases with increasing mass of IMEO-silica. This unexpected trend could be a result of agglomeration of IMEO-silica in the buffer solution: Although the sample mass has increased, the simultaneous increase in free surface area would be smaller. Consequently, the adsorption of Trp molecules on the silica surface was too short proportional to the mass changes.

The amount of adsorbed Gly, His, Phe and Trp on IMEO silica (A-7) powder is shown in Fig. 30. All adsorbed amounts are related to 20 mg IMEO-silica.
Remarkably, Gly, His and Phe dissolved in a pH 5 buffer adsorbed on IMEO-silica in nearly the same quantity (ca. 10 µmol per gram sample), whereas no adsorption of Trp was found. As shown in Fig. 30, a change of the pH of the adsorption buffer from 5 to 6 also changed the adsorption capacity of Gly and His. The isoelectrical point of Gly is stated at pH 6, so it is not charged at this pH. This charge loss could be an explanation for the drastically decrease of adsorbed Gly at pH 6.

Histidine, in turn, was adsorbed best at pH 6. This phenomenon was a result of the uncharged side chains of histidine.

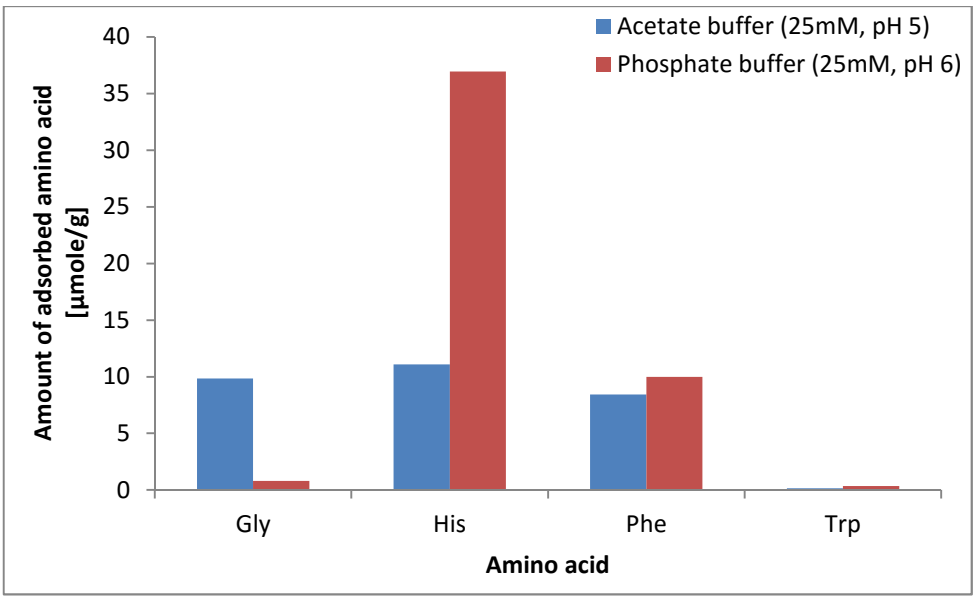

Fig. 30: Adsorption of several amino acids on IMEO-silica (A-7) powder.

4.3.3.2 Adsorption and desorption of BSA

Bovine serum albumin (BSA) served as model molecule for the adsorption of proteins onto IMEO-silica material in this study.

BSA is a plasma protein with a molecular weight of 62 kDa. The isoelectrical point lies at 4.6. [11]

It was expected that the sorption characteristics of functionalized imidazoline monoliths are based on the same principles as for histidine affinity columns [24, 25].

Histidine-like groups can bind proteins slightly above its pI, when the protein's overall charge is negative [11], as mentioned at the beginning. Since the pKa of the imidazoline groups is located at pH 11, a general positive charge of the IMEO groups had to be assumed for all mobile phases with acidic to neutral pH.

For histidine affinity chromatography, high ionic strengths direct to the elution of proteins. This is achieved through sodium chloride gradients.

As before (see chapter 4.3.3.1) 10 mg of dried and crushed IMEO-silica (sample) were exactly weighed. A BSA test solution was prepared by diluting 0.1 ml of a BSA stock solution (20 mg/ml) in 1.4 mL of the respective adsorption buffer. Then, the weighed silica sample was

suspended in one ml of this solution and incubated at 25°C with a mixing rate of 1400 rpm for 3 hours.

After the incubation the suspension was centrifuged at 20°C with 10 000 rpm for 10 min. 0.8 ml of the supernatant was dropped in a semi-micro disposable cuvette for photometrical analysis at 278 nm. The absorbance between BSA test solution and supernatant were compared for the determination of adsorbed BSA.

For the desorption of BSA, in turn, 10 mg of IMEO sample were suspended in 1 ml acetate buffer (25mM, pH 5) again and incubated with the same conditions as above overnight for a complete adsorption. Afterwards, the suspension was centrifuged with 10 000 rpm at 20°C for 10 min. The supernatant was removed and analyzed for the adsorbed amount of BSA.

The centrifugate was washed with a total volume of 3 ml adsorption buffer until no BSA could be detected in the washing solution.

After washing, the centrifugate was resuspended in 0.9 mL of the respective desorption buffer and incubated at 25°C with a mixing rate of 1400 rpm for 3 hours again. After centrifugation, the supernatant was analyzed photometrically at 278 nm for its BSA concentration.

The respective adsorption and desorption buffers used for this experiment are listed in Table 12.

Table 12: Buffers used for the BSA adsorption and desorption test on IMEO-silica (A-7) powder.

Sample #	Adsorption buffer	Desorption buffer
1	25mM Acetate buffer (pH 4)	25mM Acetate buffer (pH 5) with 2M NaCl
2	25mM Acetate buffer (pH 5)	25mM Acetate buffer (pH 4) with 0.5M NaCl
3	25mM Phosphate buffer (pH 7)	PBS (pH 7.4)
4	25mM Acetate buffer (pH 4) with 20% ACN	25mM Acetate buffer (pH 4) with 20% ACN
5	25mM Acetate buffer (pH 5) with 20% ACN	PBS with 0.1M KSCN
6	25mM Acetate buffer (pH 5) with 0.5M NaCl	
7	25mM Acetate buffer (pH 5) with 1M NaCl	
8	25mM Acetate buffer (pH 5) with 2M NaCl	
9	PBS (pH 7.4)	
10	25mM TRIS buffer (pH 9)	

The photometrical analysis was made by a two-beam spectrometer with semi-micro disposable cuvettes (PMMA) at a wavelength of 278 nm. The reference solution was pure buffer without BSA.

The results of this experiment are presented in Fig. 31. The experiments were limited to ACN concentrations below 30% and ionic strengths of smaller than 2 M, because of denaturation effects of albumin.

The molar adsorption capacity of IMEO-functionalized silica for BSA could be calculated by equation (9).

$$Q_{ads} = (A_0 - A) \cdot \frac{V_{liq}}{\varepsilon_{BSA} \cdot d \cdot m_{silica}} \qquad (9)$$

Q_{ads}	…	Molar adsorption capacity [µmol BSA /g silica]
A_0	…	Initial absorbance [-]
A	…	Absorbance [-]
V_{liq}	…	Volume of adsorption buffer [ml]
ε_{BSA}	…	Molar extinction coefficient at 280 nm [41.2 $mM^{-1}cm^{-1}$] [11]
d	…	Cuvette thickness [1 cm]
m_{silica}	…	Weighed mass of silica [g]

The highest adsorption effect was achieved with 25 mM acetate buffer at a pH of 5, as in Fig. 31 shown. As expected, this is near the pI of BSA (4.6). As a result, the protein was slightly negatively charged (see Fig. 31). Lower or higher pH values drastically decreased the binding capacity. Except for pH 5 the binding capacity of BSA was comparable with normal silica (normal phase), which lies in the range of 7-20 nmol BSA per gram silica. Normal silica has a rather negatively charged surface. The binding capacities of both silica sorts for BSA were similar above and below the albumin´s pI. This indicates that hydrophobic interactions affected the adsorption onto normal phase silica.
Acetonitrile seemed to affect the adsorption behavior of albumin onto silica only minimal (data not shown).

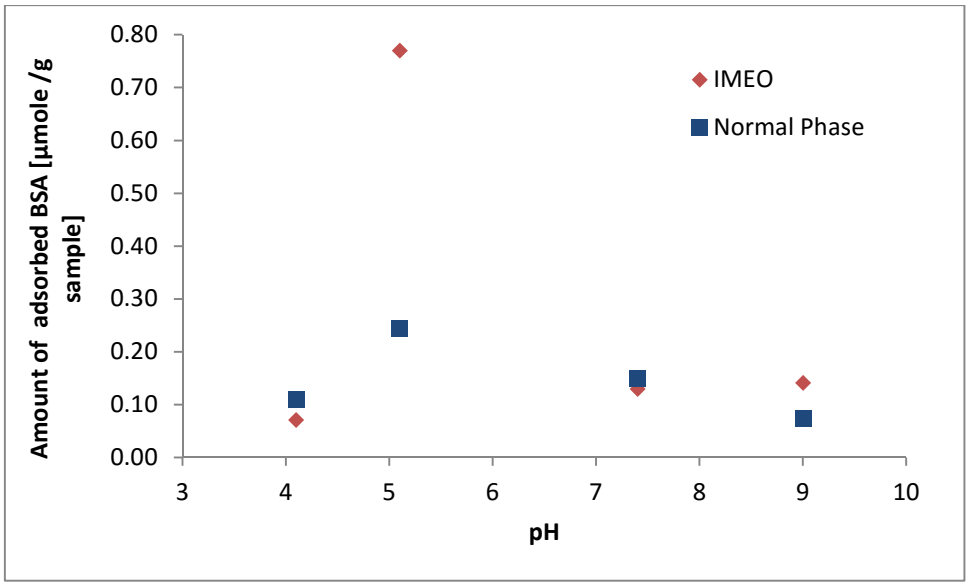

Fig. 31: Adsorption of BSA with various pH buffers. IMEO and normal silica were used; ionic strengths of the buffer media was set to 25mM

In addition, the adsorbed amount of BSA in dependence of the ionic strength is shown in Fig. 32.

The addition of 0.5 M sodium chloride to the adsorption buffer decreased massively the amount of adsorbed BSA. The adsorption effect even disappeared with sodium chloride concentrations of 2 M for IMEO modified silica, whereas normal phase silica apparently kept a basic level at ca. 0.01 mmol BSA per gram normal silica.

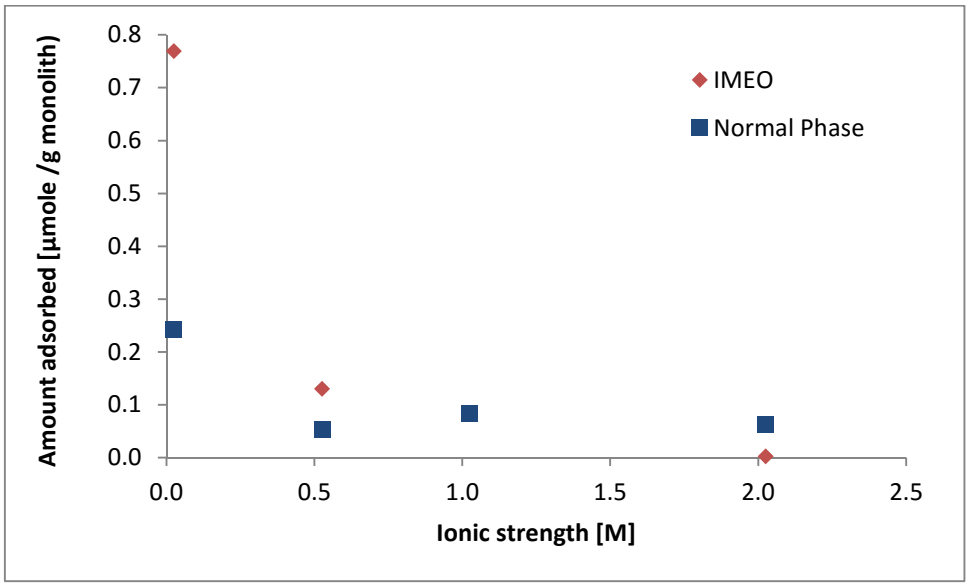

Fig. 32: Adsorption capacity of BSA versus ionic strength of the adsorption buffer. IMEO and normal silica were used; the pH of the adsorption buffer was 5

Another parameter, the molar amount of desorbed BSA, could be calculated by equation (10) for the desorption process. The results are shown in Fig. 33.

$$Q_{elu} = \frac{N_{BSA,elu}}{N_{BSA,tot}} \cdot \frac{1}{m_{silica}} = \frac{A}{\varepsilon_{BSA} \cdot d \cdot c_{stock}} \cdot \frac{V_{elu}}{V_{stock}} \cdot \frac{1}{m_{silica}} \qquad (10)$$

$N_{BSA,tot}$	…	Molar amount of total albumin [mmol]
$N_{BSA,elu}$	…	Molar amount of eluted albumin [mmol]
Q_{elu}	…	Ratio of desorbed albumin to total albumin per g silica [% /g silica]
A	…	Sample absorbance [-]
c_{stock}	…	Concentration of BSA stock solution [0.32 mM]
V_{stock}	…	Volume of BSA stock solution [ml]
ϵ_{stock}	…	Molar extinction coefficient at 280 nm [41.2 $mM^{-1}cm^{-1}$] [11]
d	…	Cuvette thickness [1 cm]
V_{elu}	…	Volume of elution solution [ml]
m_{silica}	…	Weighed mass of silica [g]

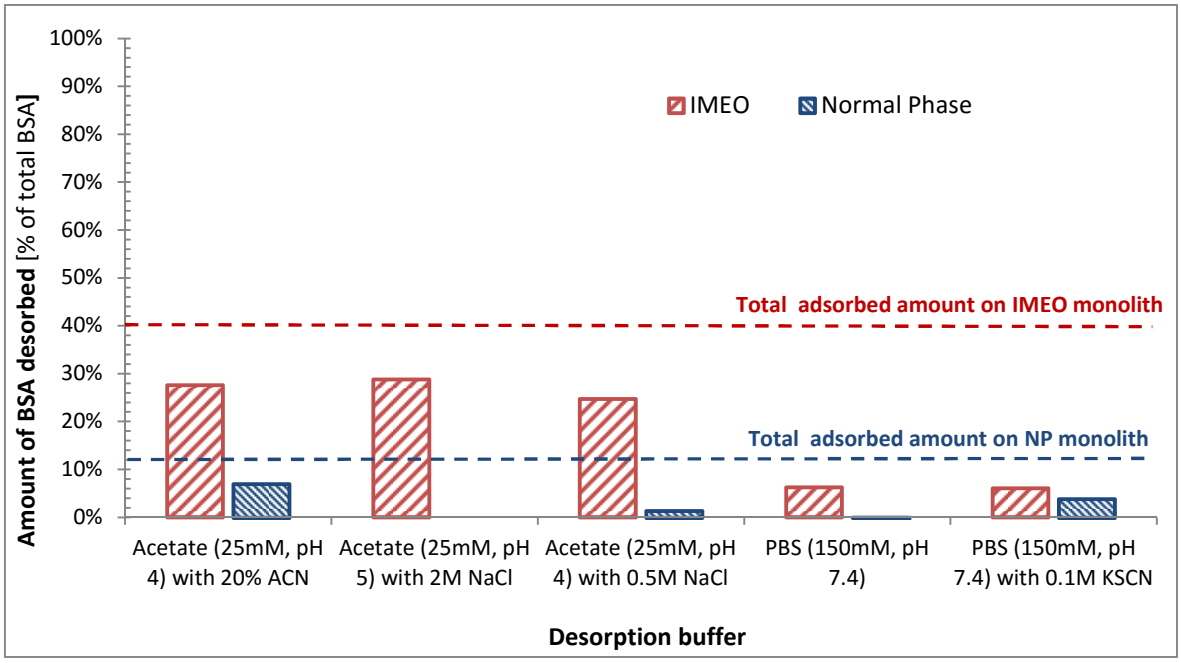

Fig. 33: Desorption of BSA from silica samples by various desorption buffers. IMEO and normal silica samples were used; the dotted-lines indicate the total amount of adsorbed BSA in relation to the total available BSA in solution

The highest desorption of BSA was performed with an ionic strength of 2 M sodium chloride, but also a pH shift from 5 to 4 has desorbed most of the protein from the IMEO functionalized silica samples (see Fig. 33). However, the recovery rate is only 70% of the total adsorbed albumin, which indicates that around 30% of the adsorbed protein has remained on the sample material.

In any case, the desorption effects of PBS and the chaotropic KSCN are rather small.

4.3.3.3 Adsorption and desorption of Immunoglobulin G

In cooperation with T. Unteregger and the Institute of Pharmaceutical Chemistry (Uni Graz) we have tested the adsorptive effect of IMEO functionalized silica on immunoglobulin G (Ig G) in batch experiments.

The experiments are described elsewhere [44], whereby dried powder samples of IMEO-monolith type A-7 and NP silica for comparison (see chapter 11.1) were used.

Unteregger [44] found a maximal binding capacity of 0.8 mg for antibodies per gram IMEO-silica, when PBS was used as adsorption buffer, which is very low related to adsorptive capacities found by Öztürk et al. [24, 25], which are located at 840 mg Ig G per gram IMEO nanoparticles and 55 mg Ig G per gram IMEO beads, respectively. However, the surface areas of the IMEO beads and nanoparticles are 2.5 to 185 times larger than the IMEO-silica particles used in this study.

It was another big problem to found an effective desorption buffer: Only the use of final sample buffer (FSB) resulted in desorption of bound antibodies. But the harsh desorption conditions and the buffer itself led to the denaturation of the antibodies. The reason for this strong immobilization may be caused by the small pores sizes of the silica. The pores are approximately in the same size range as the antibodies. In consequence, the antibodies were able to plug the pores.

Elsewhere, Deere et al. [11, 14] it was already mentioned that large molecules like proteins could hinder diffusive transport and even block pores on mesoporous silica columns. For chromatographic columns, too small pores lead to peak broadening and decrease the column efficiency. With this in mind, a suitable pore size distribution represents a critical factor for the efficiency of silica-based monolithic columns and mesoporous silicates. Furthermore, it is also mentioned that buffers with high ionic strength are not enough to desorb Cyt C, for example, from cyano-modified silicates.

In addition, a competing binding effect between albumin and antibodies with IMEO-silica could be noticed, which could be used for chromatographic purposes. [44]

4.3.4 Elution test of biomolecules

An IMEO monolithic column was prepared with the aim of separating and purifying biomolecules like proteins and amino acids.
The chromatographic characteristics of these IMEO monoliths were tested with the same model molecules as above.

IMEO-monolith (type A-15) was filled and aged in an empty solid phase extraction (SPE) column made of polypropylene (PP).

The equilibration was done with aqueous loading buffer. Subsequently, the column was loaded with a biomolecule test solution, which contained either bovine serum albumin or amino acids. The eluates were collected in separate 1 ml-fractions, unless stated otherwise. All fractions were analyzed photometrically and used to create an elution profile, to find the column capacity (for albumin) and to calculate the column´s dead volume.

4.3.4.1 Elution of amino acids (experiment 1)

Separate amino acid stock solutions (5 mg/ml) were made from glycine, L-histidine, L-phenylalanine and L-tryptophan. From all stock solutions 0.4 ml were mixed together and filled to a volume of 10 ml with acetate buffer (25 mM, pH 6.1). The end concentration of this amino acid test solution was 0.1 mg of each amino acid per ml.
The IMEO-monolith was equilibrated with 9 ml of acetate buffer (10 mM, pH 6.1, loading buffer) and subsequently loaded with 13 ml of amino acid test solution. After washing the column with further 12 ml loading buffer the amino acids were eluted with 15 ml acetate buffer (25 mM, pH 4.8) containing 2 M sodium chloride (elution buffer). The drop rate during the run was amount to 7-10 drops per minute (0.05 ml/drop, 0.4 – 0.5 ml/min).
Each collected fraction was analyzed photometrically at 280 nm for tryptophan. Afterwards, it was derivatized with ninhydrin at 570 nm (see chapter 11.2) for the determination of the total amino acid concentrations.

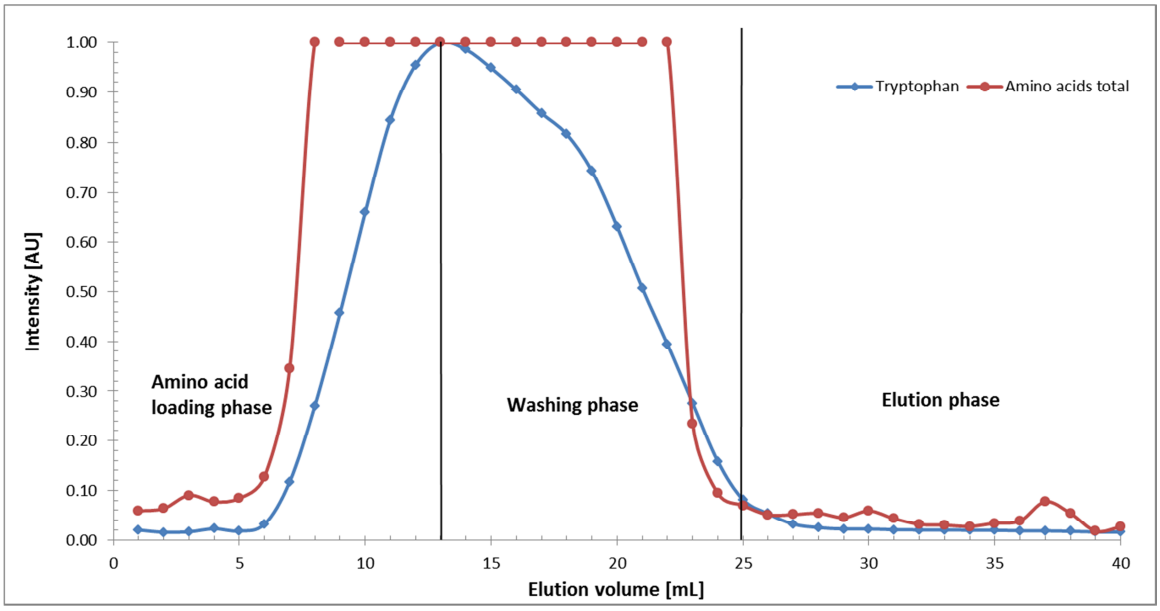

Fig. 34: Elution of a mixture of Gly, His, Phe and Trp from an IMEO-monolith (A-15). The intensity was related to the elution volume with maximum absorbance (normalized)

The elution of the amino acids is shown in Fig. 34.

It is a small retarded peak (elution volume 36 to 39) after the main peak (elution volume 5 to 26) visible. Tryptophan shows no retention, as in the experiments before (see chapter 4.3.3.1. on p. 52).

The dead volume (difference of elution volume from start to the initial signal increase) was determined to 6 ml. This corresponds to the results of the BSA elution (see chapter 4.3.4.4 on p. 65).

4.3.4.2 Elution of amino acids (experiment 2)

For a second test the same amino acid test solution was used as before.

This time the column was loaded with 1 ml of amino acid test solution, so that 200 µg of Gly, His, Phe and Trp were loaded on the column. For the first 15ml eluate an acetate buffer (25 mM, pH 6) was used, followed by an acetate buffer (25 mM, pH 6) containing 2 M sodium chloride for further 15 ml.

All eluated fractions were analyzed photometrically as described in chapter 4.3.4.1. The profile of this elution is shown in Fig. 35.

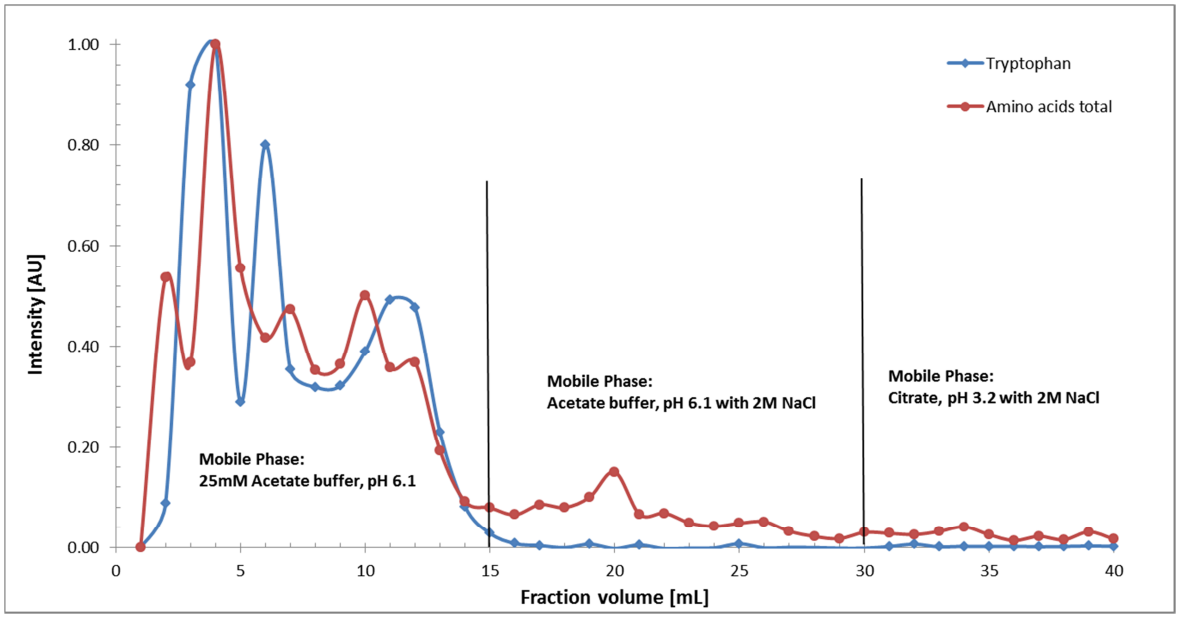

Fig. 35: Second elution of Gly, His, Phe and Trp from an IMEO-monolithic column (A-15). The intensity was related to the elution volume with maximum absorbance (normalized)

It shows a short dead volume of 2-3 mL for the same column, in contrast to Fig. 34, which points to a possibly formed sample channeling. Furthermore, Trp and the amino acids in total were eluted in multiple peaks, which also points either to sample channeling or to handling problems: A reason could be discrete backmixing of amino acid test solution with the elution buffer during loading, for example.

Evidently, all amino acids were eluted in the first phase with acetate buffer (25 mM, pH 5) at constant ionic strength. However, the small peak in fraction 20, led us to assume that minor retention to either one of the amino acids had existed. Trp can be excluded because of the missing peak in the elution profile of Trp (blue line).

4.3.4.3 Elution of amino acids (experiment 3)

For the third experiment the same column (IMOE-monolith A-15, 9 ml) as before was used. The equilibration was performed with 10 ml of carbonate buffer (25 mM, pH 10). The drop rate was determined with 7.5 drops per minute (0.05 ml/drop, 0.4 ml/min). An amino acid stock solution was prepared with 0.2 mg/ml of His, Trp and Phe containing 0.86% NaCl (HPT test solution). One ml of this test solution was applied to the column and eluted in 1ml eluate fractions as in the experiments before (see chapter 4.3.4.1 and 4.3.4.2). The mobile phase was a carbonate buffer (25 mM, pH 10). After an elution volume of 11 ml the mobile phase was changed into phosphate buffer (25 mM, pH 6) for further 9 ml. For the last 10 ml of elution the mobile phase was changed into phosphate buffer (25mM, pH 6) containing 2M

NaCl. (Note: The drop rate slowed down to 5.5 drops per minute (0.3 ml/min) in the last phase.)

The third elution of histidine, phenylalanine and tryptophan is presented in Fig. 36.

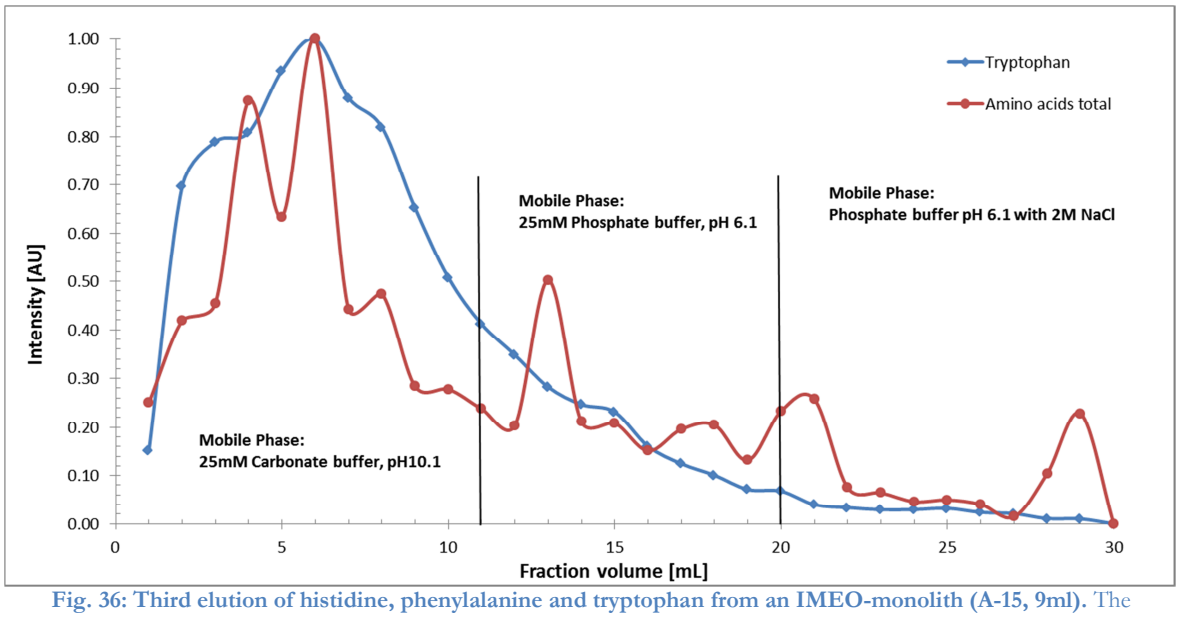

Fig. 36: Third elution of histidine, phenylalanine and tryptophan from an IMEO-monolith (A-15, 9ml). The intensity was related to the elution volume with maximum absorbance (normalized)

The determination of tryptophan and the total amino acid concentration of the eluates were performed as before (see chapters 4.3.4.1 and 4.3.4.2).

Fig. 36 reveals a few peaks that were eluted later in the third phase of the run, when Trp was already completely eluted. These peaks could indicate retention of one of the left amino acids (His or Phe).

Moreover, it is to mention that the dead volume shortened to 1-2ml in this experiment.

Subsequently, 1ml methylene blue solution (0.2 mg/ml) was applied to the column to determine the dead volume of the column. The Mb solution was eluted with 60% EtOH as mobile phase. After an elution of 10 ml, the mobile phase was changed into PBS buffer (pH 7.4). Although some Mb has still remained on the column, the test was cancelled after a total elution volume of 18 ml.

As in Fig. 37 shown, the Mb channeled and did not elute uniformly. A large quantity of Methylene blue rinsed down at the wall. For this reason, the determined dead volume of 2 ml (Fig. 36) can be regarded as too short and not significant.

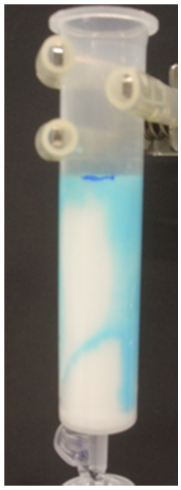

Fig. 37: Elution of Methylene blue from an IMEO-monolith (A-15).

4.3.4.4 Elution of BSA

For the elution of albumin, an IMEO-monolith (A-15, 9 ml) was equilibrated with 14ml of acetate buffer (25 mM, pH 5; loading buffer).

The albumin test solution was prepared out of 3ml BSA stock solution (10 mg/ml), which were diluted with loading buffer to an end concentration of 1.5 mg BSA. The drop rate was determined to 7-10 drops per minute (0.05 ml/drop, 0.4 – 0.5 ml/min)).

At the beginning of the experiment, the column was saturated with 15ml BSA test solution.

After loading, the column was washed with 15ml of pure loading buffer followed by elution with 15 ml of acetate buffer (25 mM, pH 5) containing 2 M NaCl.

All eluates were analyzed photometrically at a wavelength of 280 nm. The extinction coefficient of albumin was set to 0.589 ml·mg^{-1}·cm^{-1} calculated from absorbance of the BSA test solution.

The complete elution of BSA from the IMEO-monolith is shown in Fig. 38.

The column´s capacity for BSA was calculated with equation (11). It was amount to 0.85 mg BSA per ml of monolith.

$$C_{BSA} = \frac{1}{n} \cdot \sum_{f_{start}}^{f_{end}} c_i \cdot V_i \qquad (11)$$

C_{BSA}	…	Column capacity for BSA [mg BSA /ml monolith]
n	…	Number of elution fractions [8]
f_{start},f_{end}	…	Start, End fraction [#36, #43]
c_i	…	BSA concentration of individual fraction i [mg/ml]
V_i	…	Volume of fraction i [1 ml]

The dry weight of the IMEO-monolith was 5.9 grams for a column volume of 9ml (0.66 g/cm^3). In consequence, the columns capacity for BSA related to dry weight of IMEO-monolith comes to 1.3 mg BSA per gram IMEO-monolith.

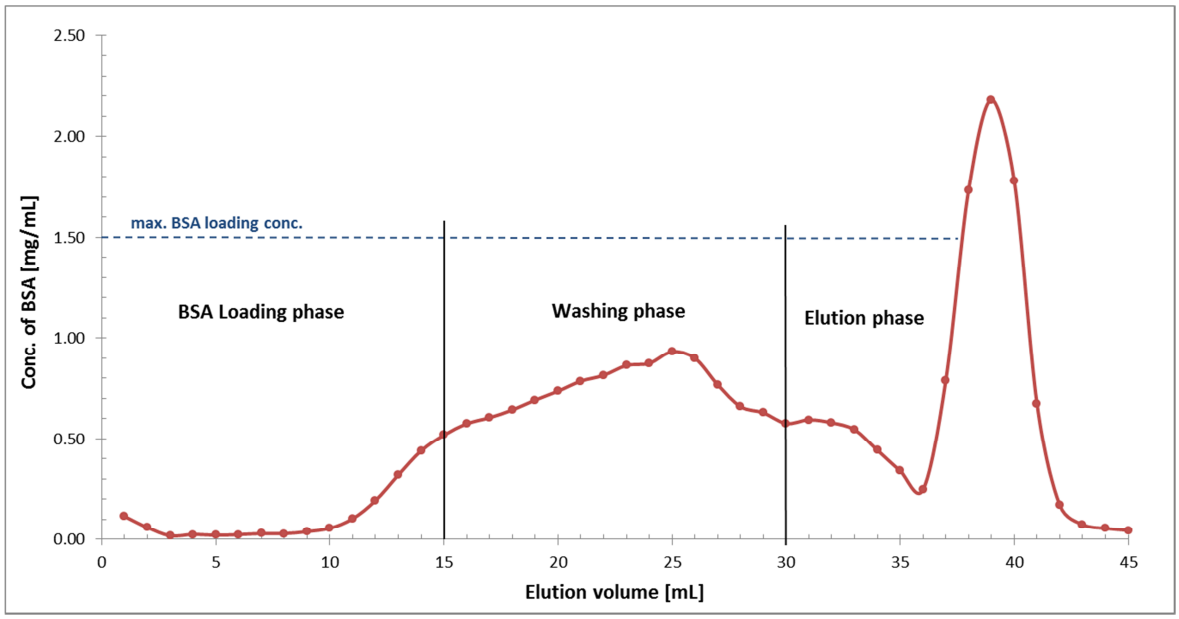

Fig. 38: Elution of BSA from an IMEO-monolithic column (A-15, 9ml).

The volume delay in the elution phase from Fig. 38 implies a dead volume of 6 ml for this IMEO-monolith, whereas, for the loading, 11ml of BSA test solution were required for a significant signal change. The eluted BSA peak was notably higher concentrated than at the start.

It is also to mention that the BSA concentration has still not reached zero after an elution volume of 45ml.

5 Conclusions

The goal of this study was to find an alternative chromatographic method to purify biomolecules like antibodies, which are able to be used in CAEC.
Therefore, a novel silica based histidine affinity column for chromatographic purposes based on imidazoles was developed in this work.
Since there wasn´t an imidazole functionalized siloxane precursor available, we had to find an alternative, which was found in IMEO. The IMEO-monolith development turned out as long-term challenge, because of two properties of IMEO: For one thing, high amounts of it weaken the monolith´s stability. In consequence, high levels of IMEO kept the batch fluid and no gelation occurred. As a result, mechanical stability competed with binding capacity. Flow rates of 2 ml per minute (by a peristaltic pump) led to the complete destruction of the IMEO-monolith.
For another thing, IMEO has catalyzed the silica based gelation reactions, i.e. the gelation time was extremely short at high concentrations. In fact, with IMEO the gelation has happened within minutes, whereas the reaction would have taken hours to even days without IMEO. The extremely short gelation times caused handling problems in the mold filling process and seemed to interfere the formation of the typically double-porous structures. Actually, any IMEO functionalized monolith neither showed a distinctly macroporous structure nor high flow rates with more than a few drops per min.

Nevertheless, infrared spectra and elementary analysis had shown the incorporation of high imidazoline concentrations into the monolith´s structure. In this context, a working silica based monolith with imidazoline-functionalization could be prepared for solid phase extractions. However, the imidazolines located on the monolith´s surface could not be determined.

BET analysis and microscopic images of IMEO-monoliths has revealed a weak emphasized double-pore system, which consisted mainly of micro- and mesopores. The absence of macropores resulted in low flow rates, but high surface areas. The existing micropores are adverse for protein diffusion because of their too small size. Unfortunately, neither an increase in porogen content nor a treatment with aqueous ammonium hydroxide solution could eliminate the micropore formation or could distinctly increase the pore sizes.
High pH values (12 and more) led to degradation of the IMEO-columns, which could be unfavorable for prospective standard cleaning procedures containing sodium hydroxide.

In sorption tests, albumin could be easily ad- and desorbed onto and from IMEO-monoliths. Adsorption and desorption were caused by ionic strength gradients of by pH changes.
Unexpectedly, we could not find a specific binding effect to IgG, which was in contrast to [24, 25]. Simple batch tests have only shown slightly unspecific adsorption, which was even lower than of normal silica. This phenomenon could be affected by the free hydroxyl groups on the IMEO-monolith´s surface. Their negative charge could interfere the interactions of the positive charged imidazolines with the antibodies. Remedial actions could be found in either endcapping the superficial hydroxyl groups or to elongate the alkyl spacer arms, which were short propyl chains in all tests. However, an endcapping would presumably influence the EOF negatively in respect of an application for CAEC.

The monolith was also tested for the sorption and retardation of several amino acids. The effect, however, was not unambiguous: The used amino acids could not be separated and eluted in distinct single peaks. In addition, the batch tests had only shown minor adsorption effects to amino acids.

Moreover, solid-phase extractions of several dyes revealed a partially inhomogenous and unstable nature of the IMEO-monoliths. The mobile phases ran faster near the walls and led to distortion and channeling effects. Nevertheless, the separation of two different dyes could be observed.
However, the kind of the retarding and separating effect stays questionable:
El-Kak et al. [21] ascribed the affinity between IgG and histidine to electrostatic mechanics and hydrogen bond interactions.
Imidazolines do not feature an aromatic ring like imidazoles and its pKa is at 11 [22]. Consequently, imidazolines are positively charged in phosphate buffers with pH 7, whereas imidazoles are uncharged at the same time. Despite of this difference, Özturk et al. [24, 25] found specific interactions between IgG and imidazolines as well as El-Kak and Vijayalakshmi [23] could demonstrate specific interactions between IgG and histidine with the same conditions.
Tests with several different charged dyes point to a weak anion exchange mechanism for imidazolines functionalized monoliths.

In summary, a silica based column with immobilized imidazolines could be developed, which showed a binding affinity to proteins like albumin by presumably weak anion exchange mechanism, but no specific tendency to antibodies.

But amino acids like tryptophan, glycine, histidine and phenylalanine interacted rarely with imidazoline-functionalized silica.

6 Outlook

IMEO-monoliths have the potency to retard proteins like albumin and could be employed as weak anion exchange system. Nevertheless the monoliths do not show any affinity to antibodies. In this context, the system needs to be strongly optimized and adjusted for antibody purification purposes.
Such an improvement could be an endcapping of the monolith.
Studies with longer spacer arms between silicium atom and imidazoline would also be sensible. Additionally, the use of alternative functional moieties (histidines, imidazoles, etc.) could also improve the antibody binding efficiency.
More details about its separation properties might bring a direct application as HPLC or CEC column, which would have gone beyond the scope of this study, however.
Nevertheless, further investigations in respect to the combination of histidine affinity chromatography and monolithic column techniques seems to be worthwhile: Antibody therapeutics are concentrated on IgGs [1] and histidine affinity chromatography could already prove its high affinity for this class of antibodies as well as for the separation of other important proteins [20, 21, 45]. Purification can be directly made from the blood serum by simple salt gradients.

Additionally, monolithic double-pore columns take care for high throughput and capacity. The production of such a functionalized silica-based column can be done easily in a one-pot synthesis as in this study shown. Furthermore, the synthesis is nontoxic, easy and fast.

A further task is to scale-up IMEO-monoliths and test it for CAEC applications. Although, the general scale-up and the applicability of silica-based monoliths for CAEC has been proven by Braunbruck et al. [10], the adaption of (imididazoline) functionalized monoliths to CAEC will be another major challenge, but it might be worth …

7 Experimental

7.1 Chemicals

- Acetic acid, ≥99% (Sigma-Aldrich, A6283)
- Albumin from bovine serum, ≥98% lyophilized powder (Sigma, A7906, Lot SLBD5326V)
- Ammonium Hydroxide 28.0-30.0%, ACS reagent (J.T. Baker, 9721)
- Brilliant Green, Dye content ~90% (Sigma, B6756)
- Calconcarboxylic acid (Sigma, H3128)
- Diethylamine, p.a. (Sigma, 31730)
- Ethanol denatured, ≥99.8% with -1% MEK (Roth, K928)
- Glycine, ReagentPlus ≥99% (HPLC) (Sigma, G7126)
- Hexadecyltrimethylammonium bromide, ≥99% (Sigma, H6269)
- Hydrochloric acid 1N, volumetric standard solution (Roth, K025)
- Hydrochloric acid fuming 37%, p.a. (Roth, 4625)
- Isopropanol, ROTISOLV® HPLC (Roth, 7343)
- L-Histidine, ReagentPlus ≥99% (TLC) (Sigma, H8000)
- L-Phenylalanine, reagent grade ≥98% (Sigma, P2126)
- L-Tryptophan, reagent grade ≥98% (HPLC) (Sigma, T0254)
- Methanol, ROTISOLV® HPLC Gradient Grade (Roth, 7342)
- Methyl red, ACS reagent, crystalline (Sigma 250198)
- Methylene blue, for microscopy (Merck, 1283)
- N,N-Dimethylformamid, ≥99.5% z. syn. (Roth, 6251.2)
- N,N-Dimethylformamide, ≥99.5% (Roth, 7342)
- ortho-Phosphoric acid 85%, p.a. (Roth, 6366)
- Poly(ethylene glycol), average Mn 300 (Aldrich, 202371)
- Poly(ethylene glycol), average Mn 6000 (Aldrich, 81260)
- Potassium acetate, puriss p.a. ≥99% (Sigma 32309)
- Potassium phosphate monobasic, ReagentPlus (Sigma, P5379)
- Sodium chloride, >99.8% (Roth, 9265.2)
- Sodium hydroxide in pellets, ≥99% p.a. (Roth, 6771)

- Sodium hydroxide, ≥99% p.a., (Roth, 6771.1)
- Tetraethyl orthosilicate, ≥99.0% (GC) (Aldrich, 86578)
- Triethoxy-3-(2-imidazolin-1-yl)propylsilane, ≥97.0% (NT) (Aldrich, 56760; Lot BCBL0518, BCBP9562)
- TRIS, Pufferan ≥99.3%, buffer Grade (Roth, AE15.1)

7.2 Lab equipment

- FTIR spectrometer: VERTEX 70, Bruker, Software: OPUS
- Elemental analysis vario EL III Element Analyzer, elementar Analysensysteme GmbH (Institute of Anorganic Chemistry, TU Graz)
- Gas pycnometer AccuPyc II 1340, Micromeritics Instrument Corp.
- Microscope DM 4000 M, Leica, Software: Leica Application Suite
- Particle size analysis with laser diffraction HELOS/BR with RODOS (dry disperser), Sympatec GmbH
- Surface area & porosity Tristar II 3020, Micromeritics Instrument Corp.
- UV-VIS spectrometer Lambda 950, Perkin Elmer

7.3 Other materials

7.3.1 For monolith preparation

- Pasteur pipettes, without cotton stoppers (Roth, 4522)
- Chromabond empty columns, 15 ml, PP (Lactan, 730230)

7.3.2 For monolith characterization

- Disposable semi-microcuvettes (Lactan, 297872810)

8 REFERENCES

[1] A.A. Shukla, B. Hubbard, T. Tressel, S. Guhan, D. Low, Downstream processing of monoclonal antibodies--application of platform approaches, Journal of chromatography. B, Analytical technologies in the biomedical and life sciences 848 (2007) 28–39.

[2] P. Latza, P. Gilles, T. Schaller, T. Schrader, Affinity polymers tailored for the protein A binding site of immunoglobulin G proteins, Chemistry (Weinheim an der Bergstrasse, Germany) 20 (2014) 11479–11487.

[3] P. Gagnon, Technology trends in antibody purification, Journal of chromatography. A 1221 (2012) 57–70.

[4] S. Kanoun, L. Amourache, S. Krishnan, M.A. Vijayalakshmi, New support for the large-scale purification of proteins, Journal of Chromatography B: Biomedical Sciences and Applications 376 (1986) 259–267.

[5] Y.H. Tan, M. Liu, B. Nolting, J.G. Go, J. Gervay-Hague, G.-y. Liu, A nanoengineering approach for investigation and regulation of protein immobilization, ACS nano 2 (2008) 2374–2384.

[6] R. Hahn, R. Schlegel, A. Jungbauer, Comparison of protein A affinity sorbents, Journal of Chromatography B 790 (2003) 35–51.

[7] R. Laskowski, Hydrodynamik und Joulesche Wärme in der präperativen kontinuierlichen anularen Elektrochromatographie (CAEC). Dissertation, Kaiserlautern, 2015.

[8] M.-G. Braunbruck, H. Gruber-Wölfler, P. Feenstra, R. Laskowski, H.-J. Bart, J.G. Khinast, Funktionalisierte mesoporöse Monolithen für kontinuierliche Ringspalt-Elektrochromatographie, Chemie Ingenieur Technik 84 (2012) 1400.

[9] M.-G. Braunbruck, Development of a stationary phase for continous annular electro chromatography. Diplomarbeit, Graz, 2009.

[10] M.-G. Braunbruck, Preparation, Characterization and simulation of functionalized monolithic materials for electrochromatography. Dissertation, Graz, 2013.

[11] J. Deere, E. Magner, J.G. Wall, B.K. Hodnett, Mechanistic and Structural Features of Protein Adsorption onto Mesoporous Silicates, J. Phys. Chem. B 106 (2002) 7340–7347.

[12] M. Wu, R. Wu, Z. Zhang, H. Zou, Preparation and application of organic-silica hybrid monolithic capillary columns, Electrophoresis 32 (2011) 105–115.

[13] J. Díaz, K.J. Balkus, Enzyme immobilization in MCM-41 molecular sieve, Journal of Molecular Catalysis B: Enzymatic 2 (1996) 115–126.

[14] L. Rieux, H. Niederländer, E. Verpoorte, R. Bischoff, Silica monolithic columns: Synthesis, characterisation and applications to the analysis of biological molecules, J. Sep. Science 28 (2005) 1628–1641.

[15] A.-M. Siouffi, Silica gel-based monoliths prepared by the sol–gel method: facts and figures, Journal of Chromatography A 1000 (2003) 801–818.

[16] N. Tanaka, H. Kobayashi, K. Nakanishi, H. Minakuchi, N. Ishizuka, Peer Reviewed: Monolithic LC Columns, Anal. Chem. 73 (2001) 420 A–429 A.

[17] M. Stiess, Mechanische Verfahrenstechnik: Partikeltechnologie, third., vollständig neu bearbeitete Aufl., Springer Berlin Heidelberg, Berlin, Heidelberg, 2009.

[18] O. Núñez, K. Nakanishi, N. Tanaka, Preparation of monolithic silica columns for high-performance liquid chromatography, Journal of chromatography. A 1191 (2008) 231–252.

[19] N. Tanaka, H. Kobayashi, N. Ishizuka, H. Minakuchi, K. Nakanishi, K. Hosoya, T. Ikegami, Monolithic silica columns for high-efficiency chromatographic separations, Journal of Chromatography A 965 (2002) 35–49.

[20] M. Vijayalakshmi, Pseudobiospecific ligand affinity chromatography, Trends in Biotechnology 7 (1989) 71–76.

[21] A. El-Kak, S. Manjini, M.A. Vijayalakshmi, Interaction of immunoglobulin G with immobilized histidine: mechanistic and kinetic aspects, Journal of Chromatography A 604 (1992) 29–37.

[22] Information on https://scifinder.cas.org/scifinder/view/scifinder/scifinderExplore.jsf (access on 6th August 2015)

[23] A. El-Kak, M.A. Vijayalakshmi, Study of the separation of mouse monoclonal antibodies by pseudobioaffinity chromatography using matrix-linked histidine and histamine, Journal of Chromatography B: Biomedical Sciences and Applications 570 (1991) 29–41.

[24] N. Öztürk, N. Bereli, S. Akgöl, A. Denizli, High capacity binding of antibodies by poly(hydroxyethyl methacrylate) nanoparticles, Colloids and surfaces. B, Biointerfaces 67 (2008) 14–19.

[25] N. Öztürk, M.E. Günay, S. Akgöl, A. Denizli, Silane-modified magnetic beads: application to immunoglobulin G separation, Biotechnology progress 23 (2007) 1149–1156.

[26] M. Al-Bokari, D. Cherrak, G. Guiochon, Determination of the porosities of monolithic columns by inverse size-exclusion chromatography, Journal of Chromatography A 975 (2002) 275–284.

[27] A. Soleimani Dorcheh, M.H. Abbasi, Silica aerogel; synthesis, properties and characterization, Journal of Materials Processing Technology 199 (2008) 10–26.

[28] T. Amatani, K. Nakanishi, K. Hirao, T. Kodaira, Monolithic Periodic Mesoporous Silica with Well-Defined Macropores, Chem. Mater. 17 (2005) 2114–2119.

[29] S. Constantin, R. Freitag, Preparation of stationary phases for open-tubular capillary electrochromatography using the sol–gel method, Journal of Chromatography A 887 (2000) 253–263.

[30] M.T. Dulay, R.P. Kulkarni, R.N. Zare, Preparation and characterization of monolithic porous capillary columns loaded with chromatographic particles, Analytical chemistry 70 (1998) 5103–5107.

[31] L.L. Hench, J.K. West, The sol-gel process, Chem. Rev. 90 (1990) 33–72.

[32] X. Wang, Lin, Kyle S K, Chan, Jerry C C, S. Cheng, Direct synthesis and catalytic applications of ordered large pore aminopropyl-functionalized SBA-15 mesoporous materials, The journal of physical chemistry. B 109 (2005) 1763–1769.

[33] N. Ishizuka, H. Minakuchi, K. Nakanishi, N. Soga, N. Tanaka, Designing monolithic double-pore silica for high-speed liquid chromatography, Journal of Chromatography A 797 (1998) 133–137.

[34] K. Kajihara, M. Hirano, H. Hosono, Sol-gel synthesis of monolithic silica gels and glasses from phase-separating tetraethoxysilane–water binary system, Chem. Commun. (2009) 2580.

[35] A. Drescher, Herstellung und Charakterisierung von Monolithen zur kontinuierlichen katalytischen Synthese. Bachelorarbeit, Graz, 2014.

[36] A. Rao, M.M. Kulkarni, Effect of glycerol additive on physical properties of hydrophobic silica aerogels, Materials Chemistry and Physics 77 (2003) 819–825.

[37] C. Baleizão, Periodic mesoporous organosilica incorporating a catalytically active vanadyl Schiff base complex in the framework, Journal of catalysis 223 (2004) 106–113.

[38] S.L. Hruby, B.H. Shanks, Acid–base cooperativity in condensation reactions with functionalized mesoporous silica catalysts, Journal of catalysis 263 (2009) 181–188.

[39] X. Wang, Lin, Kyle S K, Chan, Jerry C C, S. Cheng, Preparation of ordered large pore SBA-15 silica functionalized with aminopropyl groups through one-pot synthesis, Chemical communications (Cambridge, England) (2004) 2762–2763.

[40] A. Venkateswara Rao, S.D. Bhagat, Synthesis and physical properties of TEOS-based silica aerogels prepared by two step (acid–base) sol–gel process, Solid State Sciences 6 (2004) 945–952.

[41] K.S.W. Sing, Reporting physisorption data for gas/solid systems with special reference to the determination of surface area and porosity (Recommendations 1984), Pure and Applied Chemistry 57 (1985).

[42] K. Nakanishi, H. Minakuchi, N. Soga, N. Tanaka, Structure Design of Double-Pore Silica and Its Application to HPLC, Journal of Sol-Gel Science and Technology 13 (1998) 163–169.

[43] W.M. Haynes, CRC handbook of chemistry and physics, ninththirdrd ed., twentiethtwelfth-twentieththirteenth, CRC; Taylor & Francis [distributor], Boca Raton, Fla., London, 2012.

[44] T. Unteregger, Development of Methods for the Continous Purification of Biopharmaceuticals Using Electrophoresis and Monolithic Stationary Phases. Master Thesis, Graz, 2015.

[45] X. Wu, K. Haupt, M.A. Vijayalakshmi, Separation of immunoglobulin G by high-performance pseudo-bioaffinity chromatography with immobilized histidine I. Preliminary report on the influence of the silica support and the coupling mode, Journal of Chromatography B: Biomedical Sciences and Applications 584 (1992) 35–41.

[46] R.B. Chavan, G. Nalankilli, Observations on the estimation of amino groups in silk using ninhydrin reaction, Indian Journal of Fibre & Textile Research 18 (1993) 129.

[47] Information on http://www.eng.umd.edu/~nsw/ench485/lab3a.htm (access on 23th October 2015)

[48] S. Balakrishnan, N.J. Zondlo, Design of a protein kinase-inducible domain, Journal of the American Chemical Society 128 (2006) 5590-5591.

9 List of figures

Fig. 1: Structure of IgG.. 3
Fig. 2: Typical downstream process for (monoclonal) antibodies. 4
Fig. 3: Scheme of a continuous annular electro-chromatography system 7
Fig. 4: Prototype of a CAEC with monolithic stationary phase. 7
Fig. 5: Overview of chromatographic affinity ligands. 13
Fig. 6. Precursor for the imidazoline ligand (IMEO). 15
Fig. 7: Structures of the immobilized pseudoaffinity ligands, histidine and imidazoline. 16
Fig. 8: Structure of an IMEO-functionalized monolithic column. 18
Fig. 9: Hydrolysis and Condensation reactions of alkoxysilanes 22
Fig. 10: Relative hydrolysis and condensation rates vs pH of the reaction mixture. 23
Fig. 11: Ternary phase diagram of TEOS-alcohol-water. 28
Fig. 12: Relationship of Silica-PEG-solvent mixtures for monolith preparations 30
Fig. 13: Defects of IMEO-monoliths. 35
Fig. 14: Methyl red stained IMEO-monolith. 36
Fig. 15: IMEO-monolith type A-7. 39
Fig. 16: IMEO-monolith type B-40. 39
Fig. 17: FTIR spectrum of an IMEO monolith type A 40
Fig. 18: Particle size distribution of powdered IMEO monolith A-7. 41
Fig: 19: Isotherm Linear Plot of an IMEO-monolith type A-7. 42
Fig. 20: Imidazoline moiety with propyl chain (ligand) from IMEO. 44
Fig. 21: Outer structure of dried IMEO monoliths (type A) 45
Fig. 22: Structure of dried IMEO monoliths (type A) 46
Fig. 23: Structure of dried IMEO monolith (type B) 46
Fig. 24: Swelling test of an IMEO-silica powder (type A-7) 47
Fig. 25: Concentrations of IMEO recovered in various elution buffers. 48
Fig. 26: Molecular structures of the used dyes 49
Fig. 27: Separate elution of various dye solutions 50
Fig. 28: Elution profile of the dye mixture eluted from an IMEO monolith (type A-7). 52
Fig. 29: Adsorption of Trp on IMEO-silica (A-7, powder) 54
Fig. 30: Adsorption of several amino acids on IMEO-silica (A-7) powder. 55
Fig. 31: Adsorption of BSA with various pH buffers 58
Fig. 32: Adsorption capacity of BSA versus ionic strength of the adsorption buffer 58

Fig. 33: Desorption of BSA from silica samples by various desorption buffers 59
Fig. 34: Elution of a mixture of Gly, His, Phe and Trp from an IMEO-monolith (A-15).....62
Fig. 35: Second elution of Gly, His, Phe and Trp from an IMEO-monolithic column.....63
Fig. 36: Third elution of histidine, phenylalanine and tryptophan from an IMEO-monolith...64
Fig. 37: Elution of Methylene blue from an IMEO-monolith (A-15). 65
Fig. 38: Elution of BSA from an IMEO-monolithic column (A-15, 9ml). 66
Fig. 39: Reaction of ninyhdrin with amino acids. modified according to[46].....79

10 List of tables

Table 1: Comparison between protein A and histidine affinity chromatography. 15
Table 2: Properties of typical monolithic columns. 19
Table 3: Overview of selected components for the IMEO-monolith synthesis. 37
Table 4: Composition (molar equivalents) of the two IMEO-monoliths 38
Table 5: BET nitrogen adsorption analyses of several monolithic test specimen.....42
Table 6: True density of IMEO-monolith specimen. Measured by nitrogen pycnometry 43
Table 7: CHN Elementary analysis of IMEO monolith A.....44
Table 8: Test for chemical resistance to mobile phases of IMEO-monolith A. 48
Table 9: Used mobile phases for the elution of the single dye solutions.....50
Table 10: Elution of a dye mixture from an IMEO monolith (A-7).....51
Table 11: Relevant data about the used amino acids.:.....53
Table 12: Buffers used for the BSA adsorption and desorption test on IMEO-silica 56
Table 13. Wavelengths for the photometrical analysis of various substances. 80
Table 14: List of prepared monolith batches.....81

11 APPENDIX

11.1 Normal-phase silica preparation

Normal silica (normal phase, NP) were prepared for comparison purposes according to a slight modified method of M.-G. Braunbruck [10].

At the beginning, 0.09 gram of CTAB (0.26 mmol, 0.02 equiv) were weighed in a round-bottom flask and dissolved in 3.6 ml of EtOH (62 mmol, 4.6 equiv.) and 1.2 ml of water (67 mmol, 5.0 equiv.). 3.0 ml TEOS (13 mmol, 1 equiv.) and 0.6 ml *N,N*-dimethylformamide (DMF, 8 mmol, 0.6 equiv.) were added to the solution. The mixture was heated in a sealed flask at 40°C for one hour. Then, 0.015 ml of diethylamine (DEA, 1.5 mmol, 0.11 equiv.) were added to the solution. The mixture reacted within 6 to 8 minutes and formed a solid and milky gel. After aging for 18 hours at ambient temperature the batch was washed with water, 0.01M aqueous ammonia hydroxide solution and 60% EtOH.

For silica preparation, the gel was additionally pestled and dried at 100°C in a kiln.

11.2 Ninhydrin derivatization

Ninhydrin reacts with amines in amino acids, but also with imidazolines and forms a blue to purple compound known as Ruhmann´s purple, which can photometrically detected at a wavelength of 570 nm. [46]

The reaction is very sensitive and a cheap method to detect amino acids, but also column bleeding of IMEO monolithic columns.

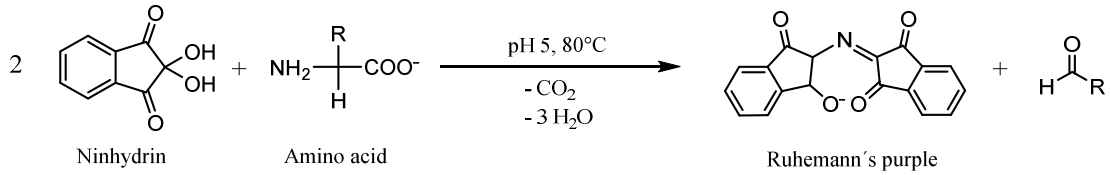

Fig. 39: Reaction of ninyhdrin with amino acids. modified according to[46]

The analysis of both amino acids and IMEO concentration was done with a modified assay from Nam Sun Wang [47]:

For the ninhydrin test solution, one gram of ninhydrin was dissolved in a mixture of 25 ml of EtOH abs. and 25 ml of acetate buffer (250 mM, pH 5).

For both, the amino acid and column bleeding analysis, 0.4 ml of sample solution were mixed with 0.6 ml ninhydrin test solution. The sample mixture reacts on a shaker with 500 rpm at 80°C for 15 min. All samples were cooled down to ambient temperature and analyzed photometrically at 570 nm.

11.3 Photometrical analysis

All photometrical analyses were done in disposable semi-micro cuvettes made of PMMA on a Lambda 950 (Perkin Elmer) UV-VIS spectrometer. Pure water or pure buffer solution, respectively, served as reference solution. All sample solutions were tested in scan-mode with a resolution of 2 nm, unless stated otherwise. The used wavelengths of each measured analyte are listed in Table 13.

Table 13. Wavelengths for the photometrical analysis of various substances.

	Wavelength		Max. absorbance	
Analyte	**From … nm**	**To … nm**	**at … nm**	**Notes**
BSA	Single WL-Mode		278	Molar extinction coeff.: 41.2 $mM^{-1}cm^{-1}$ acc. to [11]
Tryptophan	260	300	279	
Ruhmann´s purple	540	600	570 (+/- 10)	Reaction of amines with ninhydrin; WL of max. absorb. is dependent of pH and reactant

11.4 List of monolith batches

The subsequent table lists all produced monolith batches during the monolith development process. It contains component amounts, synthesis procedures, test results, notes and posttreatments. Furthermore, it references to analyses and photos of certain monolith batches. All samples are labelled with a code letter followed by a consecutive batch number. The meaning of the code letters is as follows:

C	…	Modified according to [35]
IM	…	Variable IMEO concentration
M	….	Monolith batch
P	….	Variable PEG concentration
pH	…	Variable pH values
S	…	Variable Solvent concentration

Monolithic types:

RP = reversed phase, NP = normal phase (no functionalization), NH2 = Amino functionalized, IMEO = imidazoline functionalized

All equivalents are related to the amount of either TEOS or TMOS, as already mentioned elsewhere.

Table 14: List of prepared monolith batches (raw data)
(see following pages)

	A	B	C	D	E	F	G	H	I	J	K	L	M	N	O
1	**Batch**		**M1**	**M2**	**M3**		**M5**	**M8**	**M9**	**M10**	**M11**	**M12**	**M13**	**M14**	**M15**
2	monolithic type		RP	IMEO	RP		NH2	RP	RP	RP	RP	RP	RP	RP	RP
3	Reaction vessel		rbf, 50ml	rbf, 25ml	rbf, 50ml		rbf, 50ml	rbf, 10ml	rbf, 25ml	rbf, 10ml	rbf, 10ml	rbf, 25ml	rbf, 10ml	rbf, 10ml	rbf, 10ml
4	Network former	TEOS [ml]	2	2	2		2.32	0.5	0.5	0.5	0	0.5	0.5	0.5	0.5
5		TMOS [ml]													
6	Functionalized silica	SH-TMOS [ml]													
7		C8-TEOS [ml]	1.12		1.12			0.28	0.28	0.28	0.8	0.28	0.28	0.56	0.26
8	Porogen	PEG (MW: 6000] [mg]													
9		PEG (MW: 300] [mg]													
10		CTAB [mg]	134	133	134		150	33	66.2	33.3	33.7	0	33.1	33.9	33.6
11	Solvent	MeOH [ml]						1	1	1	1	1			
12		EtOH [ml]	4	4	4		3.84						1	1	1
13		PrOH [ml]													
14	DCCA	DMF [ml]													
15	Reagent	HCl [mg]	4.01	4.01	4.01			1.02	1.02	1.02	1.02	1.02	1.02	1.02	1.02
16		HAc, glacial [ml]													
17		H3PO4 [mg]													
18		HNO3 [mg]													
19		Formic acid [ml]													
20		NaOH [mg]													
21		NH4OH [mg]													
22		H2O, total [ml]	0.47	0.44	0.47		0.64	0.11	0.11	0.11	0.11	0.11	0.11	0.11	0.11
23	Catalyst	IMEO [ml]		1											
24		DEA [ml]	0.44		0.44			0.44	0.44	0.44	0.44	0.44	0.44	0.44	0.11
25		APTES [ml]					1.2								
26		Temp. [°C] while adding catalyst	20	40	40		40	20	20	20	20	20	20	20	20
27	Solidifier	Polygosil [mg]						26	26.3	27.4	26.6	26.7	27.1	27.4	25.9
30	Usage of buffer (pH)		no	no	no		no	no	no	no	no	no	no	no	no
31	Reaction conditions	Temp. [°C]	70	70	70		70	60	60	60	60	60	60	60	60
32		Duration [h]	1	0.17	1		0.17	1	1	1	1	0.5	1	1	1
33		Vessel	open	open	open		closed	closed	closed	closed	closed	closed	closed	closed	closed
34		Stirring	yes	yes	yes		yes	yes	yes	yes	yes	yes	yes	yes	yes
35		Reaction notes													
36	Synthesis results	Solid point [min]	15	0.01	<15		2	10	16	26	n/a	16	n/a	n/a	70
37		monolith form	opaque, homogen	yellowish, transparent, rubberlike	yellowish, transparent,		milky, homogen	milky	milky	yellowish, milky	phase separation; no solid form		no solid form	no solid form	n/a
38		flushable	no	n/a	no		yes	yes	no	no	n/a	yes (MeOH)			no
39		Flow rate [drops/min]					n/a	12 (MeOH)				slow, increase with time			
40		Dried monolithic form	monolithic mass (dried): 0.27g (0.8cm^3)		keep form, contraction, cracks, hard; monolithic mass(dried): 0.27g (0.9cm^3)		monolithic mass(dried): 0.28g (1.0cm^3)	electrostatic, contraction, forms cracks	forms cracks, keeps form mainly, contraction, rosa-brownish	yellowish, contraction, brownish at the edge		electrostatic, cracks,			keeps form, smooth surface
41		Synthesis notes						monolithic mass: 1.51g;	Polygosil sedimented; drying forms cracks, keep form mainly, but contraction; monolithic mass: 1.39g;	solid sedimented partly; monolithic mass: 1.71g;		monolithic mass: 1.33g;			monolithic mass: 1.29g;
42	Photos	Casio Exilim		7823	7824		7825	7826	7827	7828		7829			7830
44		Microscope													
45	IR-analysis			yes			yes								
46	Particle analysis														
47		HELOS													
48	Curing														

	P	Q	R	S	T	U	V	W	X	Y	Z	AA	AB	AC	AD
1	**M16**	**M17**	**M18**	**M19**	**M20**	**M21**	**M22**	**M23**	**M24**	**M25**	**M26**	**M27**	**M28**	**M29**	**M30**
2	RP	RP	RP	IMEO	IMEO	IMEO	IMEO	IMEO	IMEO	IMEO	IMEO	IMEO	IMEO	IMEO	IMEO
3	rbf, 10ml	rbf, 10ml	rbf, 10ml	rbf, 10ml	rbf, 10ml	rbf, 10ml	rbf, 10ml	rbf, 10ml	ct, 15ml	ct, 15ml	ct, 15ml	ct, 15ml	ct, 15ml	ct, 15ml	ct, 15ml
4	0.5	0.5	0.5	0.5	0.5	0.5	0.5	0.5	0.5	0.5	0.5	0.5	0.5	0.5	0.5
5															
6															
7	0.28	0.56	0.56												
8															
9															
10	33.8	33.9	33.2	41.6	41.3	40.8	41.3	41.1	41.7	41.1	40.8	41.6	41.4	41.3	41.4
11	1	1		0.91		0.91							0.91		
12			1		1.33		1.33		1.32					1.32	1.32
13								1.74				1.74			
14										1.74	1.74				
15	1.02	1.02	1.02	0.82	0.82	0.82	0.82	0.82		0.82				0.82	
16									1.30E-02		1.30E-02	1.30E-02			1.30E-02
17															
18															
19															
20													0.88		
21															
22	0.11	0.11	0.11	0.11	0.11	0.11	0.11	0.11	0.06	0.11	0.06	0.06	0.083	0.11	0.06
23				0.31	0.31	0.31	0.31	0.31	0.31	0.31	0.31	0.31	0.31	0.31	0.15
24	0.11	0.11	0.11												
25															
26	20	20	20	20	20	4	4	4	4	4	4	4	4	4	4
27	26.1	25.8	25.8	20.6	20.5	20.8	20.2	19.7	20.9	20.9	20.6	19.7	19.4		
30	no	no	no	no	no	no	no	no	no	no	no	no	no	no	no
31	60	60	60	60	60	60	60	60	60	60	60	60	60	60	60
32	1	1	1	1	1	1	1	1	1	1	1	1	1	1	1
33	closed	closed	closed	closed	closed	closed	closed	closed	closed	closed	closed	closed	closed	closed	closed
34	yes	yes	yes	yes	yes	yes	yes	yes	no	no	no	no	no	no	no
35															
36	10	n/a	n/a	0.5	0.9	0.5	1	7	20	5	30	25	16	2	15
37	milky	phase separation; no solid form	phase separation; no solid form	yellowish, transparent, soft	yellowish, transparent	yellowish, transparent	yellowish, transparent	yellowish, transparent	yellowish, dull	yellow, transparent, rubber-like	yellow, milky, soft (pasty)	milky,soft	yellowish, milky, separate particles in monolith	phase separation, opaque transparent	milky
38	yes			n/a	yes	yes	yes	yes	no	yes	yes	yes	yes	yes	no
39	1.2 (MeOH)			n/a	EtOH rinses through	MeOH rinses through	EtOH rinse through	PrOH rinses through		DMF rinses through		PrOH rinses through	MeOH rinses through	EtOH rinses through	
40				N/a											
41	solvent flush changed colour (yellowish->colourless); monolithic mass: 1.48g;				no adhesion to glass wall	no adhesion to glass wall	no adhesion to glass wall	no adhesion to glass wall	polygosil on ground	polygosil on ground	bad spots, soft	no adhesion to glass wall	no adhesion to glass wall; polygosil on ground	no adhesion to glass wall	no adhesion to glass wall
42				7831	7832, 7833	7834	7835	7836	7837	7838	7839	7840	7841	7842, 7851, 7860	7843, 7852. 7861
44						632	633	648	646	649	650	651	0652, 0653	0663-0665	0666, 0667
45				yes	yes	yes	yes	yes	yes	yes	yes	yes	yes	yes	yes
46															
47															
48															

	AE	AF	AG	AH	AI	AJ	AK	AL	AM	AN	AO	AP	AQ	AR	AS
1	**M31**	**M32**	**M33**	**M34**	**M35**	**M36**	**M37**	**M38**	**M39**	**M40**	**M41**	**M42**	**M43**	**M44**	**M45**
2	IMEO	IMEO	IMEO	IMEO	IMEO	IMEO	IMEO	IMEO	IMEO	IMEO	IMEO	IMEO	IMEO	IMEO	IMEO
3	ct, 15ml	ct, 15ml	ct, 15ml	ct, 15ml	ct, 15ml	ct, 15ml	ct, 15ml	ct, 15ml	ct, 15ml	ct, 15ml		ct, 15ml	ct, 15ml	ct, 15ml	ct, 15ml
4	0.5	0.5	0.5	0.5	0.5	0.5	0.5	0.5	0.5	0.5	0.5	0.5	0	0.5	0.5
5															
6															
7															
8				381.8	676.4	65.3	0	44.2	43.4	45.3	44.5		42.1		44.6
9												2.2		2.2	
10	41.1	41.8	82.4												
11															1
12	1.32	1.32	1.32	1.32	1.32	1.32	1.32		1.32	1.32	1.32	1.32	1.32	1.32	
13															
14															
15		0.42													
16	2.60E-02		1.30E-02	1.30E-02	1.30E-02	1.30E-02	1.30E-02	4.23E-04			3.55E-05	1.30E-02	3.55E-05	3.55E-05	3.55E-05
17										21.5					
18									13.8						
19															
20															
21															
22	0.06	0.08	0.06	0.06	0.06	0.06	0.06	0.74	0.06	0.06	0.06	0.06	0.06	0.06	0.06
23	0.31	0.31	0.31	0.31	0.31	0.31	0.31	0.31	0.31	0.31	0.31	0.31	0.93	0.31	0.31
24															
25															
26	4	4	4	20	20	20	4	4	20	20	20	20	20	20	20
27															
30	no	no	no	no	no	no	no	no	no	no	no	no	no	no	no
31	60	60	60	60	60	60	60	4	60	60	60	60	60	60	60
32	1	1	1	1	1	1	1	0.5	1	1	1	1	0.17	1	1
33	closed	closed	closed	closed	closed	closed	closed	closed	closed	closed	closed	closed	closed	closed	closed
34	no	no	no	no	no	no	no	no	no	no	no	no	no	no	no
35															
36	11	3	13	63	21	33	25	5	3	0.01	10	5	n/a	13	9
37	milky	opaque, transparent	milky	milky, separate particles inside	milky,separate particles inside	milky,separate particles inside	milky	phase separation: milky solid/transparent solid;	opaque, transparent, hard	n/a	milky, soft	milky	no solid form	(opaque, transparent, soft)	(opaque, transparent, soft)
38	no	yes	no	yes	yes	yes	no	no	no	n/a	yes	yes	n/a	yes	no
39		EtOH rinses through							monolith washed out						
40															
41		no adhesion to glass wall, hard structure	no adhesion to glass wall	PEG unsoluble at RT and sedimented;	PEG unsoluble at RT and sedimented;	PEG unsoluble at RT and sedimented;		acc. to Lit#27 (Lab book. p. 30)	no adhesion at glass wall		soft			soft;	soft; low adhesion to glass wall
42	7844, 7853, 7862	7845, 7854, 7863	7846, 7855, 7864	7847, 7856, 7865	7848, 7857, 7866	7849, 7858, 7867	7850, 7859, 7868	7870, 7877	7871, 7878		7842, 7879	7873, 7880		7874, 7881	7875, 7882
44	0669, 0670	0671, 0672	0673, 0674,	0675-0677	0678-0681	0682-0686	0687-0689	0698, 0699	0700, 0701		702	703		704	705
45	yes		yes	yes	yes	yes	yes								
46															
47															
48															

	AT	AU	AV	AW	AX	AY	AZ	BA	BB	BC	BD	BE	BF	BG	BH
1	**M46**	**M47**	**M48**	**M49**	**M50**	**M51**	**M52**	**M53**	**M54**	**M55**	**M56**	**M57**	**M58**	**M59**	**M60**
2	IMEO	IMEO	IMEO	IMEO	RP	RP	IMEO	IMEO	IMEO	IMEO	IMEO	IMEO	NP	NP	NP
3	ct, 15ml	ct, 15ml	ct, 15ml	ct, 15ml	ct, 15ml	ct, 15ml	ct, 15ml	ct, 15ml	ct, 15ml	mct, 2ml	mct, 2ml	mct, 2ml	mct, 2ml	mct, 2ml	mct, 2ml
4	0.5	0.5	0.5	0.5	0.45	0.45	0.5	0.5	0.5	0.5	0.5	0.5			
5													0.34	0.34	0.34
6															
7					0.25	0.25									
8													74.7	75.3	76.3
9	1.6	1.64	1.64	1.64			1.64	1.64	1.64	1.64	1.64	1.64			
10					30.4	30.6									
11					0.9	0.9									
12	1	1	1	1			1	1	1	1	1	1			
13															
14															
15				0.82	0.91	0.91				1.09	1.09	1.09			
16		5.72E-05	3.43E-05				5.72E-05	5.72E-05	5.72E-05				4.29E-04	4.29E-04	4.29E-04
17	2.1														
18															
19															
20															
21															
22	0.06	0.10	0.06	0.10	0.10	0.10	0.10	0.10	0.10	0.12	0.12	0.12	0.75	0.75	0.75
23	0.31	0.31	0.31	0.31			0.31	0.31	0.31	0.31	0.31	0.31			
24					0.1	0.1									
25															
26	20	20	20	4	20	20	20	20	20	4	4	4	4	4	4
27							10.2	20.2	30.3	10.1	20.4	29.7			
30	no	no	no	no	no	no	no	no	no	no	no	no	no	no	no
31	60	60	60	60	60	60	60	60	60	60	60	60	4	4	4
32	1	1	1	1	1	1	1	1	1	1	1	1	0.5	0.5	0.5
33	closed	closed	closed	closed	closed	closed	closed	closed	closed	closed	closed	closed	closed	closed	closed
34	no	no	no	no	no	no	no	no	no	no	no	no	no	no	no
35															
36	5	13	15	4	18h	n/a	20	20	20	0.01	0.01	0.01	18h	18h	18h
37	milky	milky	phase separation	opaque, transparent, cracks	transparent, dull, bad spots	no solid form; single crystalls on glass wall	milky, soft	milky, soft	milky, soft	dull, inhomogen	dull, inhomogen	dull, inhomogen	phase separation: solid/fluid; cracks, hard	phase separation: solid/fluid; cracks, hard	phase separation: solid/fluid; cracks, hard
38	yes	no	no	no	yes	n/a	no	no	no	n/a	n/a	n/a	yes	yes	yes
39	EtOH rinses through		very slow	very slow			very slow	very slow	very slow				H2O rinses through	H2O rinses through	H2O rinses through
40															
41	no adhesion to glass wall		phase separation: solid/fluid; soft; Water flushed monolith out	glass walls at 40°C, when adding IMEO; limited adhesion to glass wall						vial leaky in waterbath	vial leaky in waterbath	vial leaky in waterbath	no adhesion; acc. to Lit. #27	no adhesion; acc. to Lit. #27	no adhesion; acc. to Lit. #27
42	7885	7886	7887	7898	7899	7900, 7901	7902, 7903	7904	7905				7906	7907	7908
44															
45															yes
46															available (Pool)
47															
48															

	BI	BJ	BK	BL	BM	BN	BO	BP	BQ	BR	BS	BT	BU	BV	BW
1	**M61**	**M62**	**M63**	**M64**	**M65**	**M66**	**M67**	**M68**	**M69**	**M70**	**M71**	**M72**	**M73**	**M74**	**M75**
2	IMEO	IMEO	IMEO	IMEO	IMEO	IMEO	IMEO	IMEO	IMEO	IMEO	IMEO	IMEO	IMEO	IMEO	IMEO
3	mct, 2ml	mct, 2ml	ct, 15ml	ct, 15ml	ct, 15ml	ct, 15ml	ct, 15ml	ct, 15ml	ct, 50ml	ct, 50ml	ct, 50ml	mct, 2ml	mct, 2ml	mct, 2ml	mct, 2ml
4	0.5	0.5	0.5	0.5	0.5	0.5	0.5	0.5	1	1	1	0.6	0.54	0.48	0.42
5															
6															
7															
8									5.80E+02	1.22E+03	1.91E+03	100	100	100	100
9	1.64	1.64	1.64	1.64	1.64	1.64	1.64	1.64							
10															
11															
12	1	1	1	1	1	1	1	1							
13															
14															
15									1021.00	1021.00	1021.00				
16												5.72E-04	5.72E-04	5.72E-04	5.72E-04
17															
18															
19	0.01	0.01	0.01	0.01	0.01	0.01	0.01	0.01							
20															
21															
22	0.06	0.20	0.20	0.20	0.20	0.06	0.06	0.06	14	14	14	1.00	1.00	1.00	1.00
23	0.31	0.31	0.31	0.31	0.31	0.31	0.31	0.31	0.12	0.12	0.12	0	0.08	0.15	0.22
24															
25															
26	20	20	4	4	4	4	4	4	20	20	20	20	20	20	20
27			0	15.2	30.1	0	15	26.4							
30	no	no	no	no	no	no	no	no	no	no	no	no	no	no	no
31	60	60	60	60	60	60	60	60	40	40	40	4	4	4	4
32	1	1	1	1	1	1	1	1	1	1	1	0.5	0.5	0.5	0.5
33	closed	closed	closed	closed	closed	closed	closed	closed	closed	closed	closed	closed	closed	closed	closed
34	no	no	no	no	no	no	no	no	no	no	no	no	no	no	no
35															
36	3	2	6	6	6	7 days	7 days	5 days	7 days	7 days	7 days	18h	9	9	9
37	yellowish, transparent	milky	milky	milky	milky	yellowish, transparent	yellowish, transparent	yellowish, transparent	phase separation: solid/fluid, no monolithic structure	opaque, milky	opaque, dull	milky, inhomogen	milky; separate PEG particles inside	milky; separate PEG particles inside	milky; separate PEG particles inside
38	no	no	n/a	n/a	n/a	n/a	n/a	n/a					no	no	no
39															very slow
40			milky, keep form, but contract	milky, keep form, but contract	milky, keep form, but contract	strong contraction, but keep form, yellow clear gel	strong contraction, but keeps form; yellow transparent gel;								dried at 350°C: darkbrown, kept in form mainly, strong contaction, cracks
41	vial during reaction leaky;	vial during reaction leaky;	Aging at 40°C	Aging at 40°C	Aging at 40°C	slow polymerisation after addition of water	Polygosil sedimented;	slow polymerisation after addition of water; Aging at 40°C	Aging at 40°C	Aging at 40°C	Aging at 40°C				monolith resisted 3h in aqueous ammonium hydroxide 0.01M at 100°C
42	7909	7910				7933	7932		7937	7939	7938	7934	7920, 7926	7921, 7927	7922, 7928, dried form: 7965, 7966, 7967
44															
45															
46															
47															
48															

	BX	BY	BZ	CA	CB	CC	CD	CE	CF	CG	CH	CI	CJ	CK	CL
1	**M76**	**M77**	**M78**	**M79**	**M80**	**M81**		**M83**	**M84**	**M85**	**M86**	**M87**	**M88**	**M89**	**M90**
2	IMEO	IMEO	IMEO	IMEO	IMEO	IMEO		IMEO	IMEO	IMEO	IMEO	IMEO	IMEO	IMEO	IMEO
3	mct, 2ml	mct, 2ml	mct, 2ml	mct, 2ml	mct, 2ml	mct, 2ml		ct, 15ml	ct, 15ml	ct, 15ml	ct, 15ml	ct, 15ml	ct, 15ml	ct, 15ml	mct, 2ml
4	0.36	0.45	0.4	0.35	0.3	0.5		0.7	0.63	0.56	0.49	0.5		0.5	0.47
5													0.42		
6															
7															
8	100												100	80	80.8
9								2	2	2	2	1.6		1.6	
10															
11															
12		0.4	0.4	0.4	0.4	0.4		1	1	1	1	1		1	
13															
14															
15		1.63	1.63	1.63	1.63	1.63								4.08	
16	5.72E-04												5.72E-04		5.72E-04
17															
18															
19								0.01	0.01	0.01	0.01	0.01			
20															
21															
22	1.00	0.16	0.16	0.16	0.16	0.16		0.20	0.20	0.20	0.20	0.20	1.00	0.40	1.00
23	0.3	0.06	0.12	0.18	0.25	0		0	0.09	0.17	0.49	0.3	0.2	0.3	0.24
24															
25															
26	20	20	20	20	20	20		20	20	20	20	4	20	20	4
27															
30	no	no	no	no	no	no		no	no	no	no	no	no	no	no
31	4	20	20	20	20	20		60	60	60	60	60	4	20	4
32	0.5	0.5	0.5	0.5	0.5	0.5		1	1	1	1	1	0.5	0	0.5
33	closed	closed	closed	closed	closed	closed		closed	closed	closed	closed	closed	closed	closed	closed
34	no	no	no	no	no	no		no	no	no	no	no	yes	yes	no
35															
36	9	0.01	0.01	0.01	0.01	6 days		5 days	0.01	0.01	0.01	3	0.01		3
37	milky; separate PEG particles inside	opaque, yellowish, dull	opaque, yellowish, dull	opaque, yellowish, dull	opaque, yellowish, dull	completely transparent, cracks		transparent gel, cracks				milky		three phases: fluid/monolith/gel	phase separation: monolith/fluid; milky
38	no							n/a	n/a	n/a	n/a	n/a	n/a	n/a	no
39	monolith washed out														
40															
41	soft; monolith flushed out (no retention)		good structure			Aging at 40°C		Aging at 40°C					Reaction mixture is emulsion	reaction from bottom to top; aging at 40°C	immersed in NH4OH 0.01M, cooked in 0.01M NH4OH at 100°C
42	7923, 7929					7935		7936				7930, 7931		7940	7986, 7987, 7988
44															
45															
46															
47															
48															cooked in 0.01M NH4OH at 100°C (3h): structure destroyed

	CM	CN	CO	CP	CQ	CR	CS	CT	CU	CV	CW	CX	CY	CZ	DA
1	**M91**	**M92**	**M93**	**M94**	**M95**	**M96**	**M97**	**M98**	**M99**	**M100**	**M101**	**M102**	**M103**	**M104**	**M105**
2	IMEO	IMEO	IMEO	IMEO	IMEO	IMEO	IMEO	IMEO	IMEO	IMEO	IMEO	IMEO	IMEO	IMEO	IMEO
3	mct, 2ml	mct, 2ml	mct, 2ml	mct, 2ml	mct, 2ml	mct, 2ml	mct, 2ml	mct, 2ml	mct, 2ml	mct, 2ml	mct, 2ml	mct, 2ml	mct, 2ml	mct, 2ml	mct, 2ml
4	0.47	0.47	0.47	0.47	0.53	0.5	0.44	0.37	0.31						
5										0.47	0.47	0.47	0.47	0.47	0.47
6															
7															
8	95.5	100.6	110	120.5	95.5	95.5	95.5	95.5	95.5	95.5	95.5	95.5	95.5	95.5	95.5
9															
10															
11															
12															
13															
14															
15															
16	5.72E-04	5.72E-04	5.72E-04	5.72E-04	5.72E-04	5.72E-04	5.72E-04	5.72E-04	5.72E-04	5.70E-03	2.80E-03	2.80E-04	5.70E-05		6.01E-04
17															
18															
19															
20															
21														0.35	
22	1.00	1.00	1.00	1.00	1.00	1.00	1.00	1.00	1.00	1.00	1.00	1.00	1.00	1.00	1.00
23	0.24	0.24	0.24	0.24	0.27	0.26	0.22	0.2	0.16	0.24	0.24	0.24	0.24	0.24	0.24
24															
25															
26	4	4	4	4	4	4	4	4	4	4	4	4	4	4	20
27															
30	no	no	no	no	no	no	no	no	no	no	no	no	no	no	no
31	4	4	4	4	4	4	4	4	4	4	4	4	4	4	20
32	0.5	0.5	0.5	0.5	0.5	0.5	0.5	0.5	0.5	0.5	0.5	0.5	0.5	0.5	0
33	closed	closed	closed	closed	closed	closed	closed	closed	closed	closed	closed	closed	closed	closed	closed
34	no	no	no	no	no	no	no	no	no	no	no	no	no	no	no
35															
36	3	3	3	3	3	3	3	3	3	2	3	3	3	2	3
37	phase separation: monolith/fluid; milky	phase separation: monolith/fluid; milky	phase separation: monolith/fluid; milky	phase separation: monolith/fluid; milky	milky, inhomogen, bad spots	milky, inhomogen, bad spots	milky, inhomogen, bad spots	milky, inhomogen, bad spots	milky, inhomogen, bad spots	milky	milky, phase separation: monolith/fluid, bad spots	phase separation, bad spots	phase separation, bad spots	yellowish, transparent, bad spots	transparent, phase separation
38	no	no	no	no	n/a	n/a	n/a	n/a	n/a	no					
39															
40															
41	immersed in NH4OH 0.01M; cooked in 0.01M NH4OH at 100°C	immersed in NH4OH 0.01M; cooked in 0.01M NH4OH at 100°C	immersed in NH4OH 0.01M; cooked in 0.01M NH4OH at 100°C	immersed in NH4OH 0.01M;	Reaction mixture is Emulsion; Aging at 40°C	Reaction mixture is Emulsion; Aging at 40°C	Reaction mixture is Emulsion; Aging at 40°C	Reaction mixture is Emulsion; Aging at 40°C	Reaction mixture is Emulsion; Aging at 40°C	Aging at 40°C	Aging at 40°C	Aging at 40°C	Aging at 40°C	Aging at 40°C	Aging at 40°C
42	7986, 7987, 7988	7986, 7987, 7988	7984, 7985	7981, 7982, 7983,	7957	7955	7962	7956	7961	7977, 7978, 7979, 7980	7964	7960	7959	7963	
44															
45			yes	yes						yes					
46															
47															
48	cooked in 0.01M NH4OH at 100°C (3h): structure destroyed;	cooked in 0.01M NH4OH at 100°C (3h): structure destroyed;	cooked in 0.01M NH4OH at 100°C (3h): structure destroyed;	cooked in 0.01M NH4OH at 100°C (3h): structure intact, density gradient; washable (slow);						cooked in 0.01M NH4OH at 100°C (3h): structure intact, low density gradient; slow washable;					

	DB	DC	DD	DE	DF	DG	DH	DI	DJ	DK	DL	DM	DN	DO	DP
1	**M106**	**M107**	**M108**	**M109**	**M110**	**M111**	**M112**	**M113**	**M114**	**M115**	**M116**	**M117**	**M118**	**M119**	**M120**
2	IMEO	IMEO	IMEO	IMEO	IMEO	IMEO	IMEO	IMEO	IMEO	IMEO	IMEO	IMEO	IMEO	IMEO	IMEO
3	ct, 15ml	1.5ml vial	mct, 2ml	mct, 2ml	ct, 15ml	ct, 15ml	ct, 15ml	ct, 15ml	ct, 15ml	ct, 15ml	ct, 15ml	ct, 15ml	ct, 15ml	ct, 15ml	ct, 15ml
4	0.47	0.42	0.47	0.42	0.5	0.5	0.5	0.5	0.5	0.5	0.5	0.5	0.5	0.5	0.5
5															
6															
7															
8	100	100	96	100	100	10	0	100	100	100	100	100	100	100	120
9															
10															
11															
12	1.5				1	1	1	1	1.2						
13										1	1	0.9	0.8	0.7	1.2
14															
15															
16	5.72E-04	5.72E-04	6.00E-03	6.00E-04	1.00E-02	1.00E-02	1.00E-02	1.00E-02	1.00E-02		1.00E-02	1.00E-02	1.00E-02	1.00E-02	1.00E-03
17															
18															
19										0.01					
20															
21															
22	1.00	1.00	1.00	1.00	0.20	0.20	0.20	0.20		0.20	0.20	0.30	0.40	0.50	0.20
23	0.24	0.22	0.24	0.22	0.3	0.3	0.3	0.3	0.3	0.3	0.3	0.3	0.3	0.3	0.3
24															
25															
26	20	20	20	20	20	20	20	20	20	4	4	4	4	4	4
27															
30	no	no	no	no	no	no	no	no	no	no	no	no	no	no	no
31	4	4	4	4	60	60	60	60	60	60	60	60	60	60	60
32	0.5	0.5	0.5	0.5	0.5	0.5	0.5	1	0.5	0.5	0.5	0.5	0.5	0.5	0.5
33	closed	closed	closed	closed	closed	closed	closed	closed	closed	closed	closed	closed	closed	closed	closed
34	no	no	no	no	no	no	no	no	no	no	no	no	no	no	no
35															
36	60		3	20h	3	3	2	2	12	1	15	3	2	2	13
37	milky		milky, phase separation: fluid/monolith; enclosed air bubbles	phase separation: fluid/monolith; bad spots	milky, soft	milky	milky	milky	milky	milky, enclosed air bubbles, bad spots	milky, bad spots	milky	milky, bad spots	milky, resistent structure, bad spots	milky,
38		no (capillary)			yes	no	no	no (capillary)	yes	yes	yes	no	yes	no	yes
39					0.5 (60% EtOH)							very low			
40	milky, hard, porous														
41	Aging at 40°C;	filled in capillary	Aging at 40°C	Aging at 40°C	Aging at 40°C	Aging at 40°C	Aging at 40°C	filled in capillary: no success	Aging at 40°C	Aging at 40°C	Aging at 40°C	Aging at 40°C	Aging at 40°C	Aging at 40°C	Aging at 40°C
42	7974 (dried), 7975, 7976		7998	7999	8000, 8003 (after cooking); 8026-8031 (coloured monolith)	8001, 8004 (after cooking)	8002, 8005 (after cooking)		8006	8034	8035	8036	8037	8039	
44															
45															
46															
47															
48					cooked in 0.01M NH4OH at 100°C (1h): structure intact;	cooked in 0.01M NH4OH at 100°C (1h): structure intact	cooked in 0.01M NH4OH at 100°C (1h): structure destroyed		cooked in 0.01M NH4OH at 100°C (2h): structures mainly intact;	cooked in NH4OH at 70°C(3h): structure intact; still bad spots near the wall;	cooked in NH4OH at 70°C(3h): structure intact; still bad spots near the wall;	cooked in NH4OH at 70°C(3h): structure intact;	cooked in NH4OH at 70°C(3h): structure intact;	cooked in NH4OH at 70°C(3h): structure intact;	cooked in NH4OH at 70°C(3h): structure intact; still bad spots near the wall;

	DQ	DR	DS	DT	DU	DV	DW	DX	DY	DZ	EA	EB	EC	ED	EE
1	**M121**	**M122**	**M123**	**M124**	**M125**	**M126**	**M127**	**M128**	**M129**	**M130**	**M131**	**M132**	**M133**	**M134**	
2	IMEO	IMEO	IMEO	IMEO	IMEO	IMEO	IMEO	NP	IMEO	NP	NP	SH	IMEO	SH	
3	ct, 15ml	ct, 15ml	ct, 15ml	ct, 15ml	ct, 15ml	ct, 15ml	ct, 15ml	ct, 50ml	ct, 50ml	ct, 50ml	ct, 50ml	ct, 50ml	ct, 50ml	ct, 50ml	
4	0.5	1	0.5	0.5	0.5	1	2	3	8	6	6	4.4	8	8.8	
5															
6												5.16		10	
7															
8	100	199	100	100	100	199	398		1.60E+03				1.60E+03		
9															
10								91		182	181	0.3		6.00E+02	
11															
12								3.6		7.2	7.2	10		20	
13	0.9	1.8	0.9	0.9	0.9	1.8	3.6		14.4				14.4		
14								0.6		1.2	1.2	2		4	
15															
16	1.00E-02	2.00E-02	1.00E-02	1.00E-02	1.00E-02	2.00E-02	4.00E-02		1.60E-01				1.60E-01		
17															
18															
19															
20															
21															
22	0.30	0.60	0.30	0.30	0.30	0.60	1.20	1.20	4.80	2.40	2.40	1.26	4.80	2.50	
23	0.3	0.6	0.3	0.3	0.3	0.6	1.2		4.8				4.8		
24								0.15		0.3	0.3	1		2	
25															
26	4	4	4	4	20	4	4	20	4	4	4	4	4	20	
27															
30	no	no	no	no	no	no	no	no	no	no	no	no	no	no	
31	60	60	60	60	60	60	60	40	60	40	40	40	60	40	
32	0.5	0.5	0.5	0.5	0.5	0.5	0.5	1	0.5	1	1	1	0.5	1	
33	closed	closed	closed	closed	closed	closed	closed	closed	closed	closed	closed	closed	closed	closed	
34	no	no	no	no	no	no	no	no	no	no	no	no	no	no	
35															
36	3	4	6		3			6	3	8	7	40	6	18h	
37	milky	milky	milky					milky	milky	milky	milky	milky	milky	milky	
38	no		yes					yes	no	n/a	n/a	no	yes	n/a	
39	0.1 (H2O)		0.75 (H2O)					2.9 (H2O)				n/a	0.57 (60% EtOH)		
40															
41	Aging at 40°C	Aging at 40°C	Aging at 40°C					Aging at 40°C; monolith milled, washed and dried; A128, A130, A131 pooled; yield: 0.81g (3.25ml)	Aging at 40°C; monolith milled, washed, dried; Yield: 2.89g (9.25ml); A129 and A133 pooled	Aging at 40°C; monolith milled, washed and dried; A128, A130, A131 pooled; yield: 1.59g (7.25ml)	Aging at 40°C; monolith milled, washed and dried; A128, A130, A131 pooled; yield: 1.64g (8.0ml)	became milky firstly and then solid; synthesized, aged, milled, washed and dried; yield: 4.21g (7.25ml) (strong smell); no adhesion at glass wall (during wash step)	Aging at 40°C; monolith milled, washed, dried; Yield: 2.73g (9.5ml); Column dimensions (lengthxID): 4.7x0.4cm; A129 and A133 pooled	monolith milled, washed and dried; yield: 11.7g (20ml)	
42		separation dye mix: 8045 8047,						8055, 8056	8057			8058, 8059; Dried form: 8062, 8063; after pyridine-reaction: 8061	8060		
44	0723, 0724, Leica DM4000	Leica DM4000	Leica DM4000					Leica DM4000	Leica DM4000				Leica DM4000(?)		
45								yes	yes	yes		yes	yes		
46								available (Pool)	N2-Adsorption	available (Pool)			N2-Adsorption		
47								available (Pool)	available (Pool)	available (Pool)	available (Pool)	available (Pool)	available (Pool)		
48												Reaction: SH-Monolith + 2-chloropyridine Charge 1: Yield: 0.43g (out of 1.2g			

	EF	EG	EH	EI	EJ	EK	EL	EM	EN	EO	EP	EQ	ER	ES	ET
1		**M137**	**M138**	**M139**	**M140**	**C141**	**P142**	**P143**	**P144**	**P145**	**P146**	**M147**	**P148**	**P149**	**P150**
2		IMEO	IMEO	NP	RP	IMEO	IMEO	IMEO	IMEO	IMEO	IMEO	IMEO	IMEO	IMEO	IMEO
3		ct, 50ml	rbf, 50ml	rbf, 50ml	rbf, 50ml	rbf, 25ml	rbf, 10ml	rbf, 10ml	rbf, 10ml	rbf, 10ml	rbf, 10ml	rbf, 25ml	rbf, 25ml	rbf, 25ml	rbf, 25ml
4		3	8	6	9	2.3	2	2	2	2	2	3	2	2	2
5															
6															
7					5										
8		5.98E+02	1600				202	398	600	802	998	1170	0	400	800
9															
10				180	600	152.4									
11					1.8										
12				7.2		3.8									
13		5.4	14.4				3.6	3.6	3.6	3.6	3.6	5.25	3.6	3.6	3.6
14				1.2											
15					18.20										
16		6.00E-02	1.60E-01												
17															
18															
19															
20															
21															
22		1.80	4.80	2.40	1.99	0.60	1.20	1.20	1.20	1.20	1.20	1.75	1.20	1.20	1.20
23		1.8	4.8			1.4	1.2	1.2	1.2	1.2	1.2	1.8	1.2	1.2	1.2
24				0.3	2										
25															
26		4	4	20	20	20	20	20	20	20	20	20	20	20	20
27															
30		no	no	no	no	no	yes (4)	yes (4)	yes (4)	yes (4)	yes (4)	yes (4)	yes (4)	yes (4)	yes (4)
31		60	60	40	60	70	60	60	60	60	60	60	60	60	60
32		0.5	0.5	1	1	0.2	0.5	0.5	0.5	0.5	0.5	0.5	0.5	0.5	0.5
33		closed	closed	closed	closed	closed	closed	closed	closed	closed	closed	closed	closed	closed	closed
34		no	yes	yes	yes	yes	yes	yes	yes	yes	yes	yes	yes	yes	yes
35															
36			4.5	9	1	8	4	5	6	6	7	8	6	6	7
37		in planar test cell: dull, milky; bad spots and voids;	milky	milky	yellowish tranparent gel	milky	milky	milky	milky	milky	milky	milky	milky	milky	milky
38			no	yes	yes	yes	no	yes	yes	yes	yes	yes	no	yes	no
39			0.05 (H2O)	2.0 (H2O)	H2O rinses through	2.14 (H2O)	0.2 (H2O)	0.36 (H2O)	0.69 (H2O)	1.30 (H2O)	1.82 (H2O)	8.6 (H2O, in 10ml plastic tube)	<0.1 (EtOH)	0.7 (EtOH)	0.24 (EtOH)
40						colourless, fine powder	colourless, fine powder	colourless, fine powder	colourless, fine powder	colourless, fine powder	colourless, fine powder	dried after chromatographic tests, dry weight: 5.86g;		dried after chromtographic tests, dry weight: 0.46g;	
41		filled in planar test cell (0.1mm slit): filling time: 2:50min; filling was possible before solidification	25.5g wet monolith mass;	12.4g wet monolith mass;	17.0g wet monolith mass;	acc. to APTES-monoliths of A. Drescher;						No wash with NH4OH; used for chromatographic tests;	Aging at RT;	Aging at RT;	Aging at RT;
42		8064-8066 (during synthesis), 8067, 8068 (after synthesis); 8069-8075 (Test with methyl blue); 8076-8078 (after immersion in EtOH);	after aging: 8118, 8121,8122; 8129; 8130, 8131; 8133; 8177-8178, 8181, 8182, 8194: Swelling Test;	after aging: 8119, 8123; 8132, 8133	after aging: 8120, 8124;8125; coloured column: 8127;	8148	8148; 8156	8148	8148	8148	8148	8157; 8160-8167; 8168, 8169;	8163;	8163; 8127-8132; 8133-8134; 8135-8137; 8138-8140; 8141-8144;	8163; 8164;
44						Leica DM4000	Leica DM4000	Leica DM4000	Leica DM4000	Leica DM4000	Leica DM4000		Leica DM4000		
45															
46															
47			Elementar analysis (CHO);												
48		Elutiontest with methyl blue: Solution: 1 mg methyl blue / ml EtOH	BATCH: washed with 50ml NH4OH (0.01M), cooked in NH4OH (0.01M) at 60°C for 2	BATCH: washed with 50ml NH4OH (0.01M), cooked in NH4OH (0.01M) at 60°C for 2	BATCH: washed with 50ml NH4OH (0.01M), cooked in NH4OH (0.01M) at 60°C for 2	BATCH: washed in NH4OH (0.01M) at 80°C; filtrated, washed in H2O	BATCH: washed in NH4OH (0.01M) at 80°C; filtrated, washed in H2O	BATCH: washed in NH4OH (0.01M) at 80°C; filtrated, washed in H2O	BATCH: washed in NH4OH (0.01M) at 80°C; filtrated, washed in H2O	BATCH: washed in NH4OH (0.01M) at 80°C; filtrated, washed in H2O	BATCH: washed in NH4OH (0.01M) at 80°C; filtrated, washed in H2O	Chromatographic Tests; Series A, B, C, L,		Chromatographic Tests: Series D, E, F, G, H, J, K,	P150a washed with 0.01M NH4OH; P150b washed with 0.1M NH4OH;

	EU	EV	EW	EX	EY	EZ	FA	FB	FC	FD	FE	FF	FG	FH	FI
1	**P151**	**P152**	**IM153**	**S154**	**pH155**	**pH156**	**pH157**	**pH158**	**pH159**	**pH160**	**pH161**	**IM162**	**IM163**	**IM164**	**IM165**
2	IMEO	IMEO	IMEO	IMEO	IMEO	IMEO	IMEO	IMEO	IMEO	IMEO	IMEO	IMEO	IMEO	IMEO	IMEO
3	rbf, 25ml	rbf, 25ml	rbf, 25ml	rbf, 25ml	rbf, 10ml	rbf, 10ml	rbf, 10ml	rbf, 10ml	rbf, 10ml	rbf, 10ml	rbf, 10ml	rbf, 10ml	rbf, 10ml	rbf, 10ml	rbf, 10ml
4	2	2	2	2	1	1	1	1	1	1	1	2	2	2	2
5															
6															
7															
8	1200	1600	400	750	200	200	200	200	200	200	200	400	400	400	400
9															
10															
11															
12															
13	3.6	3.6	3.6	6.75	1.8	1.8	1.8	1.8	1.8	1.8	1.8	3.6	3.6	3.6	3.6
14															
15															
16															
17															
18															
19															
20															
21															
22	1.20	1.20	1.20	2.25	0.60	0.60	0.60	0.60	0.60	0.60	0.60	1.20	1.20	1.20	1.20
23	1.2	1.2	3	1.2	0.6	0.6	0.6	0.6	0.6	0.6	0.6	6.8	13.6	27.2	61.2
24															
25															
26	20	20	20	20	20	20	20	20	20	20	20	20	20	20	20
27															
30	yes (4)	yes (4)	yes (4)	yes (4)	yes (2)	yes (6)	yes (8)	yes (10)	yes (12)	yes (3)	yes (5)	yes (4)	yes (4)	yes (4)	yes (4)
31	60	60	60	60	60	60	60	60	60	60	60	60	60	60	60
32	0.5	0.5	0.5	0.5	0.5	0.5	0.5	0.5	0.5	0.5	0.5	0.5	0.5	0.5	0.5
33	closed	closed	closed	closed	closed	closed	closed	closed	closed	closed	closed	closed	closed	closed	closed
34	yes	yes	yes	yes	yes	yes	yes	yes	yes	yes	yes	yes	yes	yes	yes
35															
36	7	7	5	9	0	5	6	5	6	3	5	6	25	31	210
37	milky	milky	yellowish-milky	milky	milky	milky	milky	milky	milky	milky	milky	milky, yellowish	milky, yellow	yellow, jellylike, slightly milky, pasty (not solid);	yellow, jellylike, pasty (not solid)
38	yes	yes	no	yes	no	no	no	no	no	no	no	no	no	no	no
39	0.47 (EtOH)	0.37 (EtOH)	<0.2 (EtOH)	2.1 (EtOH)	<0.2 (EtOH)	<0.2 (EtOH)	<0.2 (EtOH)	<0.2 (EtOH)	<0.2 (EtOH)	0.25 (EtOH)	<0.2 (EtOH)	H2O rinsed through	H2O rinsed through	H2O rinsed through	H2O rinsed through
40											strong shrinkage, but good mechanical resistance				
41	Aging at RT;	Aging at RT;	low mechanical stability; low wall adhesion	low mechanical stability											
42	8163;	8163;	8165;	8166;		8159; 8161; 8162;	8159; 8161	8159; 8160; 8161	8159; 8161	8159; 8161	8159; 8161	8165;	8165;	8165;	8165;
44															
45															
46															
47															
48				dried out, but kept in form; rehydrated with 60% EtOH;											

	FJ	FK	FL	FM	FN	FO	FP	FQ	FR
1	**S166**	**S167**	**S168**	**P169**	**C170**	**P171**	**P172**	**P173**	**M176**
2	IMEO	IMEO	IMEO	IMEO	IMEO	IMEO	IMEO	IMEO	IMEO
3	rbf, 10ml	rbf, 10ml	rbf, 10ml	rbf, 10ml	rbf, 10ml	rbf, 25ml	rbf, 25ml	rbf, 25ml	rbf, 25ml
4	0.5	0.5	1	1	2.3	1	1	1	3
5									
6									
7									
8	580	330	500	300		0	200	400	1170
9									
10					150				
11									
12					3.8				
13	5.25	3	4.5	1.8		1.8	1.8	1.8	5.25
14									
15									
16									
17									
18									
19									
20									
21									
22	1.75	1.00	1.50	0.60	0.60	0.60	0.60	0.60	1.75
23	0.3	0.3	0.6	0.6	1.4	0.6	0.6	0.6	1.8
24									
25									
26	20	20	20	20	20	20	20	20	20
27									
30	yes (4)	yes (4)	yes (4)	yes (4)	yes (4)	yes (4)	yes (4)	yes (4)	yes (4)
31	60	60	60	60	70	60	60	60	60
32	0.5	0.5	0.5	0.5	0.17	0.5	0.5	0.5	0.5
33	closed	closed	closed	closed	closed	closed	closed	closed	closed
34	yes	yes	yes	yes	yes	yes	yes	yes	yes
35									
36	18h	18h	55	7	10	5	5	7	6
37	dull, jellylike, slightly milky, pasty (not solid)	dull, jellylike-milky, pasty (not solid)	milky, pasty (not solid)	milky	milky	milky	milky	milky	milky
38	no	no	no	yes	yes	no	yes	yes	yes
39	wahed out	washed out	washed out	1.6 (H2O, 1ml syringe)		<0.2 (H2O, in syringe)	0.8 (H2O, 2ml syringe)	1.4 (H2O, 2ml syringe)	1.9 (H2O, 9ml column)
40									
41				high discharge in wash phase;	crack formation in wash phase;				
42	8166;	8166;	8158; 8157; 8158;		8195;8196-8201; 8202; 8203-8210;	8195; 8196-8201; 8202; 8203-8210;	8195; 8196-8201; 8202; 8203-8210;	8176; 8179-8180: wash solution; 8195; 8196-8201; 8202; 8203-8210;	8174, 8175; 8211-8212;
44									
45									
46									
47									
48								Chromtographic tests: Series M	